INVESTIGATION OF THE TWO PULSE CORRELATION SONAR TECHNIQUE FOR WATER CURRENT MEASUREMENT

by

Benedikt Theodor Huber

B Sc , University of Victoria, 1983

A THESIS SUBMITTED IN PARTIAL FULFILLMENT OF THE
REQUIREMENTS FOR THE DEGREE OF
MASTER OF SCIENCE

in the Department of Physics

We accept this thesis as conforming to the required standard

[redacted]

Dr D M Farmer

ACCEPTED
FACULTY OF GRADUATE S

[redacted]

[redacted]

DATE Jan 05, 1987

Dr H W Dosso

[redacted]

Dr G W Bushnell

[redacted]

Dr P van den Driessche

[redacted]

Dr J T Weaver

[redacted]

Dr A D Booth

UNIVERSITY OF VICTORIA

NOVEMBER 1986

Supervisors Dr D M Farmer and Dr H W Dosso

ABSTRACT

In this thesis the use of the two pulse correlation sonar technique for measuring water currents in the ocean is investigated New theoretical analysis is developed to study the operation of the two pulse correlation sonar, including in particular, different demodulation techniques, the effect of cross-pulse interference on the correlation coefficients and correlation accuracy estimates

New theory shows that the effect of having two acoustic pulses in the water at the same time is equivalent to having a single pulse acoustic signal returning from random scatterers with a signal to noise ratio of one The peak of the spatial correlation function of the scattered signal is lowered by the presence of this noise A new treatment of spread spectrum pulses, used to reduce the interpulse interference, is shown to be only of limited usefulness

Literature does not investigate the effect of the low signal to noise ratio on the spatial correlation function, for different demodulation techniques Different demodulation techniques evaluated in this thesis, namely complex demodulation, clipped complex demodulation and amplitude demodulation are affected differently by the low signal to noise ratio and will result in different spatial correlation functions

The theoretical accuracy of the water velocity estimate is determined by two factors The height of the correlation peak and the accuracy of each correlation value The height of the correlation peak is determined by the signal to noise ratio and by the demodulation technique, while the accuracy of the correlation values is determined by the bandwidth-integration time product of the time series that is correlated

The peak of the correlation function for water volume return drops to 0 5 for complex demodulation, while it drops to 0 25 for amplitude and clipped complex demodulation, which has not been previously shown in available literature If the two

returning pulses are well separated in time, such as a signal returning from the bottom, then the correlation peak for all three demodulation techniques is equal to one

The new theoretical predictions of correlation sonar performance for volume scatterers are confirmed with a series of experiments carried out in Saanich Inlet, British Columbia and using a computer model of the correlation sonar Theory and experiments confirm that a current measuring two pulse correlation sonar can be constructed and will give accurate velocity estimates

[redacted]

Dr D M Farmer

[redacted]

Dr H W Dosso

[redacted]

Dr G W Bushnell

[redacted]

Dr P van den Driessche

[redacted]

Dr J T Weaver

[redacted]

Dr A D Booth

TABLE OF CONTENTS

LIST OF FIGURES

LIST OF TABLES

ACKNOWLEDGMENTS

I would like to thank my supervisors Dr D M Farmer and Dr H W Dosso for their help and guidance in this work

Special thanks must go to Dr A D Booth for his suggestions and constructive comments

The research in this work would have been impossible without the facilities and staff of the Institute of Ocean Sciences (Patricia Bay), especially Netta Delacretaz, Jim Galloway, Grace Kamitakahara-King and Ron Teichrob

Special mention must go to Jim Mattock of Seastar Instruments for his efforts in setting up the Correlation Sonar and in the collection of data

I should also thank my fellow graduate students Greg Crawford, Richard Dewey, Del Huston, Svein Vagle and Len Zedel for their helpful comments

This work was funded by the National Research Council through a NSERC post-graduate scholarship and by the Department of Fisheries and Oceans

Finally, I would like to thank my wife Abigail for her support and encouragement

1 INTRODUCTION

The need for the rapid, accurate and reliable measurement of current profiles has directed the attention of the oceanographic community to the use of acoustics Oceanographic studies in upper ocean dynamics, internal waves, coastal flows, large scale ocean currents, flow over topography, mixing and ocean atmosphere interaction are only a few of the areas to which a superior method of current profile measurement may be applied

Until recently, the most common method of measuring ocean currents had been with propeller or vane type current meters, placed at the location of interest in the water With the newer acoustic velocity sensing techniques the sensor platform can be mounted either on the ocean bottom or on a ship, thus eliminating the potential disturbance of the flow field by the sensor Moreover, the rapid acquisition of depth profiles from a moving platform over a large area allows the investigation of flows with temporal and spatial resolutions unobtainable from moored instruments

An acoustic remote sensing velocity apparatus operates on the premise that there are, almost without exception, scatterers suspended in the water moving with the current In the coastal regions these scatterers are dominantly biological in origin, composed of zooplankton or fish (Stanton 1986) Wind and wave action may trap air bubbles, which can be very strong scatterers, in the top 10 meters of the ocean Suspended particles such as silt, clay or sand, from river mouths or industrial pollution, may also contribute to the scattering If none of the above scatterers are present usually there will be density microstructures, which are caused by temperature or salinity inhomogeneities (Zedel 1986) Scatterers which are stationary relative to the water will give an accurate representation of the currents Contamination of the velocity readings can occur due to such factors as actively swimming biological scatterers, air bubbles rising to the surface or slowly sinking sand, silt or clay

Two related acoustic velocity sensing techniques are the correlation sonar, towards which this thesis is directed, and the more common Doppler sonar The Doppler sonar

detects the velocity by means of the Doppler shift imparted to an acoustic signal along a narrow transmitting and receiving beam (Pinkel 1980) and has been widely used in the atmosphere (Woodman 1980) and the ocean (Zedel 1985, Woodward and Gerald 1986) The correlation sonar differs from this in that the velocity detection is based on the translation of an interference pattern at the transducer caused by the movement of scatterers perpendicular to a wide transmitting and receiving beam The two techniques initially seem fundamentally different, but closer investigation reveals that they depend upon the same fundamental principle of acoustic scattering off a moving target (Briggs 1980, Edward 1978) Although the correlation sonar uses more complicated electronics and transducers than the Doppler sonar, it offers several advantages The wide beam transducers (22 degrees) required for the correlation sonar are easy to construct because they are quite small, even at low frequencies, while narrow beam Doppler transducers (1 degree) are difficult to construct and bulky at low frequencies While only a single beam is required for the correlation sonar, to determine the velocity in three dimensions the Doppler sonar requires at least three narrow beams Since the beams of the Doppler sonar will probe different sections of water, errors can be introduced when attempting to measure small scale flows The correlation sonar will average the velocities from the scatterers inside the single wide beam

The correlation technique for velocity measurement was first proposed as a navigational aid for aircraft (Dickey 1958) and later for navigation at sea (Andermo and Mosrelıez 1978) The Andermo and Mosrelıez patent was developed into a commercial ship speed log by Junger Instrument of Sweden The patent relies on a similar technique for velocity determination as is used in devices used to measure velocity using laser speckle statistics (Churnside and Yura 1981) For this technique a continuous wave coherent signal is sent towards a scattering layer The coherent source is a laser for laser speckle statistics The coherent source illuminating the surface will reflect a random speckle pattern on a screen placed opposite the target If the target is moving, the speckle pattern will move at twice the velocity of the target Two detectors

placed in line with the target velocity v_t and separation d_s will receive the same signal except that one will be delayed by a time τ_d relative to the other, where $\tau_d = d_s/(2v_t)$ The maximum cross correlation between the two time series will therefore yield the time lag τ_d

In 1978 Dickey filed a patent of a different version of the correlation sonar which sends two pulses in rapid succession into the water, towards the bottom (Dickey 1981) The two pulses are so short that they no longer can be considered continuous wave The two pulses returning from the bottom will be well separated in time and have a high frequency interference pattern superimposed on them The interference pattern is dependent on the particular scatterer distribution and receiver location Cross correlations between spatially displaced elements give a spatial correlation function on the surface The peak displacement of the spatial correlation function is proportional to the scatterer velocity The two pulse technique resulted in the development of the Magnavox MX810 deepwater correlation sonar by General Electric The MX810 deepwater correlation sonar was developed to give a ship's velocity relative to the bottom and was found to be accurate and reliable (Dickey and Bookheimer 1983)

To measure ocean current velocities with a correlation sonar, short pulses have to be sent into the water column to give adequate range resolution The continuous wave correlation sonar as detailed in the Andermo and Mosreliez patent can therefore not be used for water current measurement The spatial correlation function is only approximately four centimeters wide for a transmit pulse at an acoustic frequency of 100khz To be able to locate the peak of the correlation function it should be sampled with a resolution of two centimeters or less To make it possible to keep the number of receiving transducers to a reasonable number (four to eight transducers for each perpendicular axis), the separation of the pulses on which the correlations are performed must be between 10msec and 50msec for a velocity range of 0 to 2m/sec For water current measurement using the correlation sonar technique two pulses have

to be sent out in rapid succession Each pulse pair can then be repeated when the reverberation dies down

Another limitation on the maximum pulse separation is the scatterer decorrelation Scatterer decorrelation results in the reduction of the correlation peak because the scatterers move with a random velocity component relative to the water No exact figures are available for the scatterer decorrelation time, since it changes with the type of biological scatterer, time of day and season, but it generally is between 100msec (Huston 1986) and 1sec (Farmer, Booth and Kamitakahara 1981, Farmer and Crawford 1983) Since the pulse separation used for the two pulse correlation sonar is smaller than this, scatterer decorrelation will usually have a minor effect on the accuracy of the correlation sonar

It should therefore be possible to build a two pulse correlation sonar to measure the velocity of water currents There is however a fundamental difference in the signal returning from the water column, compared to the signal returning from the bottom If there is a uniform scatterer distribution in the water column, signal from the two returning pulses will be received at the same time from different range gates Since in the correlation process the signal from only one of the two pulses is required at any one time, the other pulse will interfere with the required signal Since the interfering pulse can usually not be separated from the required signal, it must be treated as noise The effect of this noise on the correlation function is not discussed in available literature, but it will greatly influence the accuracy of a correlation sonar current measuring device This thesis investigates the exact nature of the interpulse interference noise and what effect it has on the correlation function A general expression for the shape of the correlation function is derived Various signal processing and storage techniques will result in different correlation functions for similar raw signals The accuracy of the correlation functions for both bottom return and volume return is investigated in terms of the different demodulation techniques

In atmospheric radars which use the spaced antenna technique, the pulse separation and the width of the spatial correlation function is of similar order of magnitude to that of the two pulse correlation sonar Interpulse interference will however not be present, since all the return signal can be received for each pulse before the next one is transmitted due to the propagation velocity of the radar pulse at the speed of light

A computer model of a two pulse correlation sonar was developed to perform a detailed analysis of the correlation sonar as a current measuring device The results from the computer model are compared to the theoretical expected correlation functions and to correlation functions obtained from a modified prototype correlation sonar which was available at the Institute of Ocean Sciences The theoretical results are confirmed by the experimental data and the computer model

The accuracy of a two pulse correlation sonar is mainly limited by the interpulse interference A technique of reducing the interpulse interference using spread spectrum pulses is also evaluated

2 THEORY OF OPERATION OF THE CORRELATION SONAR

There exist many methods to explain the operation of the correlation sonar The statistical properties of the acoustic field may be described in terms of a space-time correlation function of the type used in the correlation sonar Alternatively, it may be described as a frequency wavenumber spectrum as used in the Doppler sonar The first section of this chapter provides an intuitive explanation for the operation of the correlation sonar, which draws on theoretical and physical explanations given in the literature (Dickey and Edward 1978, Edward 1979) Following the explanation of operation, the actual shape of the spatial correlation function is given, using a derivation by Ishimaru (1978) Operational limits, such as effects of signal contamination, are briefly discussed The final section examines a variety of signal demodulation types possible with the correlation sonar

2.1 Principle of operation

The principle of operation of the correlation sonar may be explained as follows A water volume is insonified by a wide beam acoustic transducer of width θ at a frequency f_o Acoustic returns will be received from two range increments of length $T_p * c$ where c is the speed of sound in the water column One range increment will be at a range gate or integration window at time t_r, the other at time $t_r + T_s$ T_s is the pulse separation

Following the transmission of the two pulses into the water column, the returning wavefronts are monitored at several different points in space at a range gate when the two pulses pass through the water volume of interest These points are usually in a horizontal plane for convenience The waveform received at a time t by one hydrophone will be virtually the same on a second hydrophone at a time $t + T_s$ provided the displacement vector of the hydrophones is exactly twice the displacement vector of

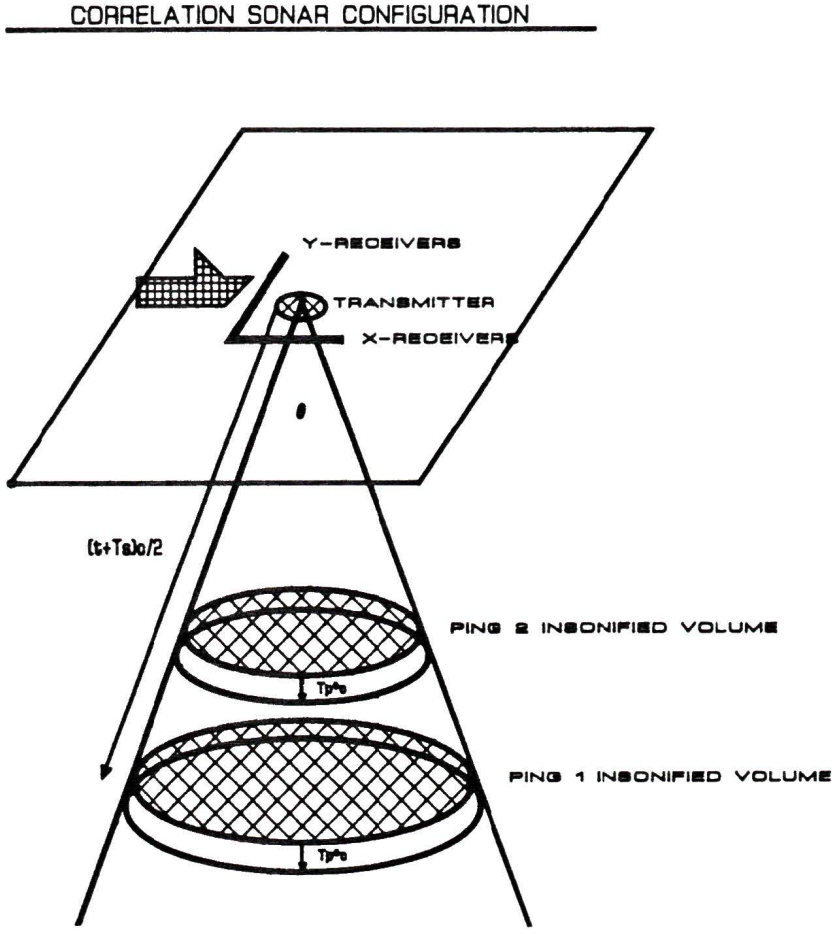

Figure 2.1

The correlation sonar system configuration An array of receivers at the surface receives signals from two insonified volumes after two pulses are transmitted with a pulse length T_p and separation T_s The transmit and receive elements have a beamwidth θ

the scatterers (figure 2 3) This process is commonly referred to as waveform invariant geometry (Edward 1979) The principle of waveform invariant geometry assumes only that the the vertical distance to the scatterers is considerably greater than the separation between transducer elements As the transducer spacing is the same order of magnitude as the wavelength of the sound, this approximation applies universally in

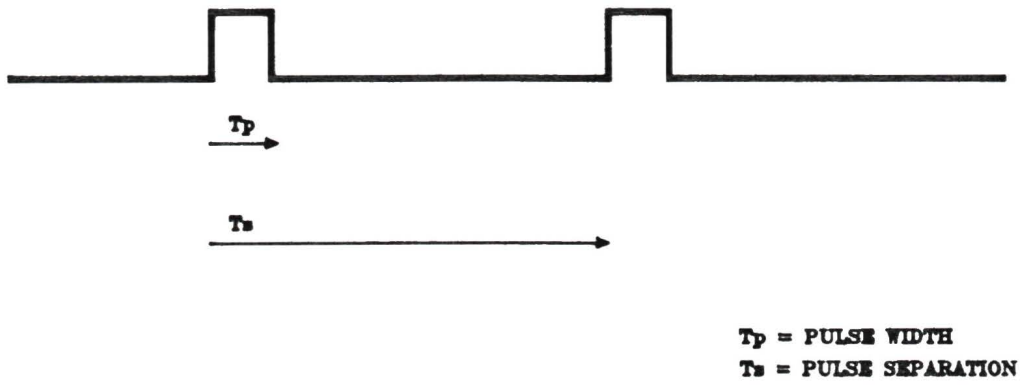

Figure 2.2

The transmission waveform envelope for the correlation sonar

the far field Waveform invariant geometry is independent of the local sound velocity

The signal $y_j(t)$ received at transducer j, is cross-correlated with the signal $y_k(t)$ received at transducer k with a time lag T_s over the water volume of interest, with an integration period T_i The cross-correlation will have a maximum value for those transducer elements having a vector separation corresponding to twice the scatterer vector displacement in time T_s By comparing the cross correlations for the different transducer elements, the correlation sonar searches out the vector displacement of the maximum value of the correlation function The velocity $\vec{v}$ of the scatterers can be calculated using the vector displacement of the peak of the correlation function $\vec{s}_{max}$

$$\vec{v} = \frac{\vec{s}_{max}}{2T_s}, \tag{2 1}$$

where $\vec{s}_{max}$ is the vector displacement of the maximum of the correlation function

In most practical situations, only a two-dimensional planar hydrophone array can be constructed The hydrophone array plane is positioned normal to the transmission

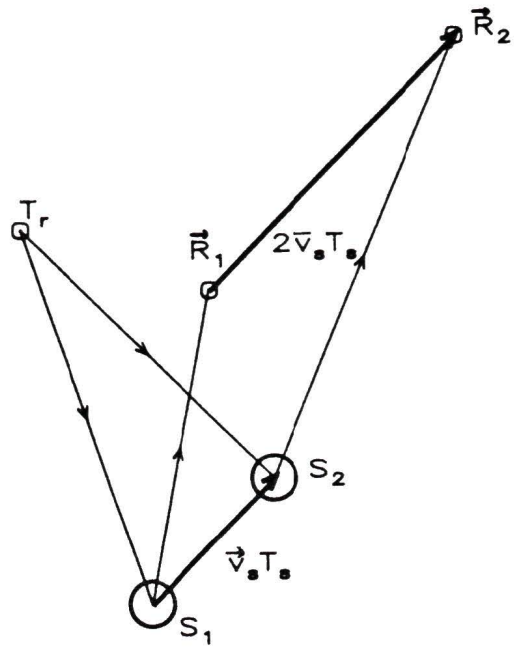

Figure 2.3

Diagram of waveform invariant geometry $\vec{\mathbf{R}}_1$ and $\vec{\mathbf{R}}_2$ are vector positions of 2 hydrophones at t_1 and t_2 respectively If $\vec{\mathbf{R}}_1 - \vec{\mathbf{R}}_2 = 2\vec{\mathbf{v}}_s T_s$, then $Y_1(t)$, the waveform received on hydrophone 1 at position $\vec{\mathbf{R}}_1$ will be equal to $Y_2(t)$, the waveform received on hydrophone 2 at position $\vec{\mathbf{R}}_2$ a time T_s later $\vec{\mathbf{v}}_s$ is the scatterer velocity

beam direction The spatial correlation vector will provide the horizontal water velocity in the v_x and v_y direction By adjusting the correlation delay time, and searching out the correlation peak in time, the vertical velocity v_z, of the scatterers may be obtained (Dickey 1981) Appropriate curve fitting and smoothing algorithms must be implemented to locate the correlation peak, as the correlation function may only be sampled at discrete points in space and time in any real world situation

2.2 The shape of the spatial correlation function

The derivation of the spatial correlation function shape is based on the development of a general random scattering correlation function given by Ishimaru (1978) The gen-

eral random scattering correlation function is adapted to the correlation sonar A layer of random scatterers is insonified with a transmitter The returning signal is received with two hydrophones at points $P_1(d/2,0,0)$ and $P_2(-d/2,0,0)$ (figure 2 4)

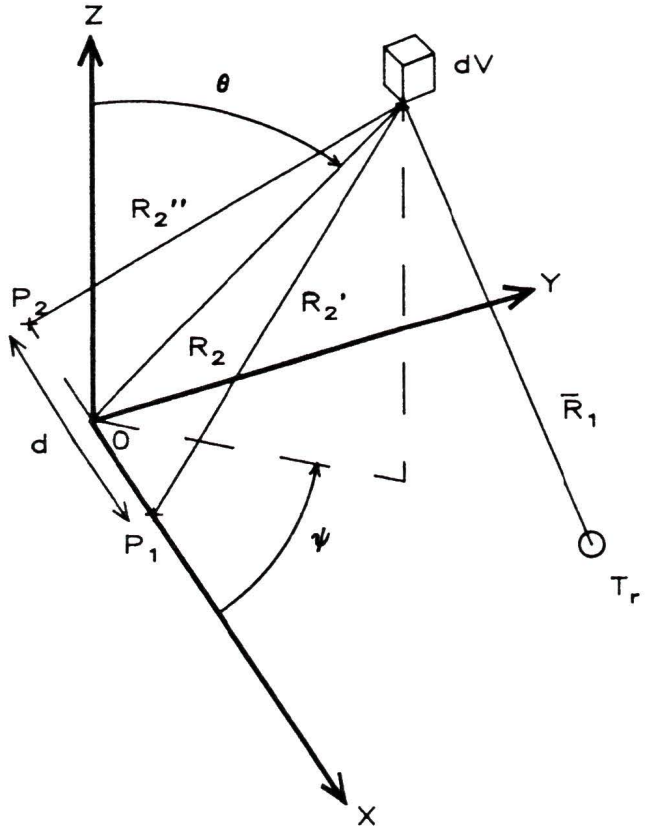

Figure 2.4

Geometry used to derive the spatial correlation function at points P_1 and P_2 for a random scattering medium

For a field scattered from an elementary volume dV at point (R_2,θ,ϕ) the phase difference between P_1 and P_2 is given by $\psi = k(R_2' - R_2'')$, where k is the wavenumber In the far field of the receiver (ie d is much smaller than R_2), ψ can be approximated as

$$\psi = k(R_2' - R_2'') \approx -kd(\hat{\mathbf{O}}\ \hat{\mathbf{x}}), \tag{2 2}$$

where $\hat{\mathbf{O}}$ is the unit vector connecting the origin and the scattering volume dV and $\hat{\mathbf{x}}$ is a unit vector along the x axis The voltages V_1 and V_2 received on a transducer

element is directly proportional to the acoustic field at the transducers at points P_1 and P_2 respectively By using an extension of the radar equation for a bistatic system, the spatial correlation function of the voltages V_1 and V_2 can be written as (Ishimaru 1978 eq 4-71)

$$\langle V_1 V_2^* \rangle = c \int_V \frac{\lambda^2 G_t(\hat{\mathbf{i}}) G_r(\hat{\mathbf{O}})}{(4\pi)^3 R_1^2 R_2^2} \rho \sigma_{bi}(\hat{\mathbf{O}}, \hat{\mathbf{i}}) \exp(-\gamma_1 - \gamma_2 + i\psi) dV, \tag{2 3}$$

where $c = \langle V^2 \rangle / (P_r/P_t)$, G_r and G_t are the receiver and transmitter gain functions, λ is the wavelength of the sound, ρ is the density of the medium, σ_{bi} is the bistatic scattering cross section of the scattering volume dV and P_t, P_r are the transmitted and received power $\hat{\mathbf{i}}$ is a unit vector connecting the transmitter and the scattering volume and $\hat{\mathbf{O}}$ is a unit vector connecting the receiver and the scattering volume γ_1 and γ_2 are the acoustic paths between dV and the transmitter, and dV and the receiver respectively

$$\gamma_1 = \int_0^{R_1} \rho \sigma_t ds, \quad \gamma_2 = \int_0^{R_2} \rho \sigma_t ds, \tag{2 4}$$

and where σ_t is the total cross section * denotes the complex conjugate, $\langle\rangle$ is the expectation operator and $i = \sqrt{-1}$

If the transmitter is placed at the origin such that $\hat{\mathbf{i}} = -\hat{\mathbf{O}}$ the correlation is

$$\langle V_1 V_2^* \rangle = c \int_V \frac{\lambda^2 G_t(\hat{\mathbf{i}}) G_r(-\hat{\mathbf{i}})}{(4\pi)^3 R_1^2 R_2^2} \rho \sigma_b \exp[-\gamma_1 - \gamma_2 + ikd(\hat{\mathbf{i}}\ \hat{\mathbf{x}})] dV \tag{2 5}$$

Here σ_b is the backscatter cross section of the scattering volume dV Further simplifications must be made to obtain a closed expression for the correlation function The points P_1 and P_2 are located in the xz plane and line P_1P_2 is inclined at an angle φ from the x axis $(0 \leq \varphi \leq \frac{\pi}{2})$ The transmitter at the origin has a gain function $G_t(\theta) = G_o \exp(-\theta^2/{\theta_o}^2)$, where θ_o is the beamwidth The receivers at R_1 and R_2 have the same gain function as the transmitter A layer of thickness Δz is parallel to the x axis, at a distance R_o (figure 2 5)

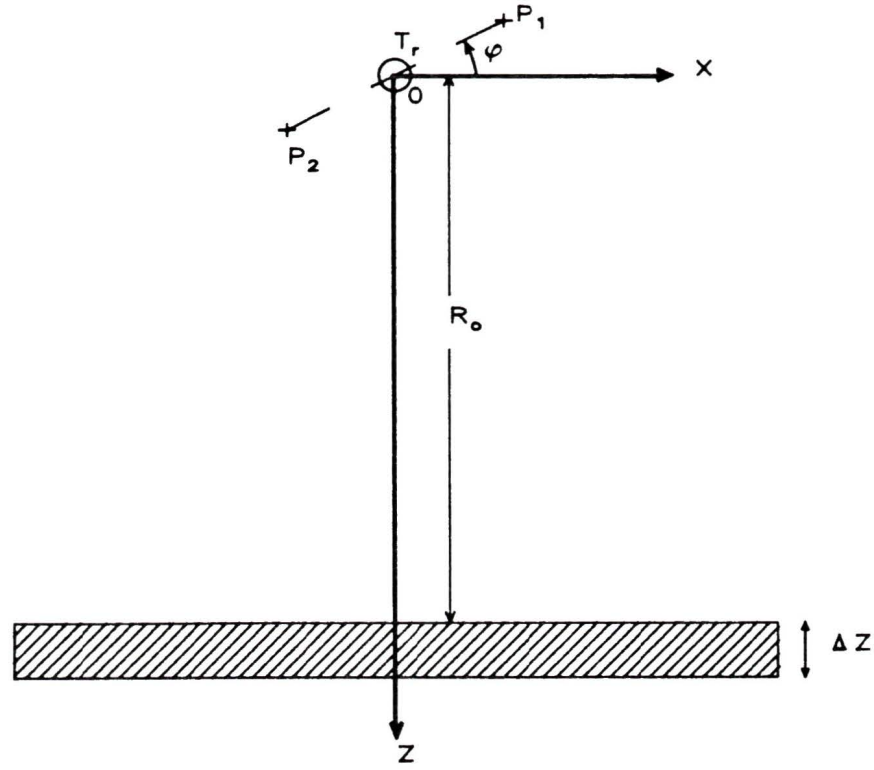

Figure 2.5

Correlation of acoustic field at points P_1 and P_2 due to a thin layer of randomly distributed particles at a distance R_o from the transmitter The line connecting points R_1 and R_2 is inclined at an angle φ from the xy plane

With the these simplifications, a simpler expression for the correlation can be obtained, using $\psi = kd(\sin\theta\cos\phi\cos\varphi + \cos\theta\sin\varphi)$

$$\langle V_1 V_2^* \rangle \approx C_o \int_0^{2\pi} d\phi \int_0^{\pi} \theta d\theta \exp[-(2\theta^2/\theta_o^2) + i\psi], \tag{2 6}$$

with $C_o \approx [c\lambda^2 G_o^2 \rho\sigma_b/(4\pi)^3 R_o^2]\Delta z$

Since $|\theta| \ll 1$,

$$\int_0^{\pi} d\phi \exp(ikd\sin\theta\cos\phi\cos\varphi) = 2\pi J_o(kd\sin\theta\cos\varphi) \approx 2\pi J_o(kd\theta\cos\varphi)$$

J_o is the bessel function of order zero Using the above integral equation 2 6 can be evaluated approximately (Ishimaru 1978)

$$\langle V_1 V_2^* \rangle \approx (\frac{\pi c_o}{A}) \exp[ikd\sin\varphi - \frac{(kd)^2}{4A}] \tag{2 7}$$

The constant A is given by

$$A = \frac{2}{\theta_o^2} + i\frac{kd\sin\varphi}{2}$$

Equation 2 7 shows that if φ is not zero, a phase shift will be introduced into the complex correlation coefficient, since the imaginary part of the correlation coefficient is no longer zero The phase shift can be shown to be proportional to the rate of change in path length from the transmitter to the scatterers and back to the receiver

If the receivers are located along the x axis, then $\varphi = 0$ and the correlation function is proportional to

$$\langle V_1 V_2^* \rangle \propto \exp[-\frac{(kd\theta_o)^2}{8}] \tag{2 8}$$

Equation 2 8 shows that the spatial correlation as a function of d, the separation, is gaussian in shape The correlation function also depends on the beamwidth θ_o and the frequency $f_o = c/\lambda = kc/2\pi$, where λ is the wavelength and k the wave number The width of the correlation function W is defined to be the point where the amplitude of the correlation coefficient drops to $1/e$ of the amplitude at the peak correlation when $d = 0$

$$W = (\frac{4\sqrt{2}}{k\theta_o}) \approx \frac{c}{f_o\theta_o} \tag{2 9}$$

A typical spatial correlation function is plotted in figure 2 6 using equation 2 8 A beamwidth of 22 degrees and a frequency of 100khz is assumed A one dimensional slice through the center of the two dimensional spatial correlation function is plotted The correlation function in the plane can be obtained by rotating the one dimensional correlation function around the center axis

2.3 The accuracy of the correlation sonar velocity estimate

The theoretical accuracy of the correlation sonar unhindered by electrical noise, platform motion, transducer missalignment and interpolation errors can be determined using an analytical model developed by J A Edward (1979) The accuracy is determined

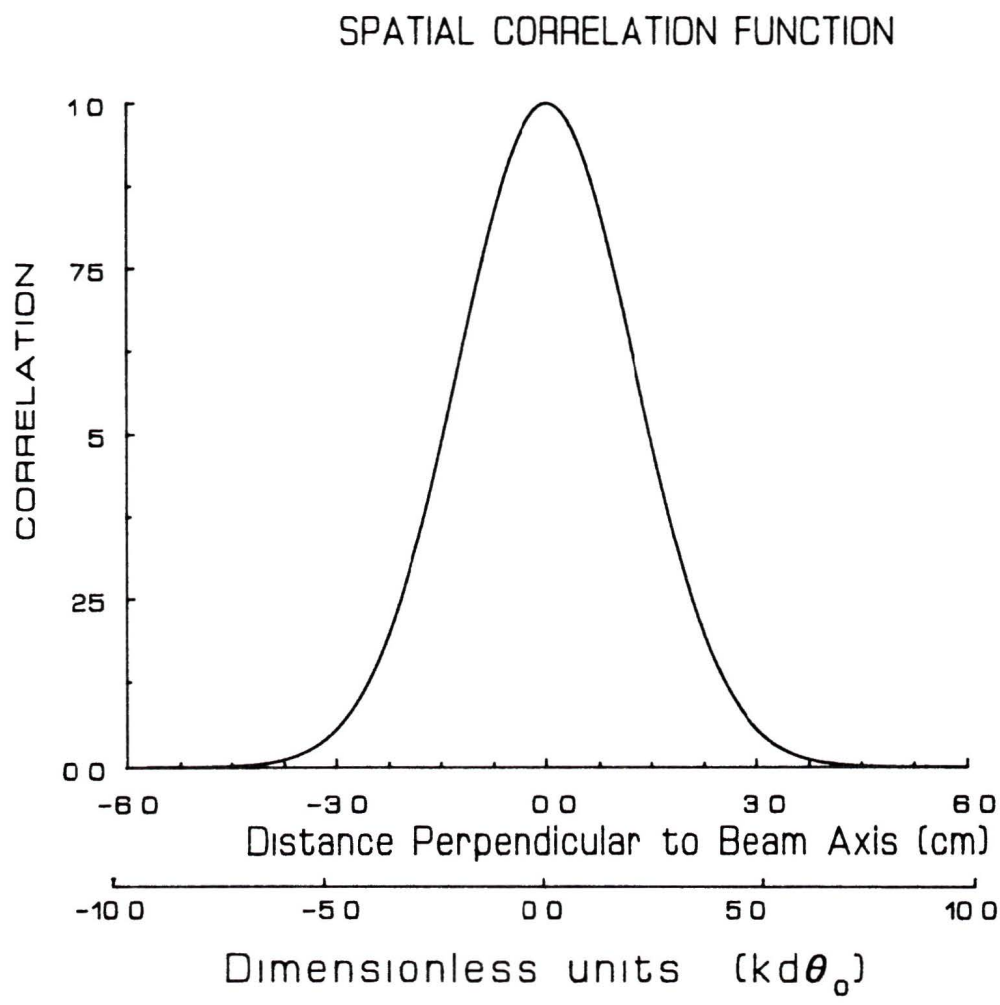

Figure 2.6

Theoretical spatial correlation function of a 22 degree beamwidth transmitter at a frequency of 100khz

by finding the statistical properties of the spatial correlation function, and is found to be approximately the same as that for the Doppler sonar The standard deviation for the velocity estimate of the correlation sonar may be approximated as

$$\sigma_v = \frac{1}{4\pi^{\frac{1}{2}} T_s}\left(\frac{W}{\sqrt{N_s}}\right)\left(1+\frac{P_n}{P_s}\right), \tag{2 10}$$

where W is the width of the correlation envelope, as given by equation 2 9 $W = \frac{c}{f_o \theta_o}$, θ_o being the round trip beam width, f_o the frequency and c the speed of sound in the water N_s is the number of independent samples available in the correlation and can

be written as

$$N_s = B_W T_I, \tag{2 11}$$

where B_W is the bandwidth of the signal and T_I is the integration time of the correlation P_n is the noise power and P_s is the signal power in equation 2 10 In the derivation of equation 2 10 no consideration was given to the effect of using different demodulation techniques on the accuracy of the correlation sonar velocity estimate The interpolation technique used to locate the peak of the correlation function also will introduce errors into the calculation of the velocity which are not included in equation 2 10

As an example, a prototype correlation sonar system at the Institute of Ocean Sciences has the following specifications B_W = 4kHz, T_s = 10 msec, f_o = 100kHz, θ_o = 22 degrees For this system a theoretical velocity standard deviation is σ_v = 22m/sec for a value of $P_n = 0$ Theoretically this should be the accuracy to which the bottom speed could be determined, if the full spatial correlation function was available for a single transmission pulse pair The actual correlation function is only sampled at four points across the peak since the peak width is about 4cm, while the transducer spacing is 1 5cm, and therefore numerical interpolation must be used to determine the exact peak location, which will introduce extra errors into the calculation of the velocity Normally the velocity estimate is based on the average of several transmissions, so that the variance is reduced to an acceptable level A typical reverberation time in the ocean is 0 5sec A one minute, 120 transmission average will have a velocity error of σ_v = $02m/sec$ Edward does not discuss the effect of water volume return on the accuracy of the velocity estimate For full water volume return the signal to noise ratio is one, as will be shown in a following chapter The theoretical 120 transmission average accuracy of the velocity, using equation 2 10, will therefore be σ_v = $04m/sec$ for full volume return

2.4 Range resolution

The range resolution is determined by both the transmitted pulse length and the length of the integration window T_i. In many cases the integration window is set to be equal to the pulse length (Edward 1979), although for deep water, where pulse spreading effect occurs due to the wide beam width and the spherical shape of the insonified volume, the integration length should be increased to accommodate the spreading effect. The maximum depth will depend on power levels, propagation losses and volume-scattering strength. Low frequencies have lower propagation losses, but may have lower scattering strength off biological targets. Therefore determination of the best frequency will be a tradeoff between scattering strength and propagation losses.

2.5 Signal contamination

Various factors contribute to deviation of the correlation function from the theoretical expected value. For instance, the signal received by each hydrophone $y_r(t)$ will the sum of the wanted signal $y(t)$ and noise $n(t)$. The correlations between transducers are performed by correlating data from transducer j at time t with data on transducer k at time $t + T_s$. Thus any noise that may be coherent between channels at zero time lag will usually be incoherent at a time lag of T_s. The general effect of incoherent noise on a correlation coefficient is the lowering of the correlation values. Different signal processing techniques used before correlation such as amplitude demodulation or complex demodulation as discussed in the next section will be affected differently by the presence of noise.

There are three major sources of noise that contaminate the signal of the correlation sonar, and thus limit the signal to noise ratio. They are environmental background noise in the ocean, transducer and electronic noise, and interpulse contamination due to the two pulses that are in the water at the same time. The environmental

noise may have natural sources such as wind or rain, or it may be man made by the ship's engines or other acoustic sensing devices such as depth sounders

The signal received at the receiving hydrophones can be very weak, requiring a large amount of amplification Any noise introduced in the amplification circuitry will contaminate the wanted signal When digitizing the demodulated waveforms, only a finite resolution analog to digital converter is available, thus digitization noise will also be introduced into the signal

When the correlation sonar receives signal from a well defined scattering layer such as the ocean bottom or the ice covered ocean surface, the two pulses that are transmitted will be well separated, provided that the pulse separation is long enough If, on the other hand the scattering layer is more or less uniformly distributed over the whole ocean depth, the signal received at each transducer will be the sum of the signal received from each pulse that was sent out, from a different range When performing the correlations, the signal required is that from one of the pulses only The return signal from a random distribution of scatterers will have a normally distributed probability density function, as will be shown in the next chapter The effect of interpulse interference can therefore be viewed as the required signal being mixed with gaussian random noise of equal amplitude as the signal Thus for a uniform, thick scattering layer the signal to noise ratio due to interpulse interference will almost never be better that one

The noise from the environment or the electronics can usually be controlled to be much smaller than the interpulse interference noise Thus the dominant noise source for a current measuring correlation sonar is the interpulse interference The precise effect of this contamination on the correlation function is not discussed in available literature concerning the correlation sonar It will however, contribute greatly to errors in the measurement of water currents Using a correlation sonar for bottom velocity measurements does not involve this problem since the two pulse returns are totally

separate Other geometries of transducer orientation, such as a bistatic geometry with intersecting beams will circumvent the inter-pulse interference problem somewhat, but will severely limit system flexibility

2.6 Type of signal demodulation

Different implementations of the correlation sonar use different demodulation techniques The relative merits of different demodulation techniques on the accuracy of the correlation sonar velocity estimate have not been investigated in available literature and will be given in a later chapter In this section, an overview of the three most common demodulation techniques is given

The signal $y_j(t)$ received on each hydrophone will be the raw carrier at a center frequency $f_o = \omega_o/2\pi$ It will have amplitude modulation and doppler shifts imposed on it, due to the moving scatterers There are several methods of demodulating and recording this signal The signal can be represented in complex notation as $y_j(t) = A(t) * \exp[i(\omega_o t + \phi(t))]$ By mixing this signal with a carrier signal of type $\sin(\omega_o t)$ and low pass filtering, the in-phase demodulated signal is obtained The in-phase signal can be written as $I(t) = A(t)sin(\phi(t))$ If the incoming signal $y_j(t)$ is mixed with $\cos(\omega_o t)$ the quadrature component $Q(t) = A(t)cos(\phi(t))$ is obtained The signal $y_j(t)$ can then be written as $y_j(t) = I(t) + i * Q(t)$ Thus by digitizing the I(t) and Q(t) signals separately the complete $y_j(t)$ signal is obtained If amplitude demodulation is performed, then only the $A(t)$ signal is digitized The amplitude signal can also be written as $A(t) = \sqrt{I(t)^2 + Q(t)^2}$

A clipped complex signal is obtained if the $I(t)$ and $Q(t)$ are clipped This means that if $I(t)$ is positive the clipped function $I_{clip}(t)$ will be a positive constant, while if $I(t)$ is negative, $I_{clip}(t)$ will be a negative constant The $Q(t)$ signal is also clipped to give $Q_{clip}(t)$ Clipping removes the amplitude signal $A(t)$ from the incoming signal $y_j(t)$

The three common demodulation techniques then are

Complex demodulation

$$y_{complex}(t) = A(t)sin(\phi(t)) + i * A(t)cos(\phi(t)) = I(t) + i * Q(t) \tag{2 12}$$

Complex clipped demodulation

$$y_{clipcomplex}(t) = I_{clip}(t) + i * Q_{clip}(t), \tag{2 13}$$

where

$$I_{clip}(t) = c \quad \text{if } I(t) > 0$$

$$I_{clip}(t) = -c \quad \text{if } I(t) \leq 0$$

$$Q_{clip}(t) = c \quad \text{if } Q(t) > 0$$

$$Q_{clip}(t) = -c \quad \text{if } Q(t) \leq 0, \quad c \text{ some constant}$$

Amplitude demodulation

$$y_{amp}(t) = A(t) \tag{2 14}$$

Amplitude demodulation only needs one digitization channel for each transducer, and the demodulation electronics are simplified The complex and the clipped complex signal need two digitization channels to record the signal for each transducer The clipped complex signal produces a self normalizing signal, thus simple hardware can be used for the correlations

Both the complex demodulation and the amplitude demodulation require high resolution digitizers, to make it possible to record the large dynamic range signals encountered in the oceans Both techniques also need very accurate gain control circuits The clipped complex signal only needs a one bit analog to digital converter since clipping is equivalent to one bit analog to digital conversion Gain control for a clipped signal is non critical since it is self normalizing

3 STATISTICAL PROPERTIES OF THE ACOUSTIC FIELD

In this chapter the statistics of the signal received at a hydrophone after a short pulse signal has been transmitted into the water column is discussed The quadrature components will be seen to have a normal distribution, while the amplitude has a Rayleigh and the phase a uniform distribution The joint probability distribution of two amplitude signals is also derived because it will be required later to calculate the correlation coefficient of two amplitude demodulated signals

3.1 Probability distribution of the scattered field

The scattered acoustic field E_s, will be received on a hydrophone in the form of a voltage V_s, where $V_s \propto E_s$ The proportionality constant will be dependent on the frequency and the hydrophone sensitivity The field E_s can therefore be written in terms of the quadrature components $I_E(t)$ and $Q_E(t)$ of the field, as discussed in chapter two

$$E_s(t) = A(t)\exp(i\phi(t)) = I_E(t) + iQ_E(t) = A_E(t)sin(\phi(t)) + iA_E(t)cos(\phi(t)) \qquad (3\,1)$$

The scatterer field E_s is the sum of the fields of many scattering particles

$$E_s = \sum_{n=1}^{N_p} A_n(t)\exp(i\phi_n(t)) = \sum_{n=1}^{N_p}(I_{En}(t) + iQ_{En}(t)), \qquad (3\,2)$$

where N_p is the number of particles It can be assumed that the contribution of each $I_{En}(t)$ and $Q_{En}(t)$ acts as an independent random variable to the sum in equation 3 2 The central limit theorem states that the probability distribution of the sum of N independent variables approaches a normal distribution as $N \rightarrow \infty$, no matter what the propability distribution happens to be for each individual variable (Davenport and Root 1958) The quadrature fields $I_E(t)$ and $Q_E(t)$ act therefore as normally distributed random variables This means that each independent sample in the times series of $I_E(t)$ and $Q_E(t)$ acts as a sample of a normal distribution

The actual number of independent samples N in a time series is related to the bandwidth B_W of the electronics and the length of the time series T_l by $N = B_W * T_l$ This assumes that the time series is sampled above the Nyquist frequency $f_n = 2 * B_W$ If the time series is sampled below the Nyquist frequency, usable signal information will be lost and less accurate correlations result

3.2 Probability distribution of the amplitude and phase

The distribution of $\phi(t)$ can be assumed to be uniformly distributed over 2π since the phase of each $A_n(t)\exp(i\phi_n(t))$ is random and uniformly distributed over 2π

$$p(\phi) = 1/2\pi, \quad 0 < \phi < 2\pi \tag{3 3}$$

The joint probability distribution function of A and ϕ is $p(A,\phi) = p(A)p(\phi)$ since A and ϕ are independent The probability distribution for the amplitude is found to be the Rayleigh distribution (Ishimaru 1978)

$$p(A) = (A/\sigma^2)exp(-A^2/(2\sigma^2)) \tag{3 4}$$

3.3 The joint amplitude probability density function of two scattered fields

The joint amplitude probability distribution $p(A_1, A_2)$ is required to calculate the correlation between two amplitude demodulated signals A derivation of $p(A_1, A_2)$ given by Ishimaru (1978) is used If the complex received signals are represented by E_1 and E_2 then

$$E_1 = A_1\exp(i\phi_1) = I_1 + iQ_1 \tag{3 5}$$

$$E_2 = A_2\exp(i\phi_2) = I_2 + iQ_2 \tag{3 6}$$

From equations 3 5 and 3 6 the joint amplitude probability function can be written as

$$p(A_1, A_2) = \int_0^{2\pi} d\phi_1 \int_0^{2\pi} d\phi_2 p(A_1, A_2, \phi_1, \phi_2) \tag{3 7}$$

The integral in equation 3 7 can be evaluated (Ishimaru 1978 eq 4-98)

$$p(A_1, A_2) = \frac{A_1 A_2}{\sigma^4(1 - r_o^2)} I_o\left[\frac{A_1 A_2}{\sigma^2(1 - r_o^2)}\right] - \left[\frac{A_1^2 + A_2^2}{2\sigma^2(1 - r_o^2)}\right], \tag{3 8}$$

where I_o is the modified Bessel function of zero order, σ^2 is the variance of the quadrature signals I and Q, and r_o is the magnitude of the normalized correlation function

$$r_o = \frac{|\langle E_1 E_2^* \rangle|}{|\langle |E|^2 \rangle|} \tag{3 9}$$

The symbol $\langle\rangle$ is the expectation operator

4 STATISTICAL PROPERTIES OF THE CORRELATION FUNCTION

In this chapter the statistical behavior of the normalized correlation coefficient r is discussed, which is defined for real time series sample vectors x and y as (Hoel 1954)

$$r = \frac{\langle xy \rangle - \langle x \rangle \langle y \rangle}{\sqrt{\langle x^2 \rangle - \langle x \rangle^2}\sqrt{\langle y^2 \rangle - \langle y \rangle^2}} = \frac{\sum xy - N\overline{x}\overline{y}}{\sqrt{\sum x^2 - N\overline{x}^2}\sqrt{\sum y^2 - N\overline{y}^2}}, \tag{4.1}$$

where N is the number of samples in the summation

If the sample vectors X and Y are complex, then the normalized correlation coefficient can be written as

$$r = \frac{|\langle XY^* \rangle|}{\sqrt{\langle |X|^2 \rangle}\sqrt{\langle |Y|^2 \rangle}} \tag{4.2}$$

To determine the effect of the interpulse interference, the correlation process is split into accuracy of raw signal correlation, effect of noise contamination on the correlation and the effect of demodulation on the correlation

In section 1 a new technique of looking at the accuracy of the complex correlation coefficient as a function of the correlation magnitude is given In the following section the effect of additive white gaussian noise contaminating the correlated time series is discussed In section 3 the effect of amplitude demodulation on the correlation coefficient is shown, while a new derivation of the effect of noise on the clipped complex demodulated correlation coefficient is given in section 4

4.1 The accuracy of the correlation coefficient

For linear correlation the value of the correlation coefficient r may be thought of as one sample in a sequence of samples $r_1, r_2, r_3,$ If the correlation were repeated another value would be obtained in the sequence The question then arises what is the accuracy of each value of the correlation coefficients, for a fixed value of $r_e = \langle r \rangle$?

Unfortunately the distribution of the samples of r is highly non-normal for values of r_e close to one Therefore the standard deviation of the samples r, cannot be used to determine the accuracy of r as an estimate of r_e There exists a change of variable from r to z that can be used to change the distribution of r to an approximately normal distribution (Hoel 1954)

$$z = \frac{1}{2}\log_e \frac{1+r}{1-r} \tag{4 3}$$

z will then be approximately normally distributed with mean μ_z

$$\mu_z = \frac{1}{2}\log_e \frac{1+r_e}{1-r_e} \tag{4 4}$$

The standard deviation of μ_z will be

$$\sigma_z = \frac{1}{\sqrt{N-3}}, \tag{4 5}$$

where N is the number of independent samples as given in section 3 1 Using equations 4 3, 4 4 and 4 5 it is possible to determine the accuracy of the correlation coefficient as a function of the magnitude of the correlation coefficient In figure 4 1 the accuracy of the correlation coefficient is plotted The accuracy is normalized relative to the accuracy at $r_e = 0$, since it is always worst there

There is always zero error in the correlation coefficient if it is one The accuracy of the correlation coefficient drops rapidly as the correlation coefficient decreases from one This shows then that the accuracy of the correlation coefficient is determined by two factors The magnitude of the correlation coefficient and the number of independent samples that were correlated The accuracy is not directly affected by the presence of noise in the signal Random noise can lower the correlation coefficient and thus will decrease accuracy, but noise cannot affect the accuracy alone

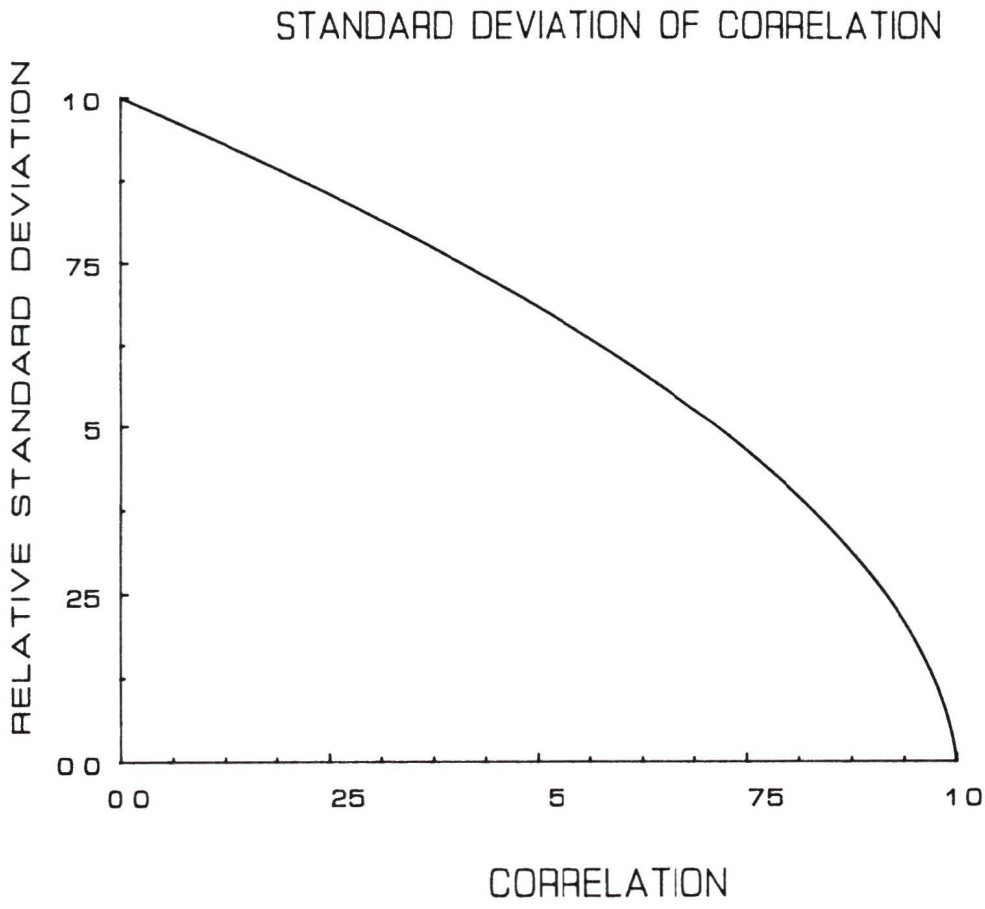

Figure 4.1

Error in the correlation coefficient r as a function of the expected magnitude of correlation r_e, normalized relative to the error at $r_e = 0$

4.2 The correlation coefficient as a function of signal to noise ratio

The correlation coefficient of two complex signals E_1 and E_2 is given by equations 3 9 or 4 2 If the two signals are contaminated with white gaussian noise signals N_1 and N_2 of equal amplitude, then the correlation coefficient can be written as

$$r_o = \frac{|\langle (E_1 + N_1)(E_2 + N_2)^* \rangle|}{|\langle |E + N|^2 \rangle|} \tag{4 6}$$

The numerator is expanded and simplified to be

$$| \langle (E_1 + N_1)(E_2 + N_2)^* \rangle | = | \langle E_1 E_2^* \rangle + \langle E_1 N_2^* \rangle + \langle N_1 E_2^* \rangle + \langle N_1 N_2^* \rangle | = | \langle E_1 E_2^* \rangle |,$$

since the noise and signal are uncorrelated

The denominator can be rewritten as

$$\langle | E + N |^2 \rangle = \langle (I_E + I_N)^2 + (Q_E + Q_N)^2 \rangle$$

$$= \langle {I_E}^2 + 2 I_E I_N + {I_N}^2 + {Q_E}^2 + 2 Q_E Q_N + {Q_N}^2 \rangle = \langle {I_E}^2 + {Q_E}^2 \rangle + \langle {I_N}^2 + {Q_N}^2 \rangle$$

$$= \langle | E |^2 \rangle + \langle | N |^2 \rangle \tag{4 7}$$

The correlation coefficient with noise therefore is

$$r_{on} = \frac{| \langle E_1 E_2^* \rangle |}{\langle | E |^2 \rangle + \langle | N |^2 \rangle} = \frac{| \langle E_1 E_2^* \rangle |}{\langle | E |^2 \rangle} \left[\frac{1}{1 + \frac{\langle |N|^2 \rangle}{\langle |E|^2 \rangle}} \right] = \frac{| \langle E_1 E_2^* \rangle |}{\langle | E |^2 \rangle} \left[\frac{1}{1 + \frac{1}{SNR^2}} \right], \tag{4 8}$$

where SNR is the signal to noise ratio Equation (4 8) shows that the correlation will be reduced as more noise is added and the signal to noise ratio decreases

4.3 The correlation coefficient of two amplitude signals

To calculate the correlation coefficient r_{amp} of two amplitude signals A_1 and A_2, a derivation given by Ishimaru (1978) is used The correlation coefficient of two real signals can be obtained as in equation 4 1

$$r_{amp} = \frac{\langle A_1 A_2 \rangle - \langle A \rangle^2}{\langle A^2 \rangle - \langle A \rangle^2} \tag{4 9}$$

For real amplitude signal returning from a random distribution of scatterers, it is known that

$$\langle A_1 A_2 \rangle = \int_0^\infty \int_0^\infty A_1 A_2 p(A_1, A_2) dA_1 dA_2, \tag{4 10}$$

$$\langle A \rangle = \int_0^\infty A p(A) dA = \sqrt{(\pi/2)\sigma^2}, \tag{4 11}$$

$$\langle A^2 \rangle = \int_0^\infty A^2 p(A) dA = 2\sigma^2, \tag{4 12}$$

where σ^2 is the variance of the complex I and Q signals If probabilty function $p(A_1, A_2)$ given in equation (3 7) is inserted into equation (4 10), the integral for $\langle A_1, A_2 \rangle$ can be expressed in the terms of elliptic integrals (Ishimaru 1978) The series expansion of these integrals can be used to give

$$r_{amp} \approx 0\,915 r_o{}^2 + 0\,058 r_o{}^4 + \tag{4 13}$$

This equation gives the normalized correlation coefficient r_{amp} of two amplitude signals A_1 and A_2 in terms of the normalized cross correlation coefficient r_o of the complex signals E_1 and E_2

4.4 The correlation coefficient of two clipped complex signals

The effect of noise on the correlation coefficient of the clipped complex signal is not given in available literature of the correlation sonar A formula relating the clipped complex autocorrelation function to the complex autocorrelation function of narrow band signals was derived by Lawson and Uhlenbeck (1950) $r_{clip} \approx \mathrm{ARCSIN}(r_o)$ This formula can be adapted to the spatial correlation function of the correlation sonar, but it was found to be inaccurate for the high signal to noise ratios obtained from volume reverberation A new method for the determination of the clipped complex correlation coefficient was therefore developed

To investigate the effect of noise on the clipped complex signal correlation, the effect of noise on the quadrature signals is studied first Since each of the quadrature signals is real, the correlation coefficient can be written as in equation 4 1

$$r = \frac{\langle xy \rangle - \langle x \rangle \langle y \rangle}{\sqrt{\langle x^2 \rangle - \langle x \rangle^2} \sqrt{\langle y^2 \rangle - \langle y \rangle^2}}$$

The correlation using the clipped signals x_{clip} and y_{clip} is self normalizing since $\sqrt{\langle x_{clip}^2 \rangle} = \sqrt{\langle y_{clip}^2 \rangle} = c$, no matter what the amplitude of the signal itself is The

constant c is the amplitude of the clipped signal If the constant c is chosen to be one, then $r_{clip} = \langle x_{clip} y_{clip} \rangle$

If the x and y signals are identical except for the noise they contain, then they can be written as $x = s + n_1$ and $y = s + n_2$, where n_1 and n_2 is additive white gaussian noise and s is the signal

The clipped correlation coefficient can therefore be written as

$$r_{clip} = \langle x_{clip} y_{clip} \rangle = \frac{1}{N_p} \sum x_{clip} y_{clip} = \frac{1}{N} \sum (s + n_1)_{clip} (s + n_2)_{clip},$$

where x_{clip} and y_{clip} represent the inphase or quadrature clipped signals

The correlation coefficient r_{clip} will then be the probability that $(x_{clip} = y_{clip})$ minus the probability that $(x_{clip} \neq y_{clip})$, since if $x_{clip} = y_{clip}$ then $x_{clip} y_{clip} = 1$ and if $x_{clip} \neq y_{clip}$ then $x_{clip} y_{clip} = -1$ As was shown in chapter three both the signal s and the noise n_1 and n_2 act as gaussian random variables Therefore their probability distribution functions will be of the form

$$\mathrm{p}(z) = \frac{1}{\sqrt{2\pi}\sigma_z} \exp\left(\frac{-z^2}{2{\sigma_z}^2}\right) \tag{4 15}$$

To calculate the probability that $x_{clip} \neq y_{clip}$ the probability of making an error p_E in the determination of the sign of x_{clip} or y_{clip} due to noise must be determined In other words the probability that the noise n is the opposite sign of the signal s and greater in magnitude

$$\mathrm{p}_E = \int_{-\infty}^{\infty} \mathrm{p}(s) \int_{-\infty}^{s} \mathrm{p}(n) dn \; ds \tag{4 16}$$

$$\mathrm{p}_E = \int_{-\infty}^{\infty} \frac{1}{\sqrt{2\pi}\sigma_s} \exp\left(\frac{-s^2}{2{\sigma_s}^2}\right) \int_{-\infty}^{s} \frac{1}{\sqrt{2\pi}\sigma_n} \exp\left(\frac{-n^2}{2{\sigma_n}^2}\right) dn \; ds \tag{4 17}$$

Once the probability of making and error p_E is found by evaluating the integral in 4 17, the correlation coefficient can be calculated

$$\begin{aligned} r_{clip} &= \mathrm{p}(x_{clip} = y_{clip}) - \mathrm{p}(x_{clip} \neq y_{clip}) \\ &= (1 - \mathrm{p}_E)^2 + {\mathrm{p}_E}^2 - 2(1 - \mathrm{p}_E)\mathrm{p}_E \end{aligned} \tag{4 18}$$

The problem then remains to evaluate the integral in equation 4 17 An analytic solution is very difficult and therefore a numerical integration technique was used Simpsons rule integration technique (Barrodale, Roberts and Ehle 1978) was chosen because it is both fast and easy to implement By adjusting the step size of the integration routine it is possible to determine the accuracy of the integration The integration is continued until a reduction of the step size by a factor of two results in a integrated value accurate to five decimal places

The above argument was carried through only for a real clipped signal such as the quadrature signals of a complex signal If the real signals are replaced by complex signals in the above argument, and the correlation coefficient of the complex signal (equation 4 2) is used, a similar value of r_{clip} is obtained as in equation 4 18 Equations 4 17 and 4 18 only give the correlation coefficient r_{clip} in terms of the signal to noise ratio $SNR = \sigma_S/\sigma_N$ If a value of the complex correlation coefficient r_o is given for two signals without noise, whose correlation coefficient is less than one, an equivalent signal to noise ratio can be calculated by inverting equation 4 8 and assuming that $|\langle E_1 E_2^* \rangle| / \langle |E|^2 \rangle = 1$

$$SNR_{equiv} = \frac{\sigma_S}{\sigma_N} = \sqrt{\frac{1}{1/r_o - 1}} \tag{4 19}$$

Once SNR_{equiv} is known, equation 4 17 and 4 18 can be solved to give the clipped complex correlation coefficient r_{clip}

Both the signal and the noise are characterized by the value of the variance σ^2 The ratio of σ_S/σ_N can be considered to be the signal to noise ratio The value of r_{clip} can be calculated for a set of values of the signal to noise ratio using equations 4 17 and 4 18 Figure 4 2 shows the correlation coefficient r_{clip} as a function of the signal to noise ratio in db It also shows the correlation coefficient of a complex demodulated signal r_o calculated form equation 4 8 and of a amplitude demodulated signal r_{amp} calculated from r_o using equation 4 13 In figure 4 2 it is assumed that

the two signals which are correlated are made up of the same wave form, except that they are contaminated with different uncorrelated noise With high signal to noise ratios ($SNR \gg 0db$) the correlation coefficient is close to one for all three demodulation techniques

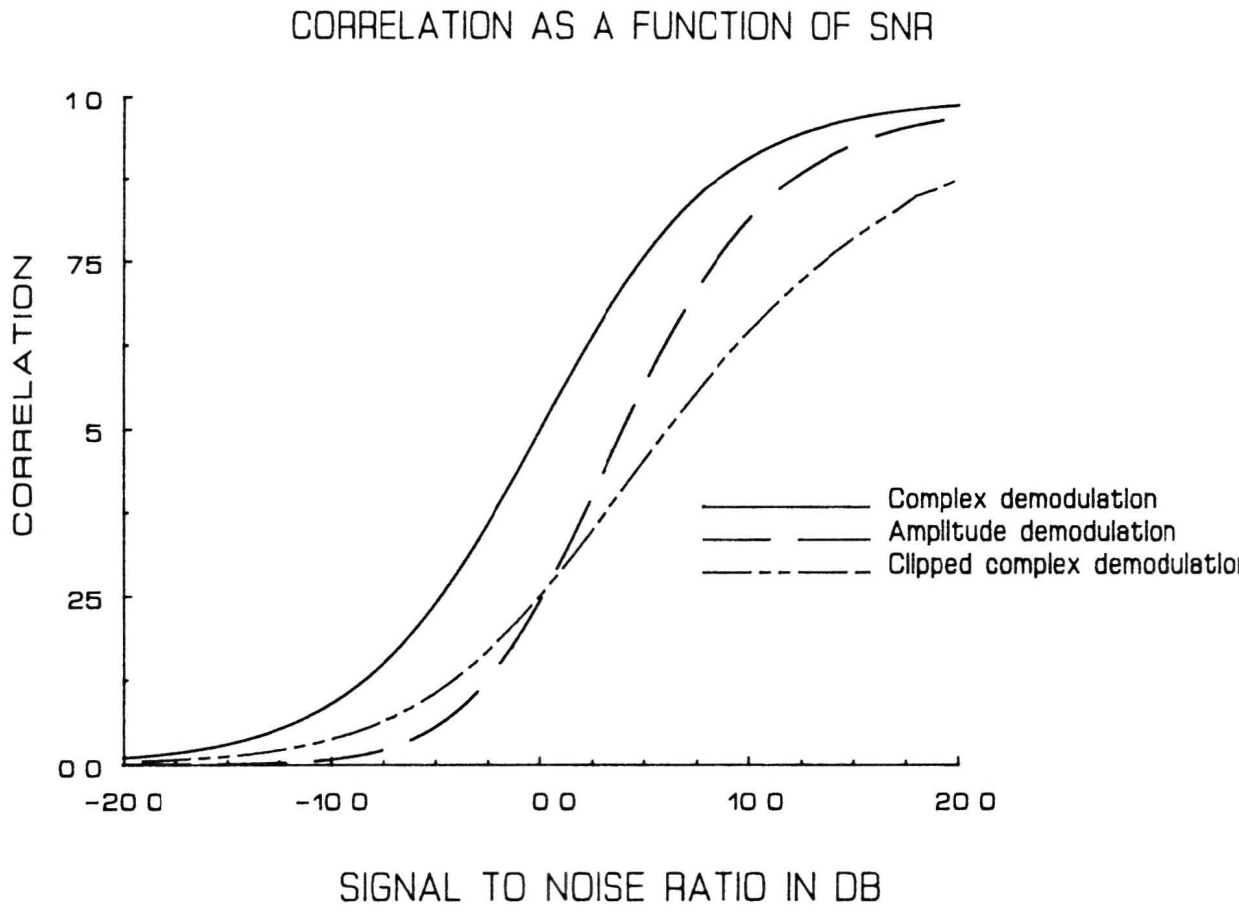

Figure 4.2

Correlation coefficient as a function of signal to noise ratio of two identical signals contaminated with uncorrelated noise for complex, amplitude and clipped complex demodulation

The highest correlations are obtained using the complex demodulated correlation

at a given signal to noise ratio Correlations of an amplitude demodulated signal are greater than correlations of the clipped complex demodulated for signal to noise ratios higher than $0db$, while the situation is reversed for lower signal to noise ratios Since the accuracy to which the location of the peak can be determined depends mainly on the height of the correlation function, amplitude demodulation will perform worse than clipped complex demodulation under high noise conditions

4.5 The effect of noise on the spatial correlation function

The effect of noise on the spatial correlation function has not been discussed in available literature on the correlation sonar, and a detailed new analysis was performed for this thesis The different demodulation techniques discussed above will give different spatial correlation functions By calculating the complex correlation coefficient r_o using equation 2 8 of noise free signals, the amplitude correlation coefficient r_a and the clipped complex correlation coefficient r_{clip} can be calculated The spatial correlation function for these different modulation schemes is plotted in figure 4 3

The correlation functions for all three demodulation techniques have a peak of one Figure 4 3 shows that both the clipped complex and the amplitude demodulation give correlation functions that are narrower than that of the complex demodulated signal To get the highest accuracy of the velocity estimate the actual shape of the correlation function should be used for interpolating the peak location Only the complex demodulated correlation function is gaussian in shape The clipped complex demodulated correlation function has a non continuous slope at zero displacement, while both r_a and r_o are continuous Thus extra care has to be taken when interpolating for the peak position with clipped complex demodulation

The signal returning from the water column will have an effective signal to noise ratio of one due to the interpulse contamination If random gaussian white noise is in-

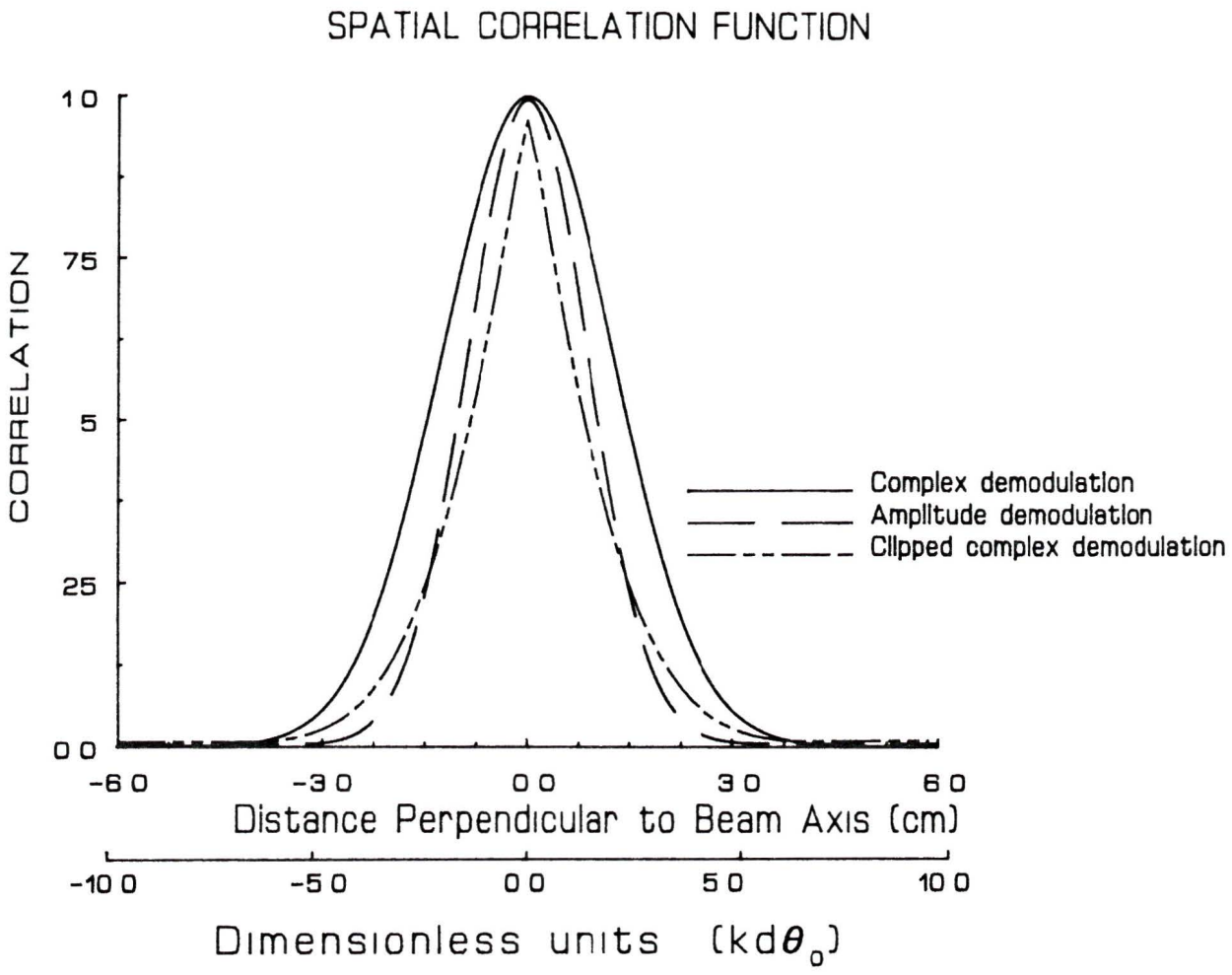

Figure 4.3

Theoretical Bottom return spatial correlation function for complex, amplitude and clipped complex demodulation

troduced into the signal of the correlation functions in figure 4 3, the correlation function of full volume water column return can be simulated The results for the three demodulations techniques are plotted in figure 4 4

The most important feature of figure 4 4 is the decrease of the correlation peak of all three demodulation techniques The peak drops from a value of one to 0 5 for complex demodulation, while it drops to 0 25 for clipped complex demodulation and to

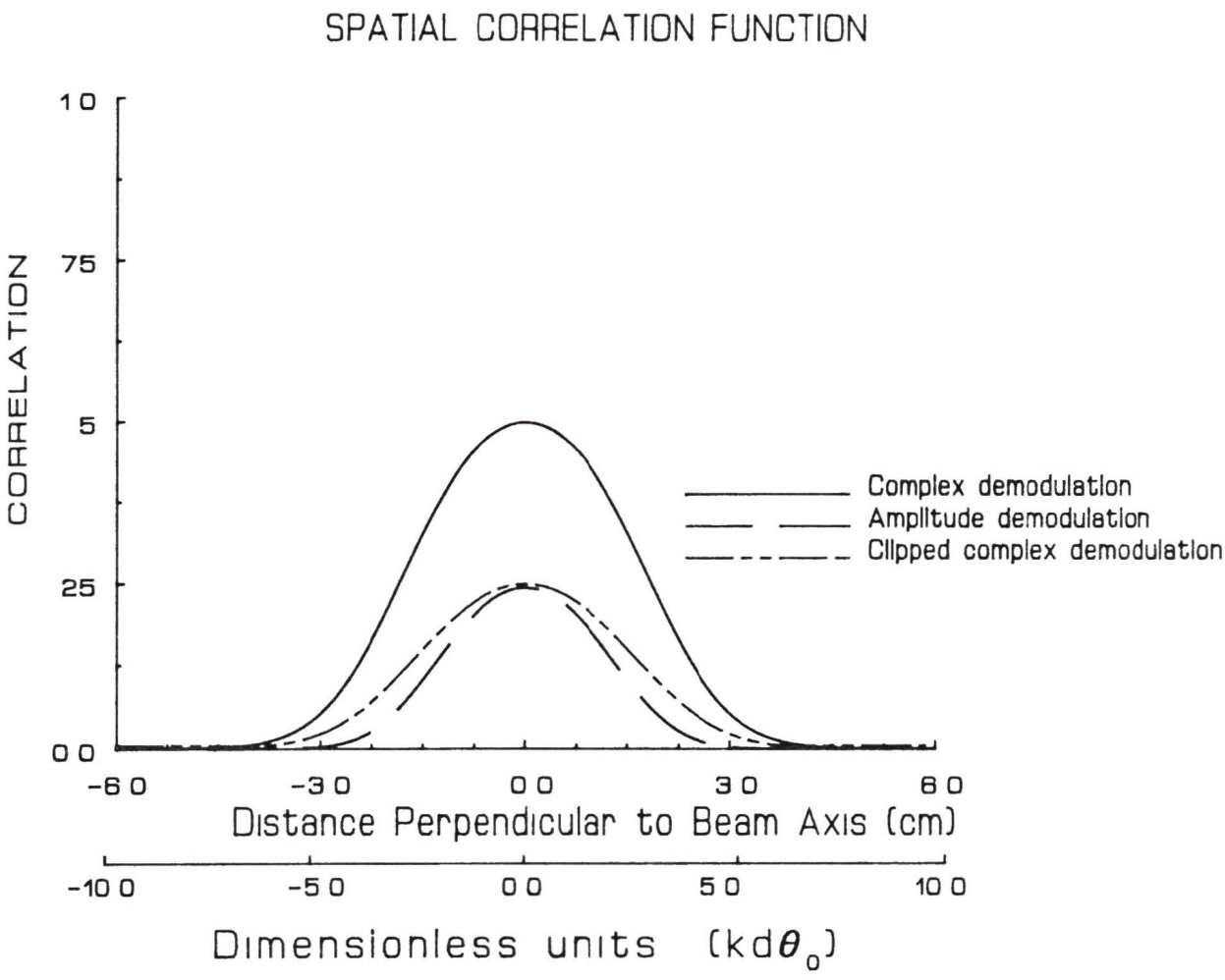

Figure 4.4

Volume scattering return spatial correlation function for complex, amplitude and clipped complex demodulation

0 23 for amplitude demodulation In other words the correlation coefficient for complex demodulation performs better than the correlation coefficient for clipped complex and amplitude demodulation Since the accuracy of the correlation coefficient is independent of the signal to noise ratio and only depends on the actual peak of the correlation function, a lower correlation coefficient will mean a decrease in accuracy This means that not only will the correlation coefficient be lower, but also less accurate

5 IMPLEMENTATIONS OF THE CORRELATION SONAR

5.1 The correlation sonar computer model

A computer model was developed to study the behavior of a two pulse correlation sonar under various operating conditions It is based on a model developed by A D Booth of Autonetics Research Associates (Booth 1985), but includes several modifications and developments Virtually all parameters of the correlation sonar operation in the computer model are adjustable In the model, a transmitting transducer located on the surface of the water illuminates a random distribution of scatterers at a distance d from the surface (figure 5 1)

The scatterers are distributed uniformly inside a water volume of thickness Δz illuminated by the transmitting beam The scatterers move with a velocity $\vec{v}_s$ which is made up of a random velocity component $\vec{v}_r$ superimposed on a velocity common to all scatterers $\vec{v}_c$ Both the random component and the common component are adjustable The model also has a single strong scatterer with an independent velocity vector $\vec{v}_f$ to simulate a large fish or other object moving through the beam The receiving transducers are located on the surface at variable locations They are chosen to be at similar locations as the receiving transducers in the IOS correlation sonar as discussed in the next section for easier data comparison The transmitting and receiving beam shape can also be included in the model

The thickness of the scattering layer is variable By using a thick scattering layer of 30m water volume return can be simulated, while a thickness of 1m can be used to imitate a rough bottom The depth of the scattering layer is adjustable and is usually set to 100m

The frequency of operation of the model was usually set to 100khz, the same frequency used on the IOS correlation sonar The pulse duration and separation is continuously adjustable It is also possible to transmit a different wide band pseudo random noise code for each pulse

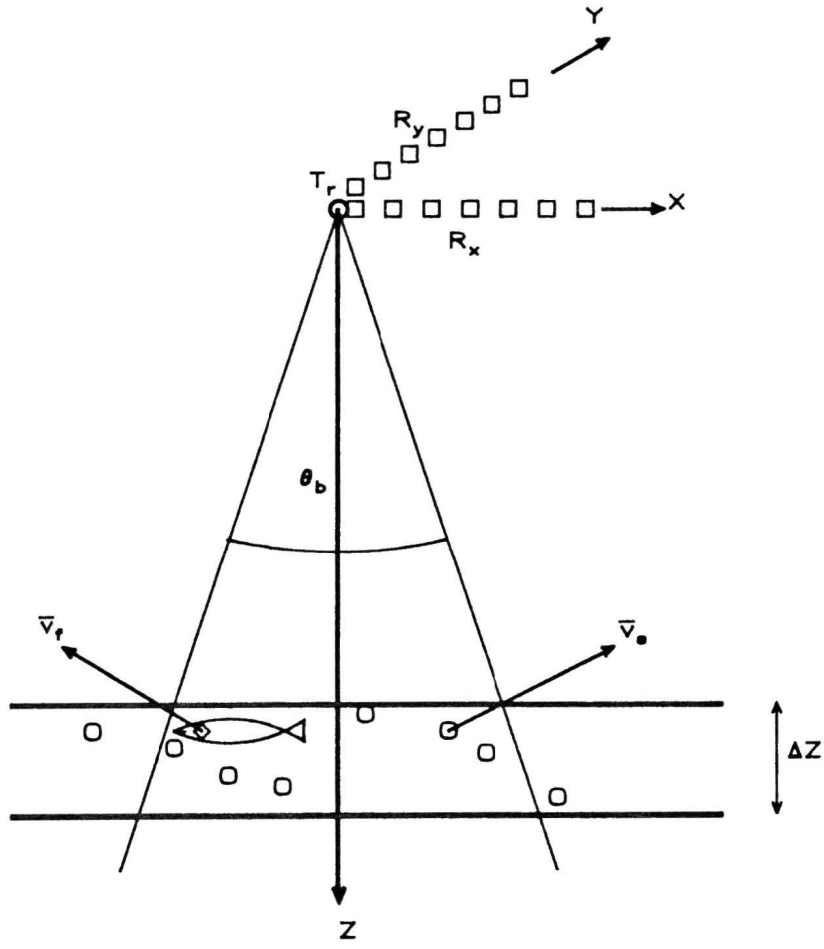

Figure 5.1

Geometry of the correlation sonar computer model A layer of uniformly distributed scatterers with thickness Δz is illuminated with a transducer of beamwidth θ_b A larger object such as a fish can move in a different direction than the scatterers

The signal received on each transducer in the model can be demodulated in several different ways The model stores the received signal in complex demodulated form The model allows gaussian white noise to be added to the complex signal The complex signal can then be amplitude demodulated or clipped complex demodulated The model also includes two new demodulation techniques, not previously discussed in available literature, both of which involve the slope (first difference) of the amplitude signal The first is called the slope demodulation and is the bipolar first difference signal of the amplitude demodulated signal The second is called the one bit slope

demodulation technique and it uses the clipped slope demodulated signal These two uncommon demodulation techniques were included because under some circumstances they were found to give better results than an amplitude demodulated signal by itself

Provisions were made in the model to include depth attenuation, variable scattering strength and Doppler shifts in the reflected signal, but were later removed because they did not affect the correlations appreciably and caused the execution time of the model to increase to a point where simulations using greater than 100 scatterers were impractical

The signal received on each model hydrophone can be written as in equation 3 1

$$y(t) = \sum_{n=1}^{N_p} A_n(t)\exp(i\phi(t)) = \sum_{n=1}^{N_p} A_n(t)\exp(i(\omega t + 2\pi\frac{r_n}{\lambda})),$$

where r_n is the distance from the transmitter to the scatterer and back to the receiver The quantity $i\omega t$ is independent of the scatterer position, and can be removed by looking at the signal in its mixed down (complex demodulated) form

$$y(t) = \sum_{n=1}^{N_p}[A_n(t)\sin(2\pi\frac{r_n}{\lambda}) + iA_n(t)\cos(2\pi\frac{r_n}{\lambda})] \tag{5 1}$$

To calculate $y(t)$ on the computer, the phase term $(2\pi\frac{r_n}{\lambda})$ is determined for each scatterer

The output data from the model is sent to the correlation program, which performs the cross correlations between the signals from all the transducer elements, determines the correlation peak and calculates the velocity from the peak location The accuracy in the correlation value of a single transmission is not high enough to determine even the approximate peak location, and therefore the correlations from more than one transmission must be averaged together before the peak is calculated Graphs of the model output can be generated at almost any stage of processing the raw signal, the demodulated signal, the correlation values for a single transmission, the correlation values for averaged transmissions and the velocity profiles can be plotted

5.2 The IOS correlation sonar hardware

The design purpose of the IOS correlation sonar was the the investigation of the correlation sonar principle for ice movement monitoring in the arctic A ship mounted system was developed to track the ocean bottom which has similar characteristics to a ice surface The ship mounted system was used to collect some data of volume return to compare to the theoretical and model results

The signals received on hydrophones from volume or deep bottom reverberation can be very small, so it is necessary to have preamplifiers mounted close to the hydrophones, to minimize noise Since the IOS correlation sonar is a prototype, it was necessary to design a system that had the data acquisition and computer electronics in the ship's laboratory area for easy servicing and modifications

The system has a transducer assembly with hydrophones mounted on a steel and aluminum frame, which can be extended below the ship's hull Preamplifiers in the transducer housing are used to amplify the signal to a level that allows the transmission of the analog signals to the data acquisition electronics in the laboratory area, without introducing any major noise components Figure 5 2 shows a typical setup of the IOS correlation sonar transducer as it was deployed on the research vessel *VECTOR* Two banks of seven receiving hydrophones are arranged perpendicular to each other A 22 degree beam ROSS transducer is mounted in the corner formed by the two transducer banks for transmitting a signal into the water

The layout of the transducer assembly can be seen in figure 5 3 Each receiving hydrophone is a ceramic element $1cm$ by $2cm$ Each seven element transducer bank is constructed so that the inner five elements have a spacing of $1\ 5cm$ and the outer two elements a spacing of $6cm$ This was done to be able to use the elements with $6cm$ spacing for high water or ship velocities, for which the correlation peak shifts more than one transducer spacing, while the spacing of $1\ 5cm$ was to be used for lower velocities

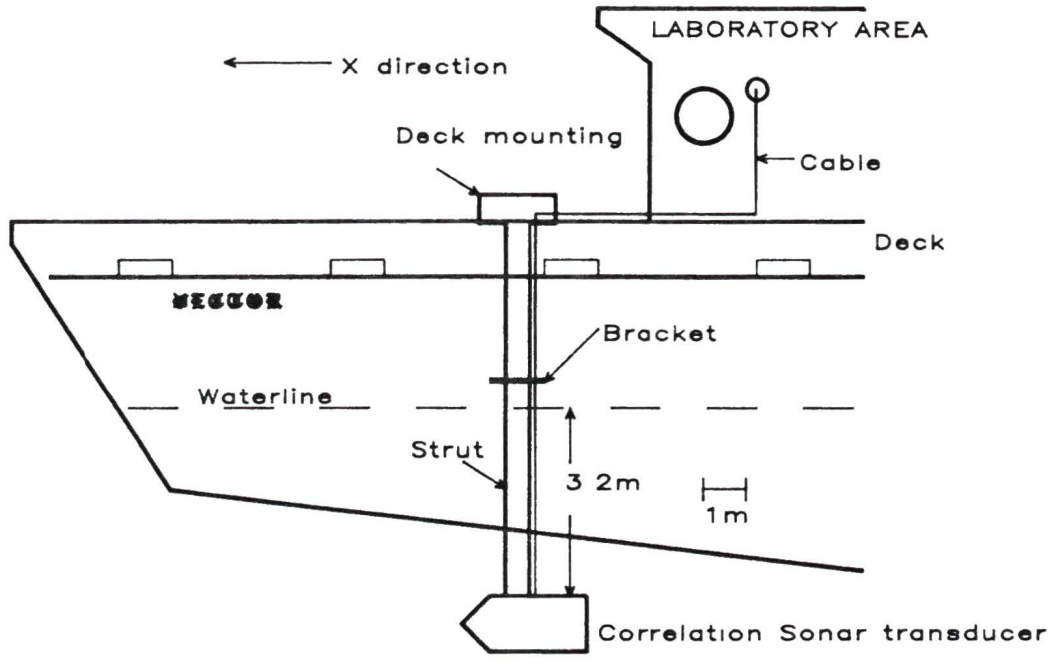

Figure 5.2

The mounting position of the correlation sonar when deployed on the research vessel *VECTOR*

The slightly amplified raw signal from the transducer assembly is sent by balanced pair shielded cables to the deck unit where the data acquisition system is located Each of the fourteen signals is applied to a variable gain amplifier, amplitude demodulated, low pass filtered, passed to a sample and hold circuit and applied to a sixteen channel to one channel analog multiplexer Each of the sixteen channels is sampled by an analog to digital converter at 40kHz to eight bit accuracy A STD bus microcomputer system controls the storage of the sampled data in memory, keys the transmitter and sets the receiving gain The sampled data can then be written to either 9-Track magnetic tape or 8-inch floppy disks

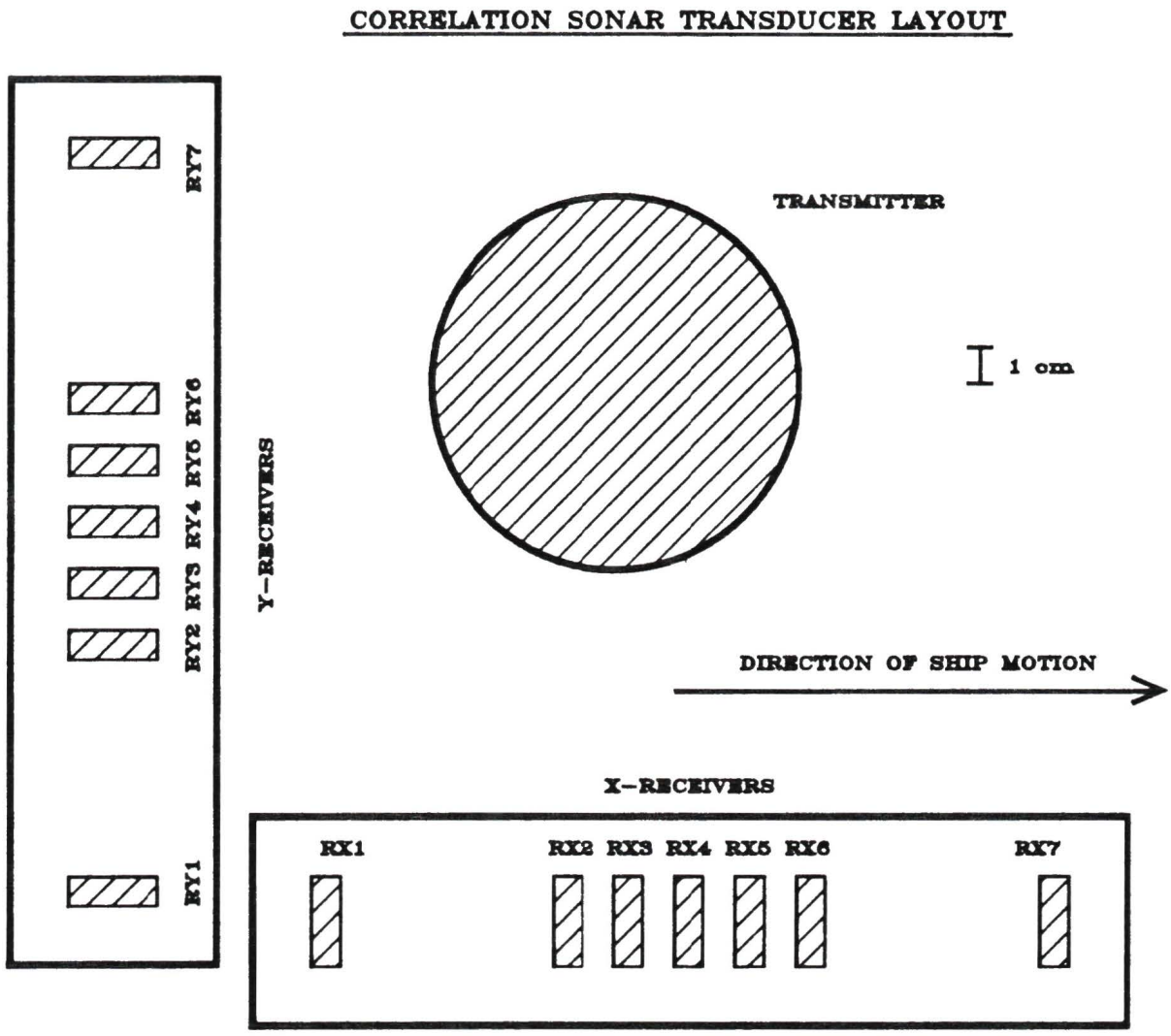

Figure 5.3

Layout of the IOS correlation sonar receiving and transmitting transducers

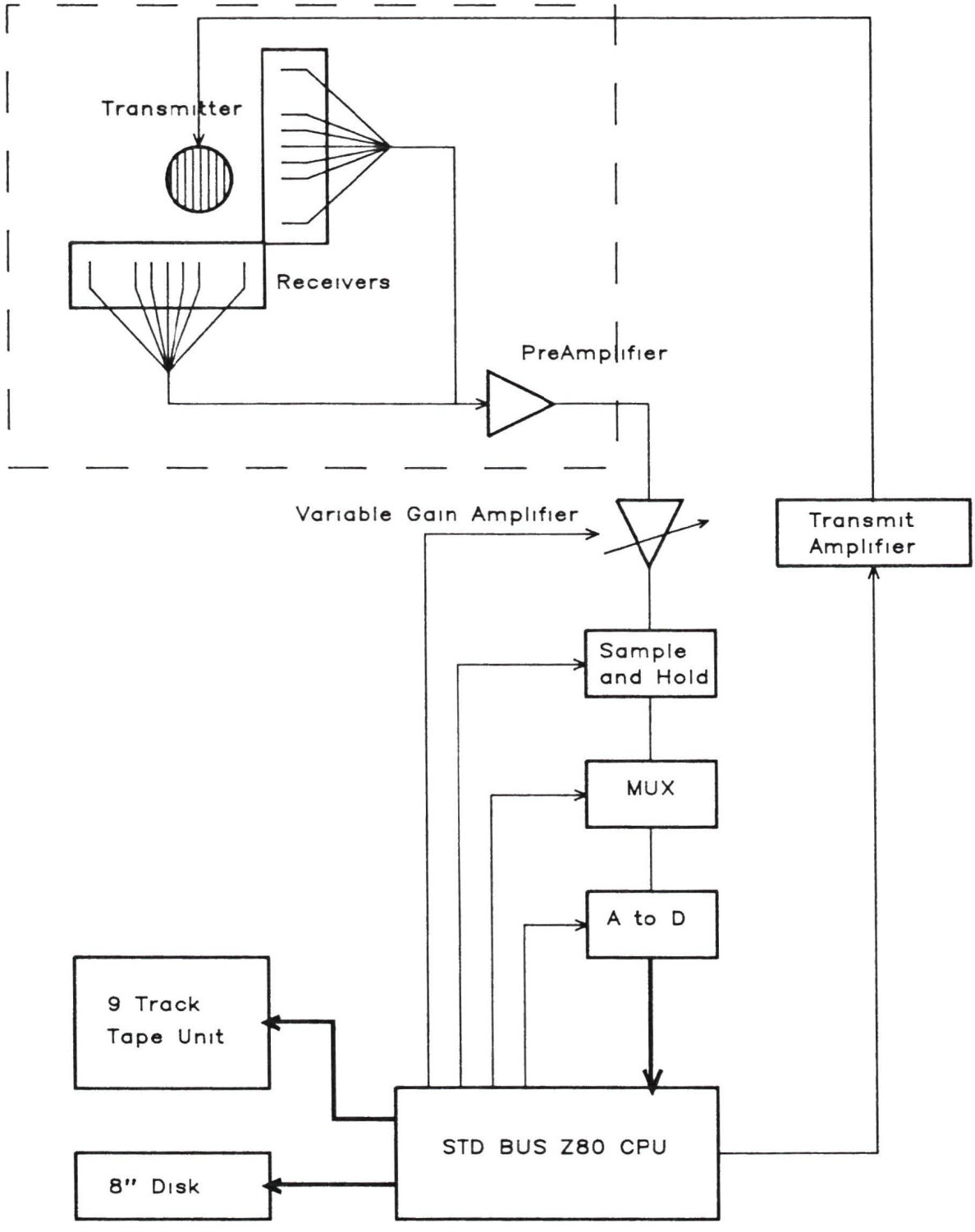

Figure 5.4

Block diagram of the IOS correlation sonar electronics

The use of the data stored on the 9-Track tape drive allowed the processing of the data on the HP1000 computer at IOS Figure 5 4 shows a block diagram of the IOS correlation sonar data acquisition and processing electronics

5.2 Operational parameters of the IOS correlation sonar

The operational frequency of the correlation sonar was chosen to be 100kHz This frequency is a compromise between transducer size, attenuation, scatterer reflectivity, and the width of the spatial correlation function The transmitting transducer beamwidth is 22 degrees according to the specifications provided with the transducer

At a transmit frequency of 100kHz and beamwidth of 22 degrees, the correlation function width can be calculated to be approximately $4cm$ This is the reason why a transducer spacing of $1\,5cm$ was chosen It allows the sampling of the correlation function with at least 3 points across the peak to facilitate the use of interpolation algorithms to find the exact peak location The memory of the data acquisition system was able to store a maximum of 48000 samples With a $40kHz$ sampling rate on 16 channels this allows the storage of only $0\,075sec$ worth of data During this time the data from approximately 56m water column can be received The water column is therefore broken up into 50m bins Using the maximum data transfer rate of the 9-track tape, it is possible to collect one bin worth of data every $1\,4sec$ and write it to tape To make it possible to average data from many transmissions together, data are usually collected for just one bin at one time

The pulse length and repetition rate are both adjustable from a minimum of $100\mu sec$ to $100msec$ or greater The pulse length always has to be less than the pulse separation, otherwise overlapping of the two pulses occurs and the two pulses merge into one longer pulse If the pulse length is too short, not enough energy is transferred into the water column resulting in poor signal to noise ratios The pulse separation

Operating frequency	100kHz
Signal demodulation type	Amplitude demodulation
Receive transducer spacing	1 5cm
Transmit beam width (3db down points)	22degrees
Transmitted pulse duration	variable (2msec typical)
Transmitted pulse separation	variable (12 8msec typical)
Channel sampling rate	40kHz
Digitization accuracy	8 bits
Total data rate	640000 samples per second
Maximum data storage per transmission	48000 8 bit samples
Length of sampled water column	50m
Acoustic transmit power	0 to 1000 watts
Maximum measurable speed -theoretical	12 m/sec
Maximum measurable speed -practical	2 m/sec

Table 5.1

IOS correlation sonar operational parameters

has to be short enough to obtain a correlation peak that is still on the array, while the pulses have to be far enough apart to give accurate velocity measurement The operational parameters of the IOS correlation sonar are summarized in table 5 1

5.4 Observational technique

The IOS correlation sonar was installed on the Department of Fisheries and Oceans research vessel *VECTOR* on June 3 1985, for operational tests under a variety of con-

ditions Data were collected near the Navy Buoy in Saanich inlet near the Institute of Ocean Sciences from June 3 1985 to June 6 1985 (figure 5 5) The protected waters of Saanich inlet have low velocities and high scatterer densities, making them ideal for the evaluation of the operation of the correlation sonar A Navy Buoy near Pat Bay provided a convenient anchor point for zero velocity tests of the correlation sonar

A 120KHz echo sounder was installed to obtain echo sounder images of the scatterers The output from the echo sounder was recorded on video cassette tape using a PCM encoder and graphical output was obtained using a EPC chart recorder The echo sounder was installed on June 5, the third day of taking correlation sonar data It was usually only turned on temporarily because the 120kHz transmitter pulse interfered with the correlation sonar return echoes

The control processor first entered into a calibration mode to collect data with the correlation sonar In this mode no data was logged or correlated, but the two pulses were sent out An oscilloscope connected to the preamplifier outputs was used to check for the correct signal level of each channel The gain for each channel was then changed to use the maximum dynamic range of the analog to digital converter without clipping the signal The number of the 50m bin in which data should be taken was also determined at this point For example if the bottom was at a depth of 210m, to obtain a bottom velocity estimate the bin number was set to 5, for a range of 200m to 250m If volume correlation was required at a depth of 130m, the bin number would be set to 3 for a range of 100m to 150m

After the calibration was complete and the correct bin number was set, data acquisition mode was entered In this mode the control processor would wait for a signal from the operator to start collecting data At the signal, the control processor would start to send out the pulses and collect data from the correct bin The data from a single pulse pair would then be written to nine track magnetic tape for later analysis At the maximum data rate of the tape drive, one profile of one bin could be logged

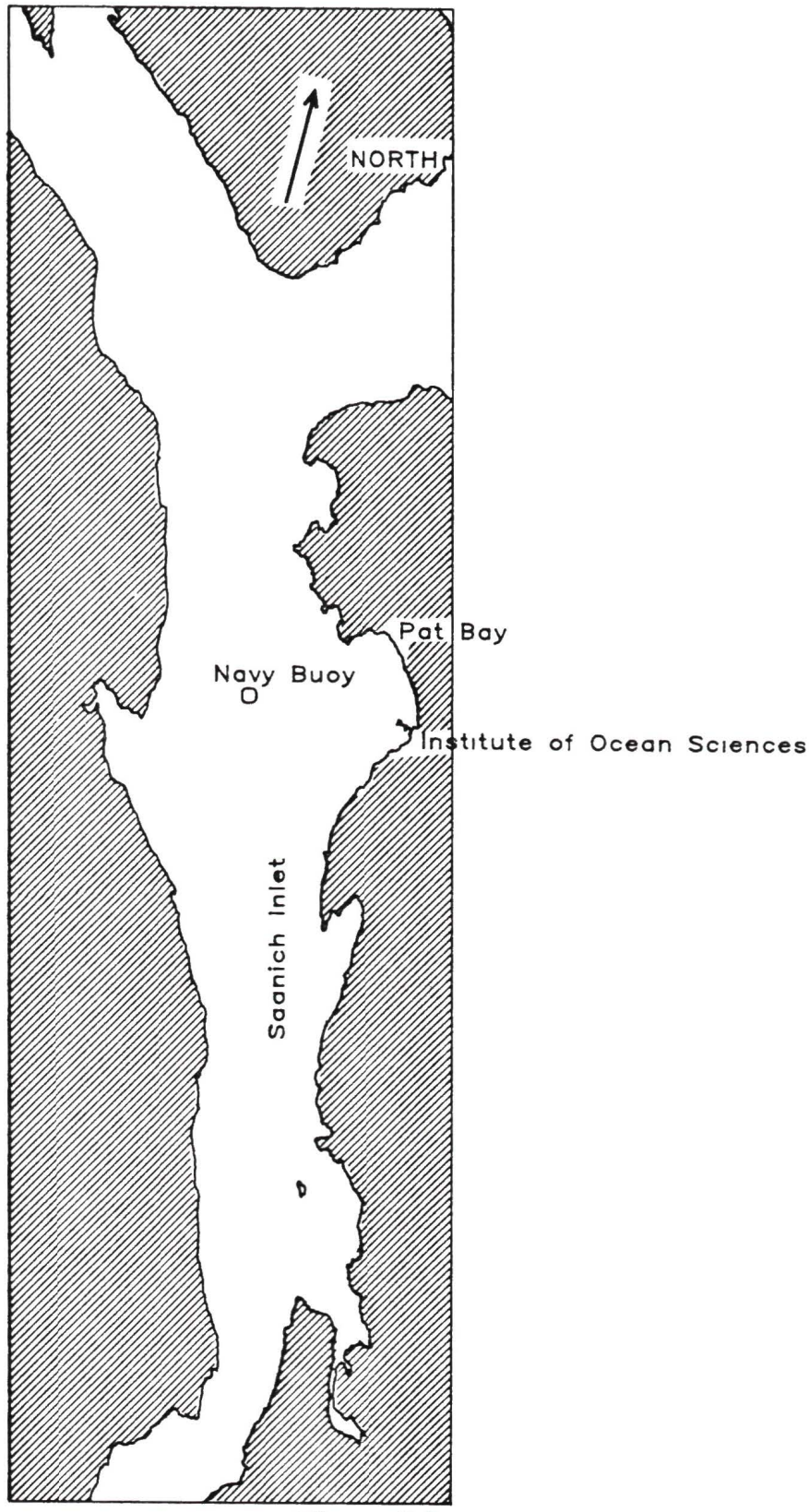

Figure 5.5

The area where data was collected with the IOS correlation sonar

every 1 4 seconds The system then logged data for 25 transmissions, before entering another wait mode The control processor would then wait once more for instructions from the operator, to take more data

In the calibration mode the control processor could also be instructed to send out pseudo random noise modulated pulses

6 THE SPREAD SPECTRUM PULSE CORRELATION SONAR

The accuracy of the correlation sonar as a current measuring device, as opposed to a device measuring speed over the ocean floor, depends to a large extend on the height of the peak of the correlation function For uniform water column return signal the two pulses which are present in the water at the same time will interfere with each other, producing a signal to noise ratio that usually is never greater than one The low signal to noise ratio will lower the height of the peak of the correlation function If it were possible to separate the pulses by labeling them in some way, the signal to noise ratio would be increased In this chapter one particular possibility of labeling the pulses, binary pseudo random noise codes, is examined A new analysis of predicting the effect of pseudo random codes on the resulting received signal is given, which is followed by a discussion and analysis of some common pseudo random noise codes

6.1 The effect of pseudo random noise codes on the acoustic signal

If a signal $s(t)$ is sent into the water column, the signal received $y_r(\vec{r},t)$ can be described as the convolution of the impulse response $h(\vec{r},t)$ with the transmitted signal $s(t)$

$$y_r(\vec{r},t) = h(\vec{r},t) \star s(t), \tag{6 1}$$

where $\vec{r}$ is the point in space where the signal is received and $\star$ represents convolution

$$f(t) \star g(t) = \int_{-\infty}^{\infty} f(\tau) g(t-\tau) d\tau \tag{6 2}$$

If the reception point is fixed in space then the received signal can be written as

$$y_r(t) = h(t) \star s(t) \tag{6 3}$$

To remove the effect of the type of signal $s(t)$ that was sent into the water column, a matched filter must be applied to the received signal It can be shown (Ziemer

and Peterson 1985) that the optimum receive filter has an impulse response that is the time inverse of the outgoing signal $s(t)$ Optimum filtering is equivalent to correlating the transmitted signal $s(t)$ with the received signal $y_r(t)$ The received filtered signal can therefore be written as

$$y_s(t) = s(t) \times y_r(t) = s(t) \times [h(t) \star s(t)] \tag{6 4}$$

Here $\times$ represents correlation in time

$$f(t) \times g(t) = \int_{-\infty}^{\infty} f(\tau) g(t+\tau) d\tau \tag{6 5}$$

Using the integrals in equations 6 2 and 6 5, equation 6 4 can be rewritten as

$$y_s(t) = h(t) \star [s(t) \times s(t)] \tag{6 6}$$

Thus the filtered signal can be viewed as the impulse response of the water column $h(t)$ convolved with the autocorrelation of the transmitted signal $s(t)$ If a signal $s_1(t)$ is transmitted and a signal $s_2(t)$ is used for filtering the received filtered signal will be

$$y_d(t) = h(t) \star [s_1(t) \times s_2(t)] \tag{6 7}$$

If it is possible to find two pseudo random noise codes such that the cross correlation is

$$s_1(t) \times s_2(t) = 0, \tag{6 8}$$

and the autocorrelation is

$$s_1(t) \times s_1(t) = s_2(t) \times s_2(t) = \delta(t), \tag{6 9),}$$

then the signal $s_1(t)$ could be sent for the first pulse and $s_2(t)$ for the second pulse A matched filter for each code would then give totally separate return echoes for the two pulses $\delta(t)$ is the Dirac delta function

$$\begin{aligned} \delta(t) &= 0 \qquad t \neq 0 \\ \delta(0) &= \infty \\ \int_a^b \delta(t) dt &= 1 \text{ if } a < 0 < b \end{aligned} \tag{6 10}$$

If these perfect conditions could be achieved with a pseudo random code, then $y_s(t) = h(t) \star \delta(t) = h(t)$ Unfortunately no pseudo random codes with both of the properties of equations 6 8 and 6 9 exist At best only approximations to the two properties can be achieved

The code is applied to the outgoing signal by mixing a carrier of type $\exp(\imath w_o t)$ with the code $u(t)$

$$s(t) = u(t)\exp(\imath w_o t), \tag{6 11}$$

where $u(t)$ alternates between 1 and -1 for 180 degree phase modulation and between 1 and 0 for amplitude modulation The minimum length over which $u(t)$ is not allowed to change is called the bit length

$$\begin{aligned} u(t) &= 0 \qquad t < 0 \quad \text{and} \quad t > k * T_b \\ &= +1 \text{ or } -1 \qquad 0 \leq t \leq k * T_b, \end{aligned} \tag{6 12}$$

where T_b is the bit length and k is the number of bits in the sequence

In the above discussion the actual demodulation and filtering process was not mentioned In practice the incoming signal is quadrature demodulated by mixing it with an in-phase and quadrature carrier, as discussed in section 2 6 Each of the quadrature channels is then correlated separately with the same pseudo random code that was transmitted This results in the filtered and demodulated complex quadrature signal If amplitude demodulation is desired, it can be obtained from the complex quadrature signal

If amplitude demodulation is used on the raw signal the proper decorrelated signal can no longer be recovered Amplitude demodulation is a nonlinear operation while correlation and convolution are linear Therefore equation 6 4 does not apply and it is not possible to recover the proper filtered amplitude demodulated signal If a single scatterer is present in the water column, then amplitude demodulation and correlation can be used, but as soon as more than one scatterer is present interference between

the two scatterers will change the received amplitude signal to such an extent that correlations will no longer yield the proper filtered signal

This effect can be visualized by reflecting a pseudo random sequence signal off the bottom If the bottom is quite smooth and the beam is narrow, the impulse response function will be close to a delta function, and proper correlation filtering of the received signal can be achieved using amplitude demodulation As the thickness of the bottom increases (ie the roughness increases) to a value greater than the length of one bit in the pseudo random code $T_b c$, the correlation filtered amplitude return signal will no longer represent the wanted signal, which would be obtained by quadrature demodulation, correlating and then recovering the amplitude signal It can therefore be concluded that amplitude demodulation should not be used with a pseudo random sequence signal returning from volume reverberation of the water column

6.2 Properties of some pseudo random codes

In this section, the theories developed in the previous section are applied to some common pseudo random codes A new look is given at the effect of pseudo random noise codes on the signal returning from volume return

A family of pseudo random noise codes, that have very low noise sidelobes, are the Barker codes For example the five bit Barker code (Farley 1982) $+++-+$ has the autocorrelation 0 0 0 1 0 1 0 5 0 1 0 1 0 0 0 A phase modulation of 180 degrees has to be used with this code since it alternates between +1 and −1 If the code were perfect only the 5 would be present in the above autocorrelation The non zero values on either side of the peak are called the noise sidelobes of the code If there is only one scatterer present in the water column, such as a fish, then the impulse response of this scatterer will then be $h(t) = \delta(t - r_o/c)$, where r_o is the range of the scatterer The impulse response $h(t)$ is correlated with the autocorrelation

function of the code to find the received and filtered signal The resulting signal will consist of the peak of 5 at the range of interest and the sidelobes of 1 at ranges just before and after the range of interest In this case the worst case signal to noise ratio can be written as

$$SNR = \sqrt{\frac{\text{mainlobe}^2}{(\text{largest sidelobe})^2}}$$

For the five bit Barker code this works out to a peak signal to noise ratio of SNR=5

If the code is sent into a uniform scattering layer, whose impulse response $h(t)$ is effectively constant $h(t) \approx c$, data will be received not only from the main peak of height 5 but also from the sidelobes of height 1 at the same range gate This occurs because a constant $h(t) = c$ is now correlated with the autocorrelation function of the code The signal to noise ratio in this case will be

$$SNR = \sqrt{\frac{\text{mainlobe}^2}{\sum \text{sidelobe}^2}}$$

This equation yields a value of the signal to noise ratio of 2 5, for the five bit Barker code, assuming there is no system noise present Thus the signal to noise ratio for a uniform layer is much less than that for a single scatterer if a pseudo random code is used in the transmission

A family of codes with zero time sidelobes are the complementary codes whose properties were first discussed by Golay (Golay 1961) This type of code is used extensively in atmospheric Doppler radars for pulse compression and improving the signal to noise ratio (Woodman 1980) The two complementary codes have the property that their noise side lobes are exactly opposite in sign and magnitude This means that if the autocorrelation of two complementary codes is added together, a true delta function combined autocorrelation will be obtained When using complementary codes, first one code is sent into the medium, such as the atmosphere, and a complex signal time series is obtained after correlating with the code Next the matching complementary code is transmitted into the scatterer medium, received and decoded into a complex

time series If the two time series from the two complementary codes are added together a single time series results that theoretically only contains signal and no sidelobe noise

Only one code can be present in the scattering medium at the same time to be able to use complementary codes properly This implies that after transmitting one code the complementary code cannot be transmitted until the echoes from the first code have disappeared In the ocean environment this time is of order of magnitude one second or longer due to the slow propagation velocity of a sound wave, while in the atmosphere it is of order of magnitude 2 msec or less, due to the propagation of the microwave radiation at the speed of light A combined correlation function with zero noise sidelobes can only be achieved if the two codes scatter off virtually identical scatterer distributions In the ocean environment the scatterer distributions change drastically relative to the transducer in one second, especially if they are moving, while the high repetition rate of 500hz of the atmospheric radar causes the scatterer distribution to stay almost constant between two transmissions Complementary codes can therefore not be used in the ocean environment for volume backscatter return

The use of a pseudo random sequences is considered for the purpose of separating the two pulses simultaneously present in the water, and to improve the system signal to noise ratio If two pseudo random codes are in the water at the same time, their cross correlations should be zero, so that they will not interfere with each other as in equation 6 8 Unfortunately codes with zero cross correlation do not exist The goal is therefore to find two codes with the minimum cross correlation possible, while at the same time each code has the smallest possible sidelobes Barker codes have the smallest possible sidelobe levels of a single code, but unfortunately there are no Barker codes longer than 13 bits and the cross correlation between two Barker codes is large Complementary codes cannot be used because there exist no two pairs of complementary codes whose cross correlation is zero

A large class of codes called maximal linear sequences or cyclic codes can be generated easily and have well known properties (Ziemer and Peterson 1985) They have the unique property that if the code is repeated indefinitely, the autocorrelation has a peak of N when the codes are aligned and a value of -1 when they are not (figure 6 1) They can be easily generated by a n bit shift register, where $N = 2^n - 1$ is the length of the code

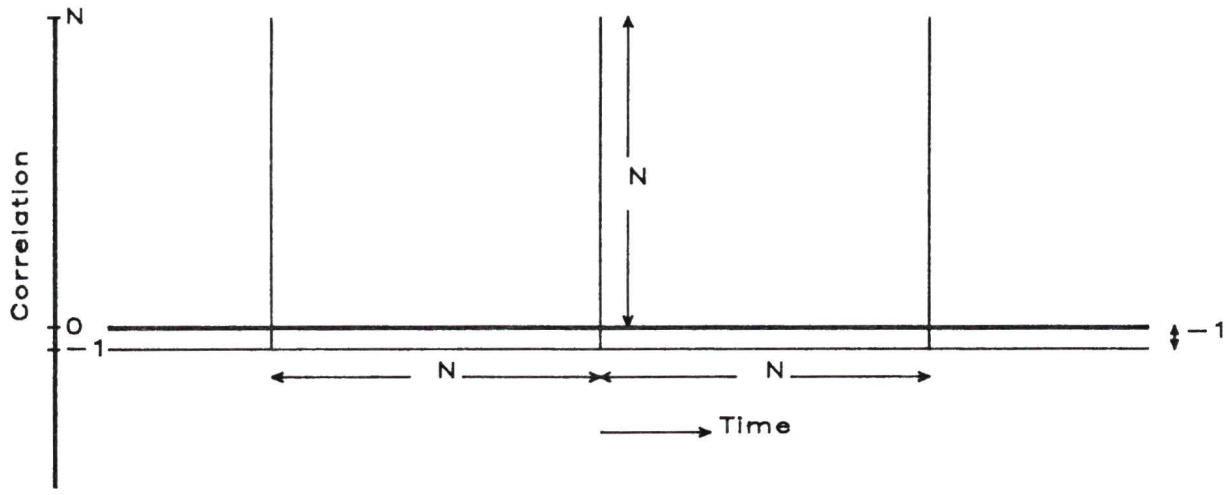

Figure 6.1

The autocorrelation function of a repeated maximal linear sequence The peak of height N repeats every N times the bit length The noise sidelobes have a constant value of -1

For pulse labeling the code is not repeated, and the autocorrelation in this case will consist of a peak of height N and noise side lobes which do not exceed $\sqrt{N}$ as shown in figure 6 2

For a 127 bit code, the signal to noise ratio of the code will be approximately 1 8, if the code is used for full volume return If care is taken when selecting the codes, the cross correlation between two maximal linear sequences will not exceed $\sqrt{N}$ If two

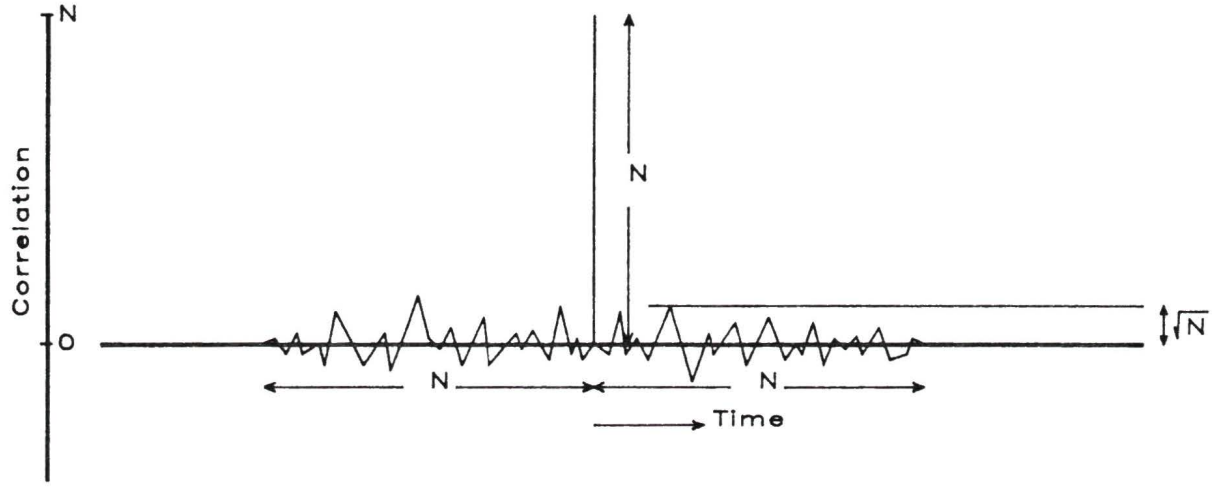

Figure 6.2

The autocorrelation of a maximal linear sequence of length N bits The peak of the autocorrelation function is of height N and the maximum noise sidelobe level is $\sqrt{N}$

127 bit codes are present in the water at the same time the signal to noise ratio, due to the codes alone, will be approximately 1 4 The signal to noise ratio due to two simple pulses in the water column at the same time is approximately 1 for uniform volume return, thus the improvement of using the pseudo random code is minimal

As an example the computer model of the correlation sonar was used to produce a 12m layer return signal for a single 127bit maximal linear sequence with a bitlength of 100μsec The return signal was complex demodulated and correlated with the code that was sent out The amplitude of the resulting complex signal is plotted in figure 6 3 The model was also run for the same layer, a single pulse being transmitted with a length of 100μsec The resulting amplitude demodulated signal can be seen in figure 6 4

In both figures 6 3 and 6 4 the 12m scattering layer can be clearly identified between 0 and 15m If a perfect code was used with zero noise sidelobes, then figures

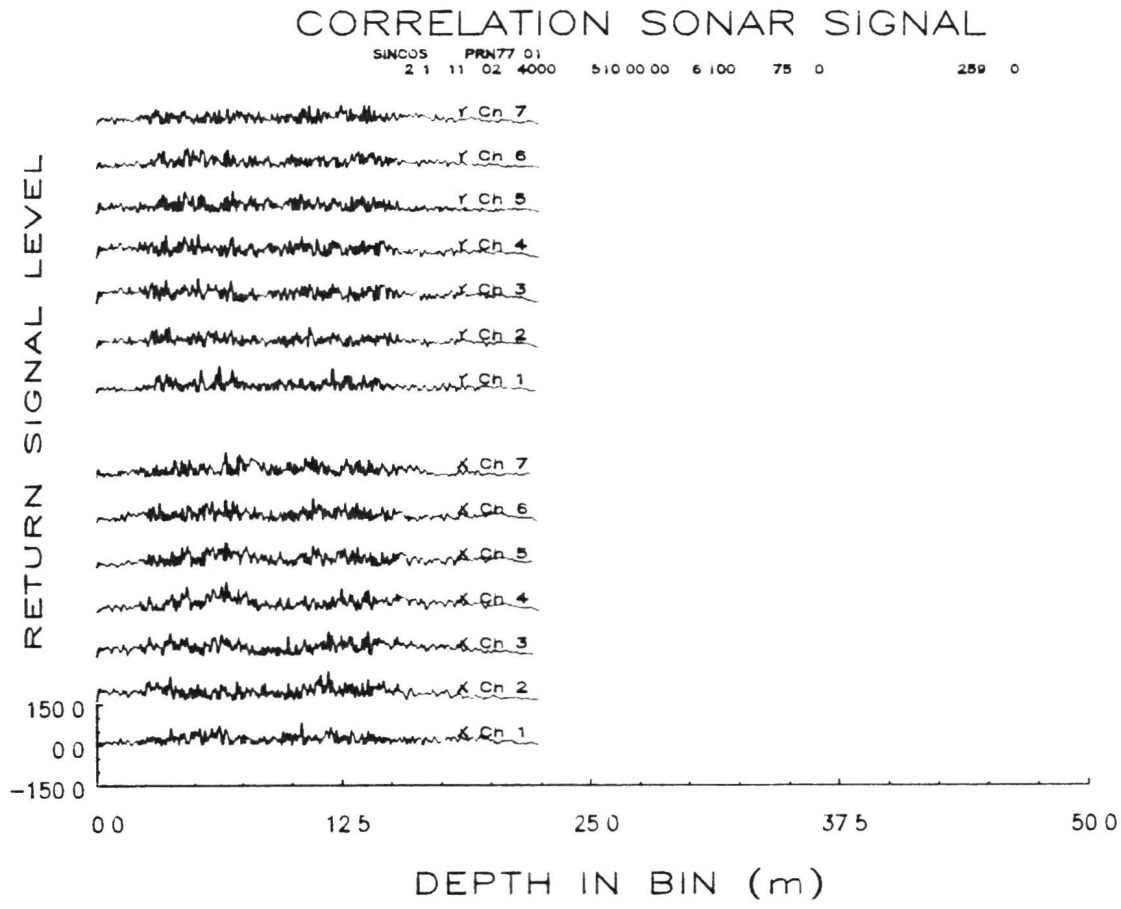

Figure 6.3

The amplitude of the correlated return signal of a 127 bit maximal linear sequence scattered off a 12m layer, generated by the computer model The bitlength was 100μsec The layer is located at a depth of 100m and the time series covers a depth from 100m to 150m The two groups of seven channels plotted correspond to the signals received by the seven hydrophones in the x and y directions

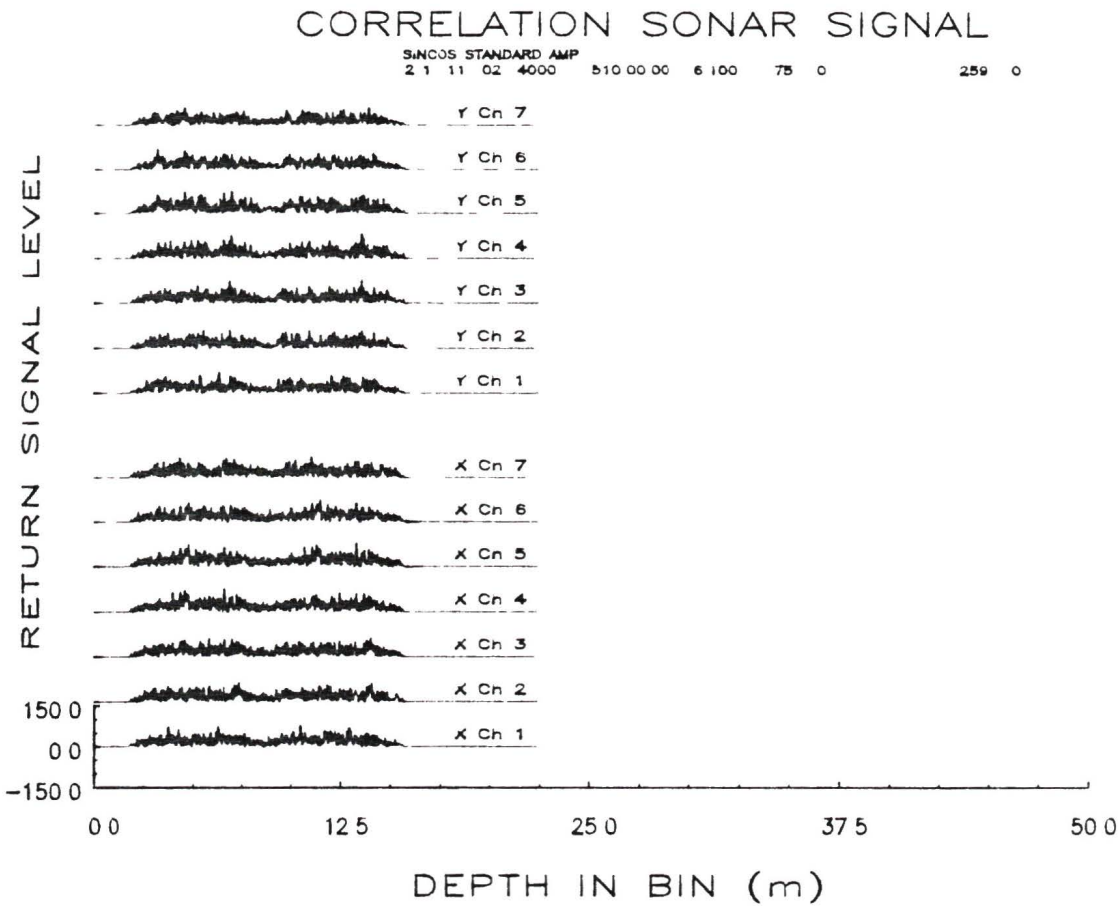

Figure 6.4

The amplitude return signal of a 100μsec pulse scattered off a 12m thick scattering layer, generated by the computer model The bitlength was 100μsec The layer is located at a depth of 100m and the time series covers a depth from 100m to 150m The two groups of seven channels plotted correspond to the signals received by the seven hydrophones in the x and y directions

6 3 and 6 4 should be identical Similarities between the signal recovered over the 12m layer can be observed, but the effect of the noise sidelobes of the maximal linear sequence can be seen at the edges of the 12m layer in figure 6 3 between a depth of 13m and 18m Any energy present at this depth is caused by the sidelobes and can be considered noise This noise is also present in the 12m layer From figure 6 3 the signal to noise ratio can be found to be approximately 2, which agrees with the value of 1 8 predicted for this type of code The raw complex demodulated signal used to obtain figure 6 3 was also amplitude demodulated before the inverse correlation filter is applied The resulting signal only consisted of noise, which depended on the code used, with no correlation to the desired signal in figure 6 3 This shows that amplitude demodulation should not be used with pseudo random pulses if proper inverse filtering is required

If the system signal to noise ratio is very low, due to a weak return signal and the large amount of gain required to bring the signal up to a satisfactory level, then the codes will improve the signal to noise ratio A useful improvement of the signal to noise ratio only occurs if the system signal to noise ratio is less than approximately 2 By proper design of receiving electronics the system signal to noise ratio should be kept well above a value of two Therefore pseudo random noise codes should not be necessary to improve the system signal to noise ratio for volume return

There may be pseudo random codes in existence which have better properties than maximal linear sequences Gray and Farley (1973) describe some codes that have a maximum auto-correlation sidelobe level of $0\,6\sqrt{N}$ These codes are hard to determine and can only be found by computer search To find two codes with low noise cross-correlation is even more difficult, if not impossible

One major difficulty when using pseudo random noise codes on scatterers in the ocean environment is the Doppler shift imposed on the signal as it is reflected The return signal is quadrature demodulated by mixing it with an in-phase and quadrature

carrier If the Doppler shift is strong enough the returning pseudo random code signal from a single scatterer can be shifted from the in phase channel to the quadrature of phase channel and back into the in phase channel with a reversed sign The effect of this after correlating may be anything from zero received and filtered signal to an incorrect sign in the decorrelated signal The usable limit will be a Doppler shift that is smaller than that required to introduce a phase change in the carrier of $\pi/4$ from the first bit to the to the last bit of the code For example if the carrier is 100khz, the bit length is 100μsec and there are 127 bits in the code, the scatterer should move less than 0 19cm in a time of 12 7 msec This means that the vertical scatterer velocity has to be less than 0 15m/sec This restraint on the scatterer velocity can often not be achieved, and therefore the code has to be shortened or it cannot be used

The use of pseudo random codes will give slight improvement of the interpulse interference signal to noise ratio, but the types of flows that can be investigated will be severely reduced by the limit set on the vertical velocity of the scatterers In a ship mounted system a large vertical velocity component can be introduced by the ship's heave, even if the scatterer vertical velocity is zero, and make the correlation sonar device with pseudo random pulses unuseable

Pseudo random noise is however an effective method of increasing the bandwidth of a pulse If the same code is applied to each of the two pulses, no inverse filtering is required and the bandwidth-integration time product of the correlations increases This results in more accurate correlation values, with the same correlation function peak height as found for the signal without the code

7 ANALYSIS OF CORRELATION SONAR BOTTOM DATA

The theories developed in previous chapters will now be tested with observations and computer model results In particular the effect of different demodulation techniques, interpulse interference and wide bandwidth pulses will be investigated The data collected for the correlation sonar can be divided into two groups Bottom or thin scattering layer return covered in chapter 7 and volume return with data received from a broad scattering layer, covered in chapter 8 The data received from the bottom usually show well separated pulses, while the data from the broad scattering layer will have indistinguishable pulses

7.1 Correlation sonar bottom return

An amplitude demodulated correlation sonar bottom return signal is shown in figure 7 1 The data were taken on June 5 1985, moored to the Navy Buoy in Saanich Inlet, thus the velocity should be zero All fourteen channels are plotted out as a function of time at a range gate covering the pulse The fourteen channels are split into two groups of seven for the two seven channel x and y transducer banks The x channel 1 is located nearest the bow of the ship, while the y channel 1 is located nearest the port side The ship that was used never came to rest completely due to wind, waves and current, thus slight velocity offsets can be expected

A two millisecond pulse length was used with a pulse separation of 10msec The two returning pulses can be clearly seen in the data The small scale features of the received pulses change going from one channel to the next, while they do not change drastically from pulse to pulse in the same time series The pulses change from channel to channel because a different spatial position gives a different interference pattern The two returning pulses are virtually identical in each time series because the platform is stationary relative to the scatterers If the platform was moving, then a different scatterer distribution would be illuminated for each pulse and the return echoes would change from pulse to pulse

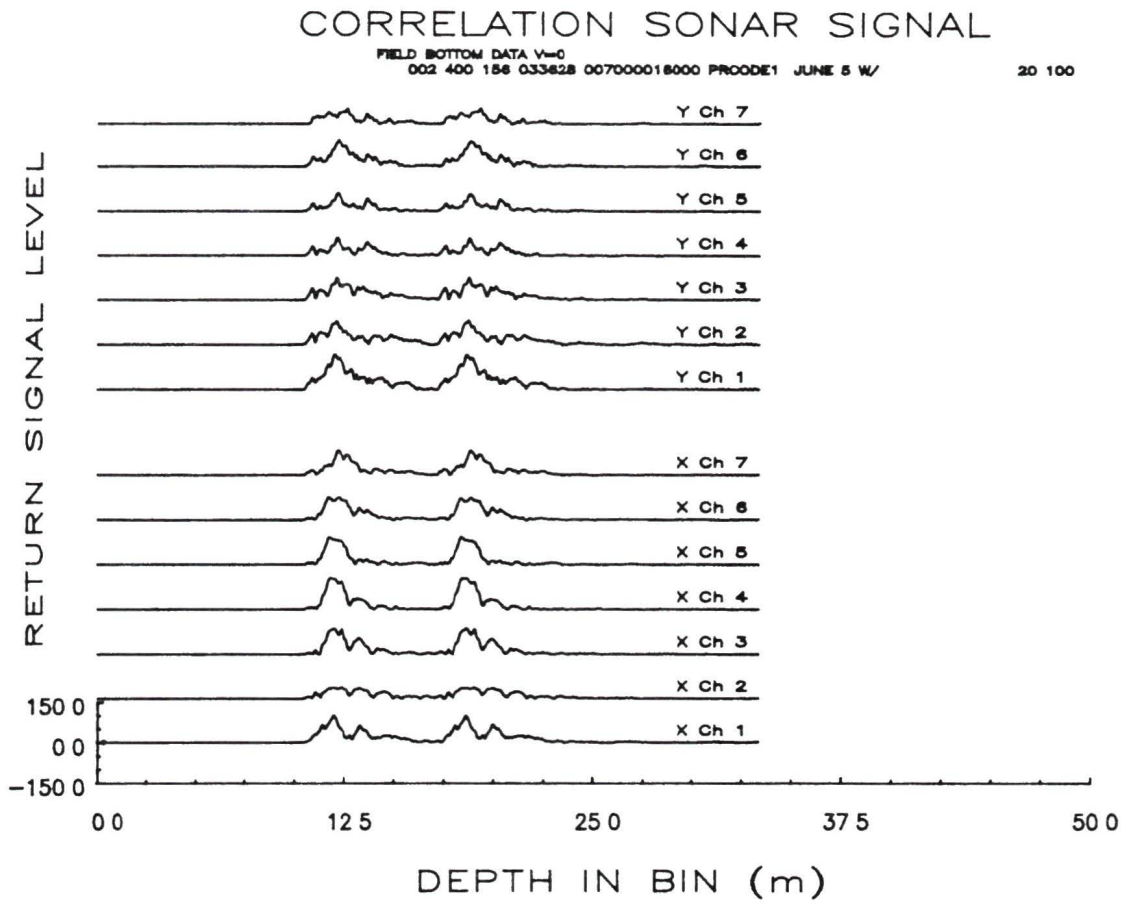

Figure 7.1

A bottom echo time series for the correlation sonar Two pulses of length 2msec were sent out with a separation of 10msec The data for the x transducer bank were plotted as the lower seven channels, while the data for the y transducer banks were plotted as the upper seven channels The ships velocity was zero for these data

The computer model can be used with the same parameters of depth, pulse length and separation as in the field data above to demonstrate how the signals change if the platform is moving A velocity of 0 75m/sec in the forward direction of the ship was chosen because it results in the translation of the interference pattern of exactly 1 5cm in the pulse separation interval into the x direction It is possible to demonstrate the effect of forward velocity using field data, but the speed can not be chosen with high enough accuracy to give the exact displacement of 1 5cm of the transducer array in the pulse separation interval The time series generated by the computer model is plotted in figure 7 2

On the x channels 2 to 6 the effect of the forward velocity of the scatterers can be clearly identified For example, the first pulse in the time series of x array channel 2 is almost identical to the second pulse time series of x array channel 3 This means that the interference pattern was translated 1 5cm on the surface in 10msec Since the interference pattern moves at twice the velocity of the scatterers, the velocity of the scatterers can be determined to be 0 75msec, which is the value that was entered in the model The outer transducer elements, channels 1 and 7, have a separation of 6cm, and thus the effect of the translation of the interference pattern to the next transducer can not be observed on these elements

When entering the velocity into the model, a velocity of 0 75m/sec was specified in the x direction This means that the velocity in the y direction is zero When studying the data from the y transducers, the return signal from the two pulses do not look similar This effect is called off axis decorrelation and will be explained in a following section

7.2 The bottom return correlation function

The raw signal data streams are cross correlated with a time lag of the pulse separation to determine the exact velocity of the scattering layer For example the data

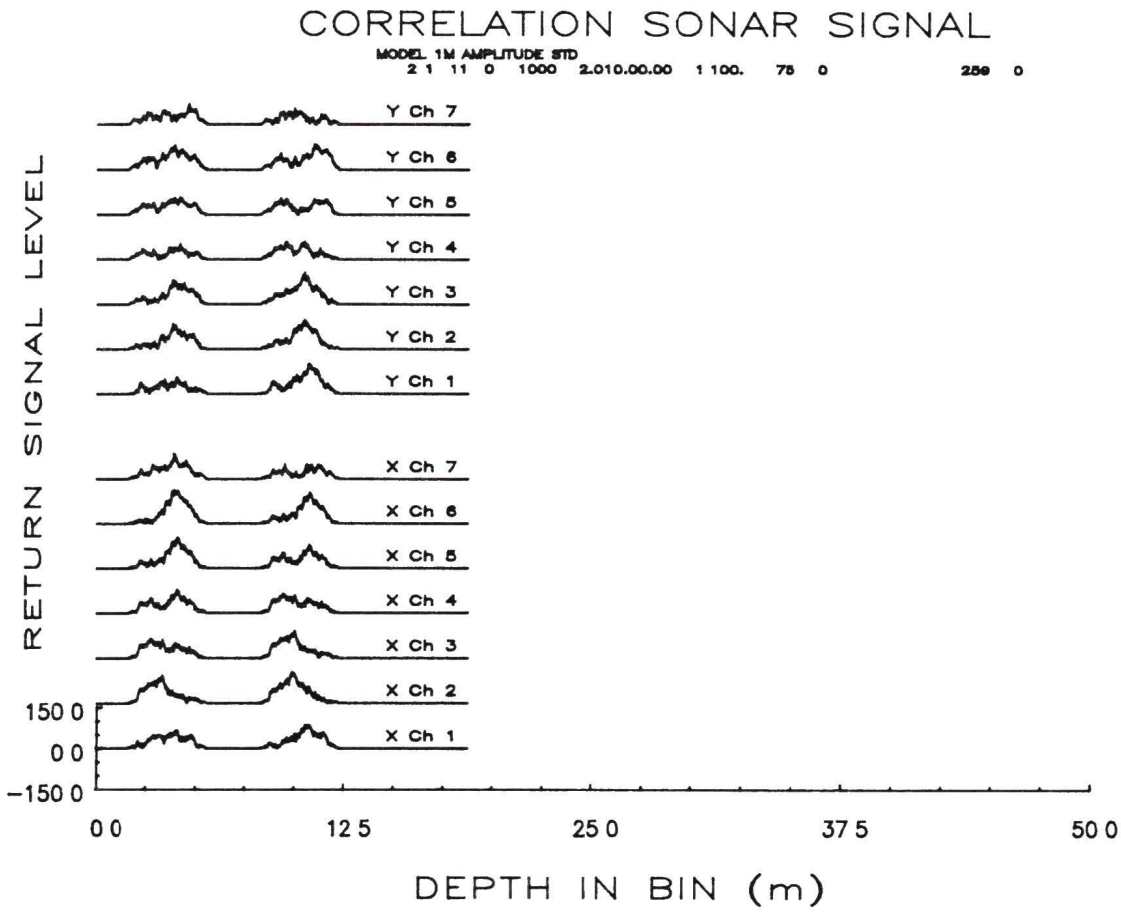

Figure 7.2

Computer model amplitude demodulated data for a 1m scattering layer at a depth of 100m moving at 0 75m/sec The pulse length is 2 msec, while the pulse separation is 10msec

from the first pulse in x channel 3 is correlated with the data from the second pulse in x channels 1 to 7 Since there are seven channels in each transducer bank, 49 cross correlation coefficients are determined for the x transducer bank and 49 channels are determined for the y transducer bank

Each of the cross correlations will have a certain separation associated with it and there will usually be more than one correlation coefficient with a given separation All correlation values with the same separation can be averaged together This will yield the correlation as a function of separation for each transducer bank The correlation as a function of separation is plotted in figure 7 3 and figure 7 4 for the field and model data discussed in the last section

The correlation obtained at each separation value is plotted in the form of a diamond, while the average of the correlation at each separation is plotted as a star The correlation function for a single transmission correlation shows large fluctuations, which means that the standard deviation on a single correlation value is large The average correlation function for 20 transmissions is plotted in figures 7 5 and 7 6 to better observe the shape of the correlation function The standard deviation for each correlation value is also determined and shown as an oval around the correlation value for easy reference

For the zero velocity field data a correlation function is obtained that shows a definite peak of amplitude 1 at zero displacement as expected from the visual inspection of the bottom echo time series in section 7 1 The standard deviation of the correlation coefficient is close to zero when the correlation is close to one, as predicted from the statistical properties of the correlation function As the distance from the peak at zero displacement increases, the correlation function decreases and the standard deviation of each correlation value shows a corresponding increase

Theory indicates that the amplitude of the correlation coefficient drops to a value that is close to zero as the distance from the zero displacement point increases to 4cm

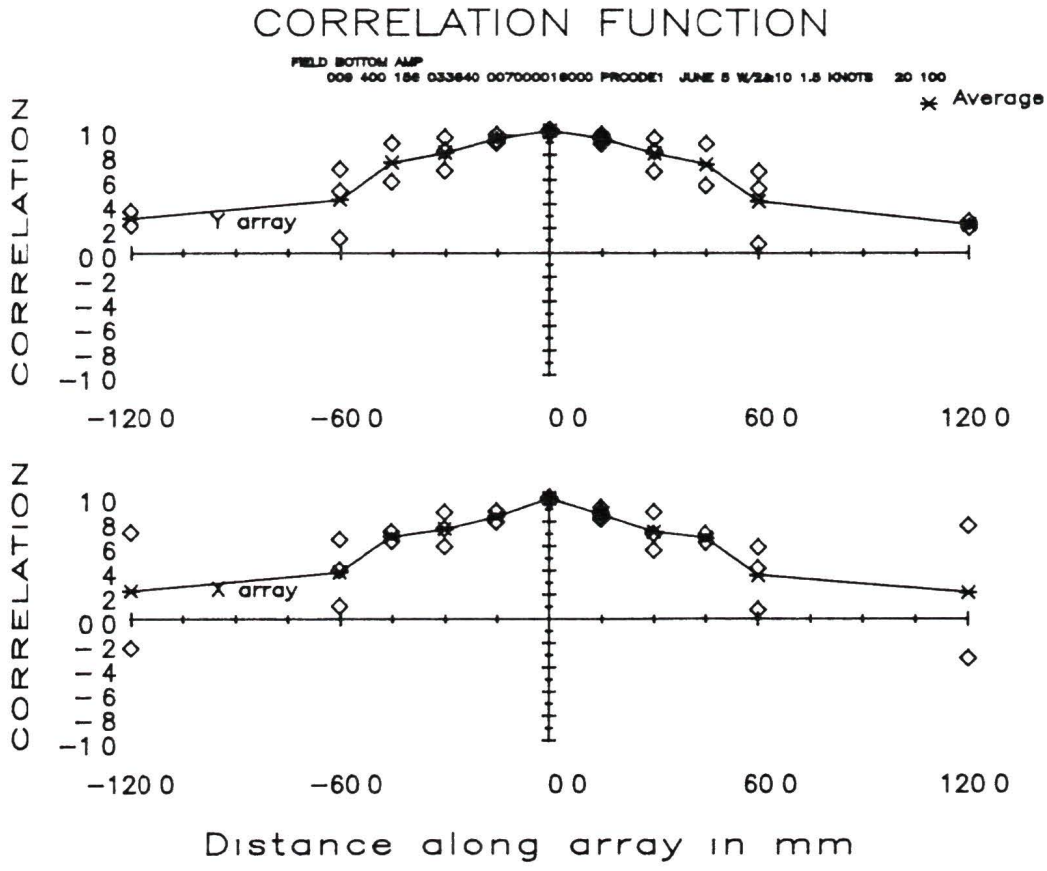

Figure 7.3

Spatial correlation as a function of distance for the field bottom data of figure 7 1 A velocity of zero means that the peak is not shifted from the zero distance point The diamonds represent the individual cross correlations between transducer elements, while the the stars represent the average of the transducer elements with the same separation

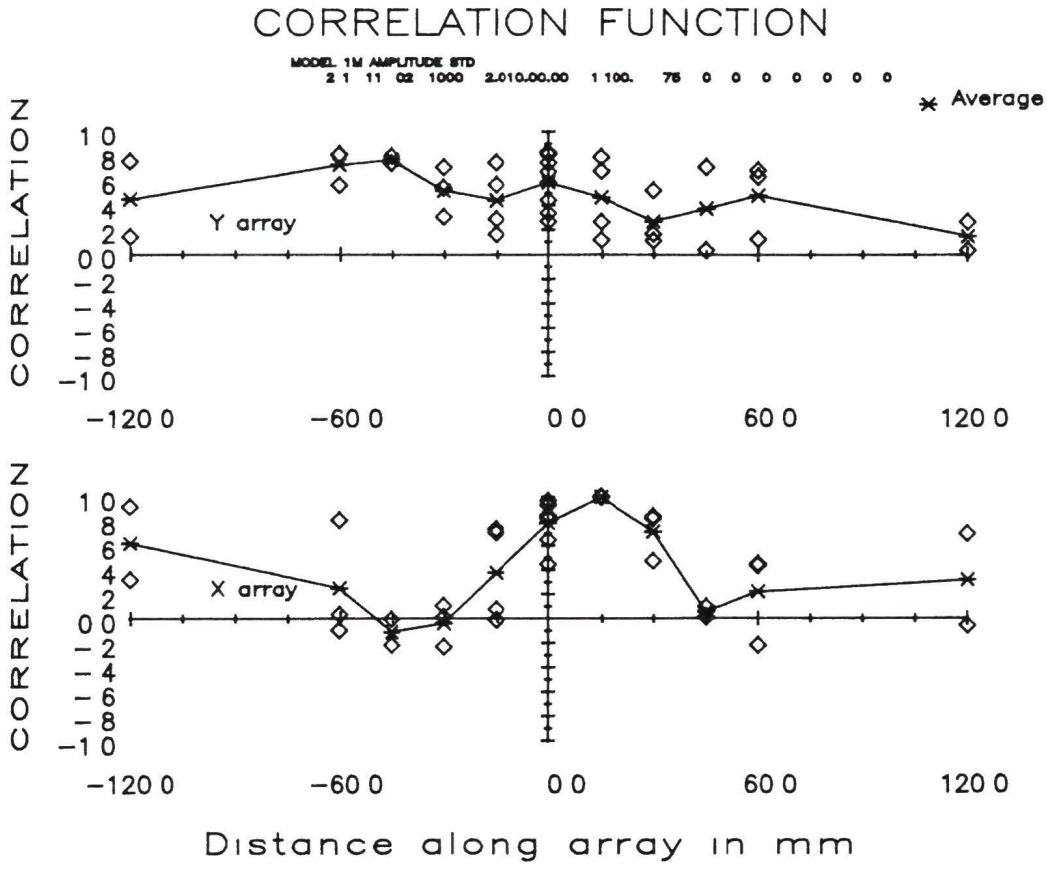

Figure 7.4

Spatial correlation as a function of distance for the computer model bottom data of figure 7 2 A velocity of 0 75m/sec in the x direction means that the peak is shifted by 1 5cm from the zero distance point The diamonds represent the individual cross correlations between transducer elements, while the the stars represent the average of the transducer elements with the same separation

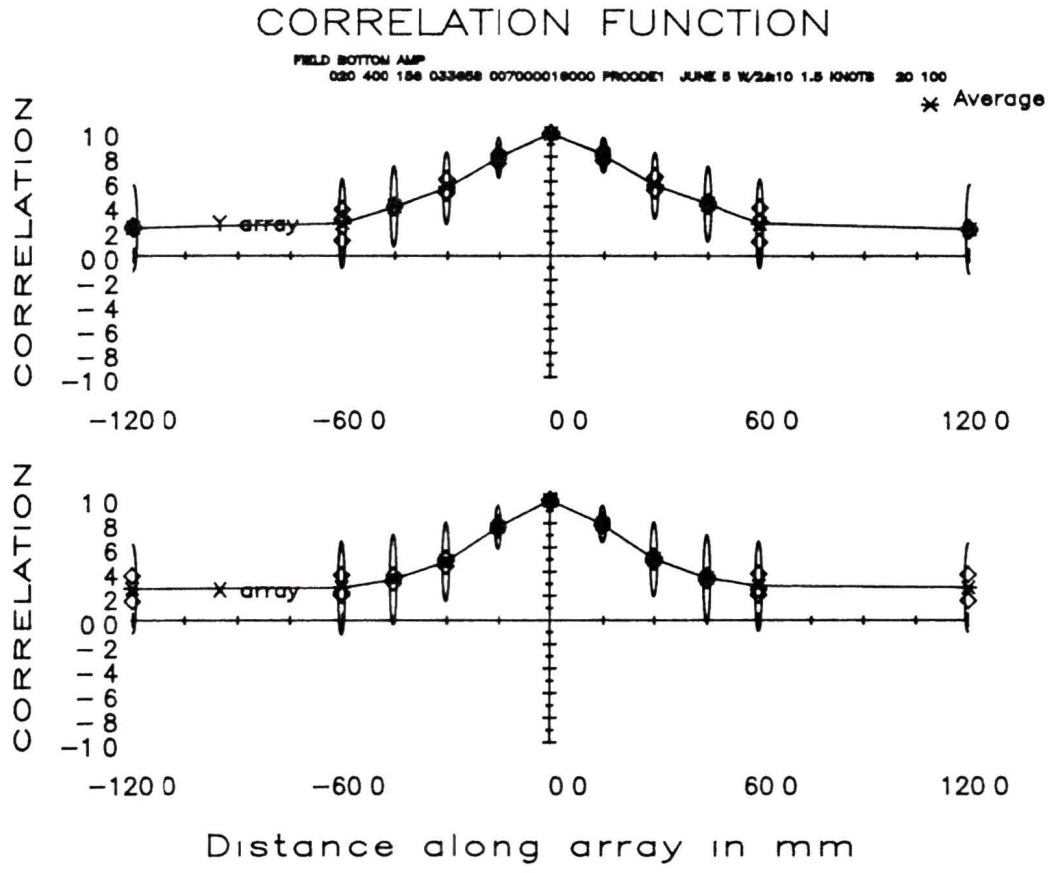

Figure 7.5

Spatial correlation as a function of distance for the field bottom data averaged over twenty transmissions The ship's velocity was zero

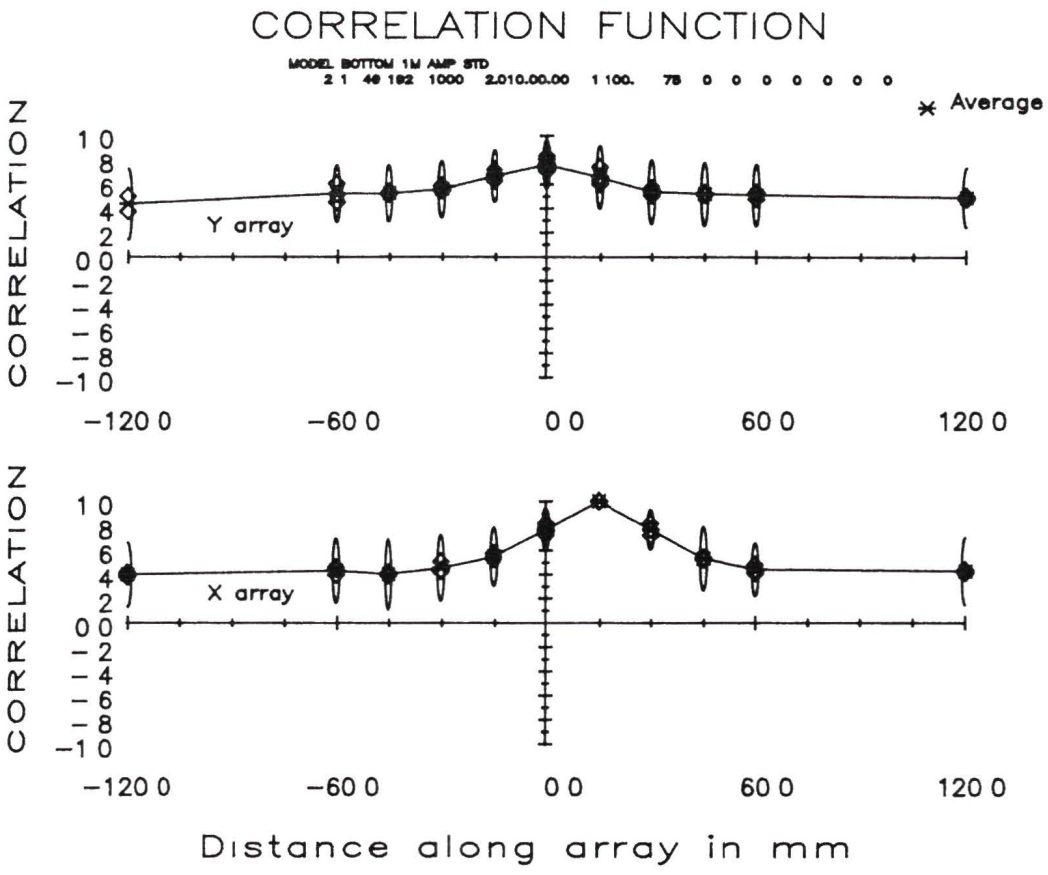

Figure 7.6

Spatial correlation as a function of distance for the computer model 1m layer data averaged over 20 transmissions A velocity of 0 75m/sec in the x direction was entered into the model

or more A decrease can be observed in the correlation function, but it only drops to a low of 0 3 The amplitude demodulated signal returning from the bottom can be viewed as a triangle function common to all the channels plus an individual signal function separate for each transducer The common basis for each signal pulse will result in an increase of the correlation, while the individual fine detail will decrease correlation far from the zero separation point This does not occur with complex demodulation as will be shown later, since the signal in each channel will be bipolar with unknown sign

Some field data were collected with a ship's velocity of 0 7m/sec This data resulted in a correlation function that was almost identical to the x and y correlation functions of the 0 75m/sec model data in figure 7 6

7.3 The off axis decorrelation

The 1m model correlation function of figure 7 6 has been obtained at a scatterer velocity of 0 75m/sec in the x direction The peak of the correlation function is shifted therefore by 1 5cm in the x direction which can be readily seen in the plot of the correlation function The velocity along the y axis is zero, therefore the peak along this axis should be at zero The peak at zero can actually be observed, but it has a height of only 0 75 This can be explained by viewing the correlation function as a two dimensional peak in a plane At zero velocity the x and y axis sample this correlation function through the center of the peak as shown in figure 7 7

If a scatterer velocity is introduced in the x direction, then the x axis transducer still samples the correlation function through the peak, while the y axis will sample the correlation function off to one side of the peak as shown in figure 7 8

A x axis velocity will therefore effectively decrease the correlation amplitude on the y channels, and will result in a less accurate y axis velocity The correlation peak

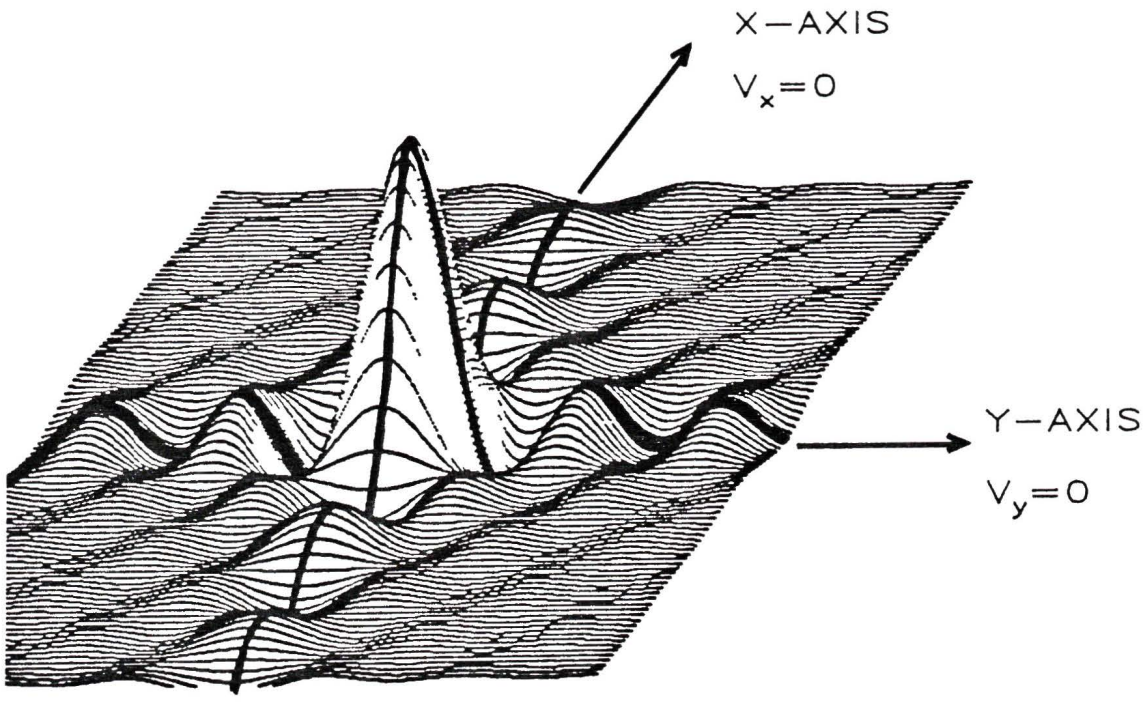

Figure 7.7

The two dimensional correlation function The correlation functions sampled by the x and y arrays intersect the peak exactly for zero velocity

on the y axis decreases to the value of the x axis correlation function at zero displacement If the x axis velocity is so large that the hydrophone array moves a distance greater than the width of the peak of the correlation function, then the y axis correlation will drop to a value which is close to zero The peak along the y axis will still be at the correct location, but it will be so small that an accurate velocity estimate can no longer be recovered If both the x axis and the y axis have a large velocity component, then both the x and y axis velocity information will be degraded

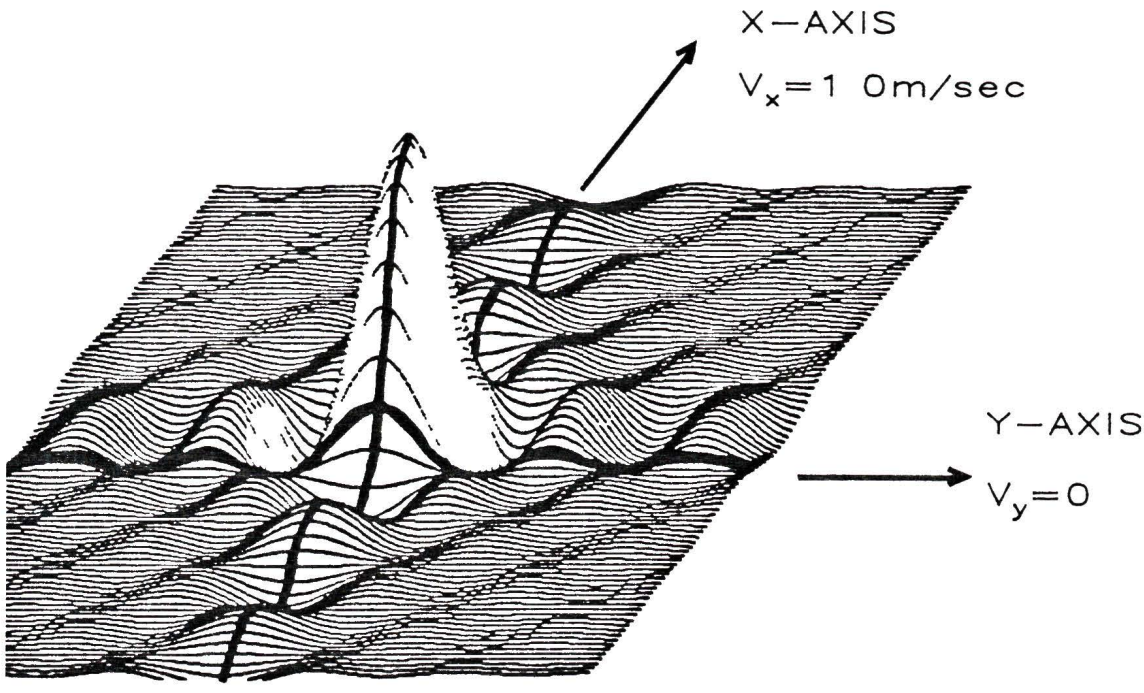

Figure 7.8

The two dimensional correlation function plotted in a plane The x axis velocity is 0 75cm/sec The x axis correlation function still intersects the correlation function peak through the center, while the y axis correlation function slices the peak off to one side

To circumvent the problem of off axis decorrelation, the correlation function must be sampled in the plane, not just along two axes It can be shown that by using a transducer array which has the elements aligned in a U or T shape, cross correlations for all the vector separations in a plane can be obtained The MX810 deepwater correlation sonar developed by General Electric uses such an array to track the bottom velocity The correlation function could not be determined in the plane with the prototype IOS correlation sonar since only a L shaped transducer array was available The

computer model receiving hydrophone layout was modified to be able to calculate the correlations in a plane and it was found that it is possible to obtain the correlation vector in a plane, without degradation of the velocity accuracy if an off-axis velocity component is present

7.4 Slope demodulation

If the amplitude demodulated time series for each transducer is differentiated, the slope demodulated signal is obtained By taking the first difference a bipolar signal is obtained, which is made up mostly of the high frequency detail of the pulse The correlation function for the slope demodulated signal will therefore drop closer to zero at points removed from the correlation peak This can be seen in figures 7 9 and 7 10 for the field data and model data

Since the accuracy of the velocity estimate depends on the relative peak height, the first difference correlation should give a more accurate velocity estimate The first difference signal also is a higher bandwidth signal, and thus there are more independent samples available in the correlation calculation, which in turn means a smaller standard deviation on the correlation coefficient The decrease in the standard deviation if slope demodulation is used can be observed in both the field and model data

By clipping the bipolar first difference signal the one bit slope signal is obtained The correlation coefficients for the one bit slope signal is plotted out in figures 7 11 and 7 12 for field and model data The relative peak height and standard deviation is approximately the same as that for the first difference correlation, and consequently the accuracy of the velocity estimate will also be better than that for the standard amplitude demodulation

A big advantage of the clipped signal is that the correlations are self normalizing and the much faster unnormalized correlation coefficient calculation can be used

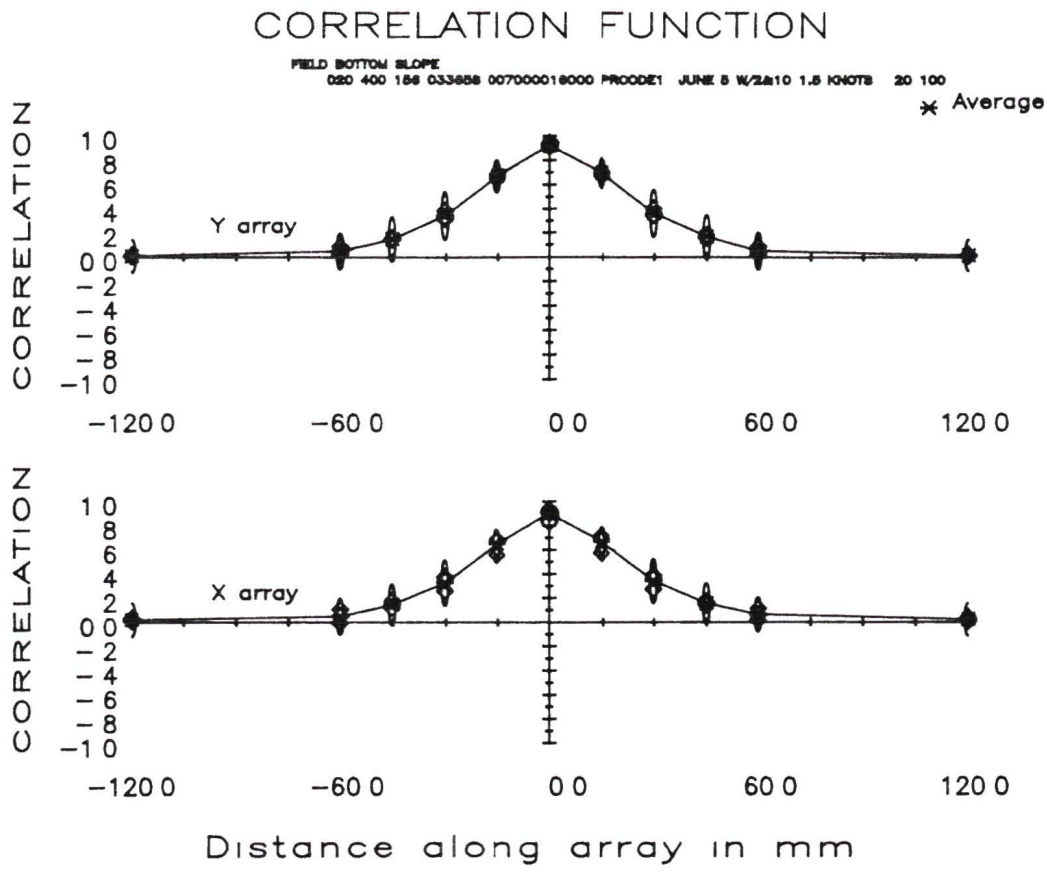

Figure 7.9

Spatial correlation function for the slope demodulated signal of the field bottom data averaged over 20 transmissions The ship's velocity was zero

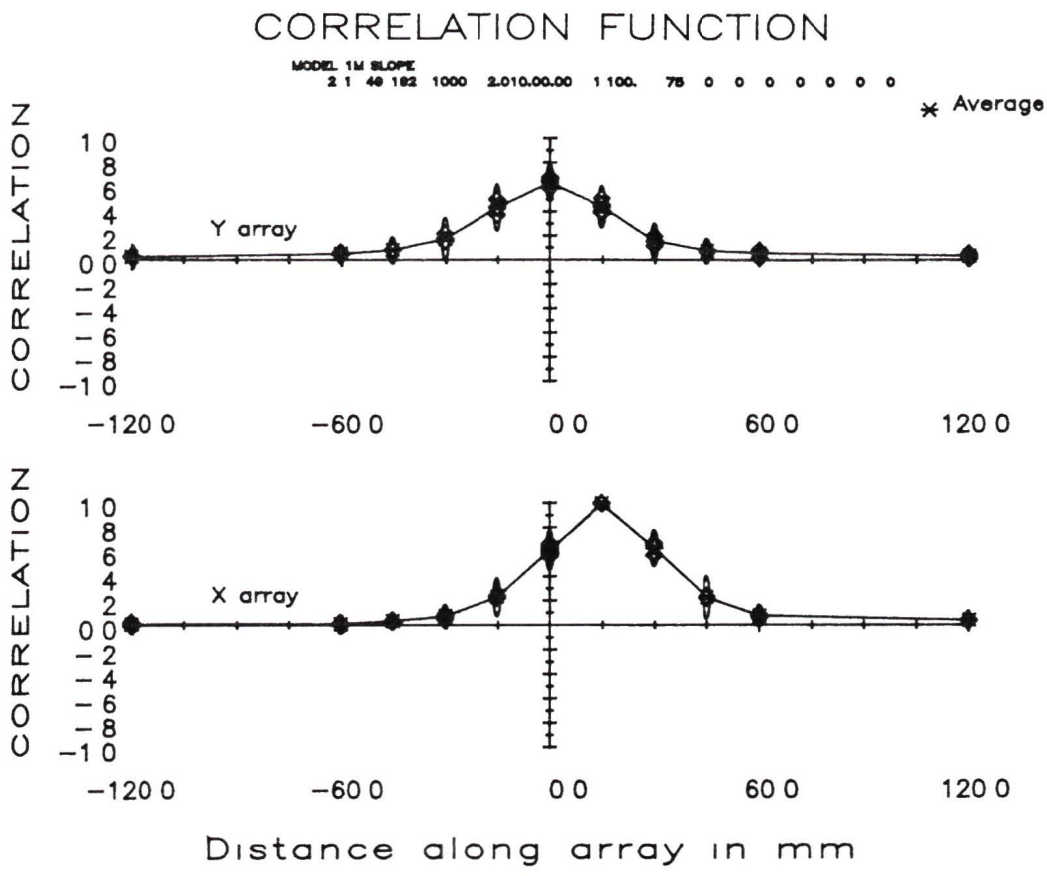

Figure 7.10

Spatial correlation function for the slope demodulated signal of computer model generated data for a 1m thick scattering layer averaged over 20 transmissions moving with a velocity of 0 75m/sec

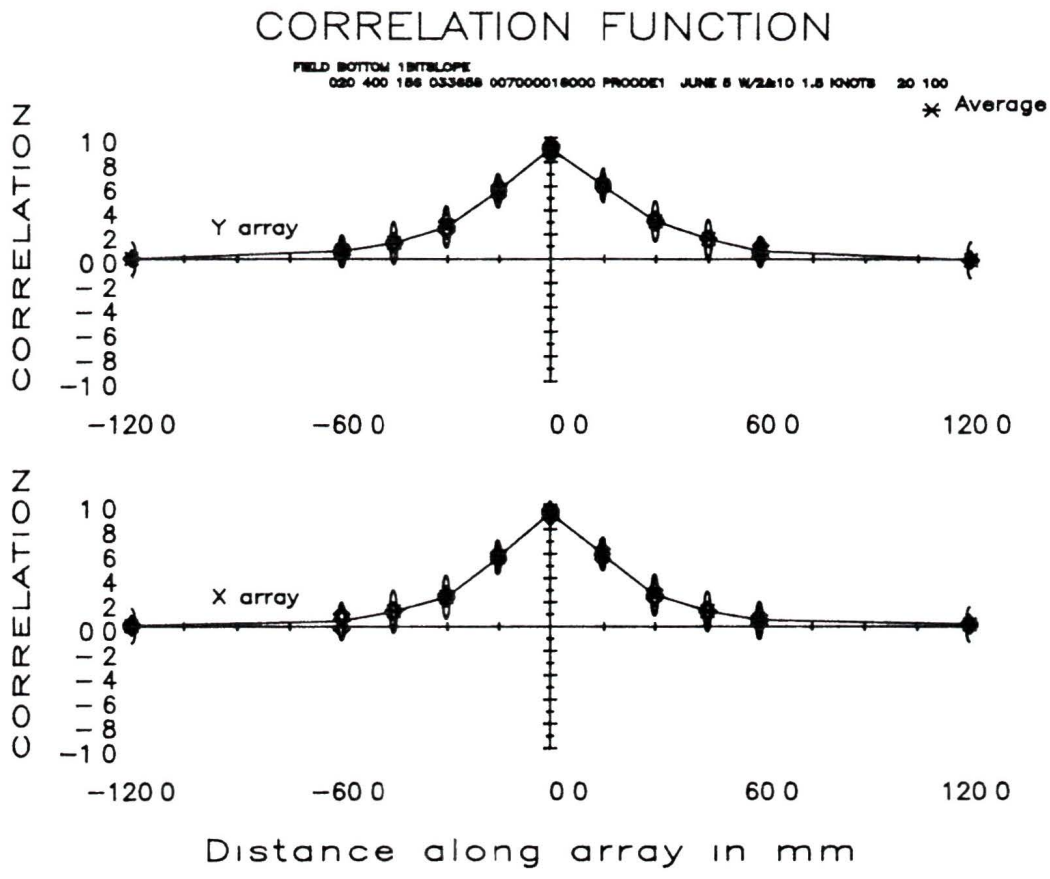

Figure 7.11

Spatial correlation function for one bit slope demodulated signal of the field bottom data

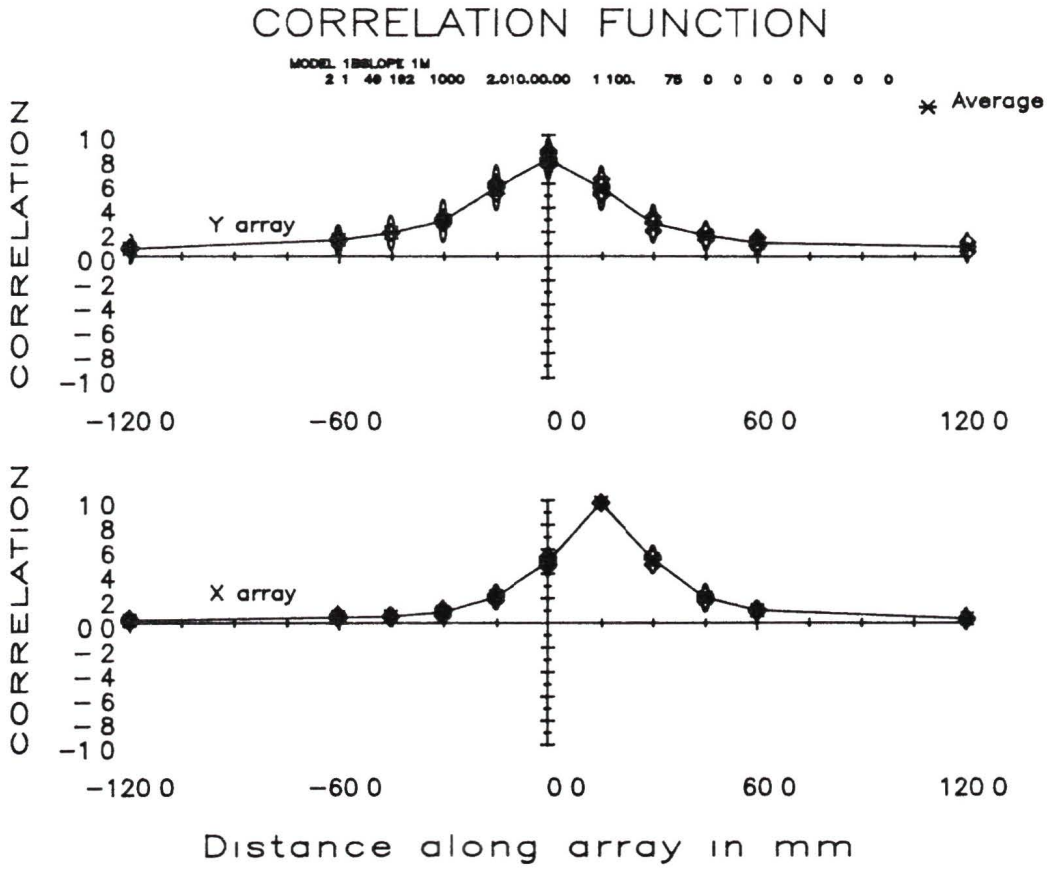

Figure 7.12

Spatial correlation function for one bit slope demodulated signal of computer model generated data for a 1m scattering layer

7.5 Wide bandwidth transmission pulses for bottom return signals

If the transmitted waveform is amplitude or phase modulated with a random binary sequence, the bandwidth of the received signal will increase A higher bandwidth means that the bandwidth-integration time product increases and the standard deviation of the correlation value decreases In the computer model and in the IOS correlation sonar the transmitting waveform could be keyed on and off with a predetermined binary random sequence The modulation used was phase modulation in the model and amplitude modulation for the field data The pseudo random sequence had a length of 127 bits with a bit length of 100μsec This effectively gives a bandwidth of the pulse of 10 khz, while without the spread spectrum code a 2msec pulse has a bandwidth of 500hz

Some data were taken moored to the navy buoy in Saanich Inlet with zero velocity using the wide bandwidth pulses The correlation function taken with these data was plotted in figure 7 13 The correlation peak does not reach an amplitude of one because the gain of the amplifiers was increased which introduced some noise into the system The correlation at a distance from the peak drops down to zero This means that the peak is well defined and accurate values can be determined for the bottom velocities

If the first difference signal is correlated, an almost identical correlation function to the amplitude correlation function is obtained If one bit slope demodulation is used, a slight increase in the correlation coefficient can be observed, while the standard deviation of each correlation value is less than that for amplitude demodulation, as shown in figure 7 14 Since the peak is higher and the standard deviation is smaller for the one bit slope correlation function, it should be possible to determine velocities more accurately using the one bit slope technique

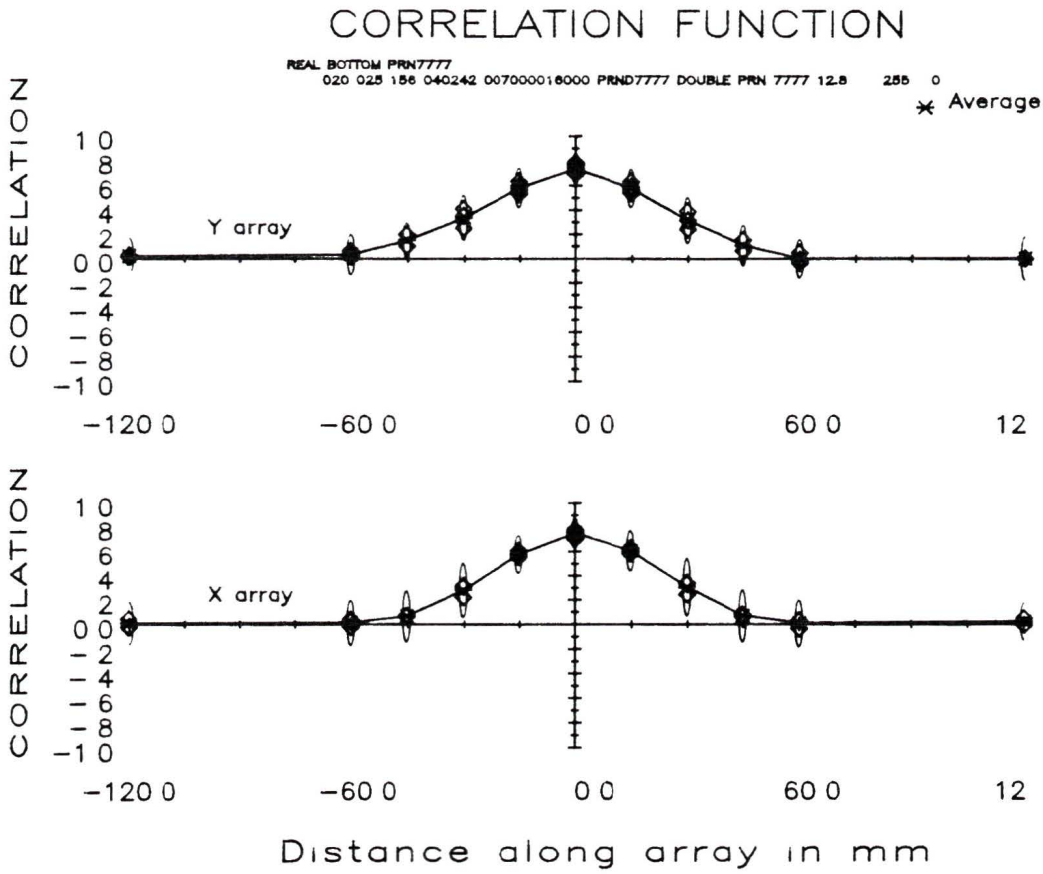

Figure 7.13

Spatial correlation function of the amplitude demodulated field data bottom echo of two wide bandwidth pulses

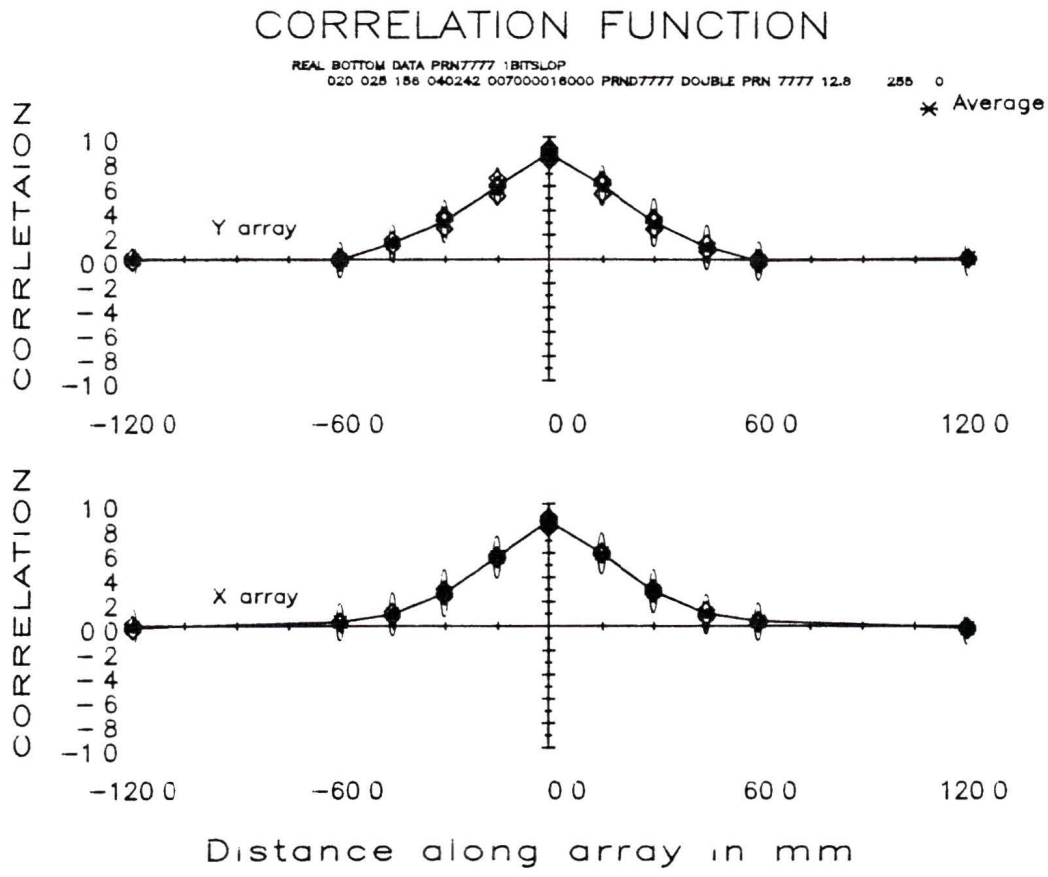

Figure 7.14

Spatial correlation function of the one bit slope demodulated bottom echo of two wide bandwidth pulses

7.6 Complex and clipped complex demodulation of bottom echoes

The computer model can be used to investigate different types of demodulation The correlation functions for complex demodulation and clipped complex demodulation were obtained for the 1m scattering layer and can be seen in figures 7 15 and 7 16 Special care must be taken when averaging the correlations from a complex signal to prevent the noise components in the correlation from interfering with the calculation of the proper correlation coefficient This can be accomplished by averaging the complex correlation coefficients and only calculating the amplitude of the correlation coefficient from the averaged complex correlation coefficient

The width of the correlation function for the complex demodulated data is wider than that for the amplitude demodulated and clipped complex demodulated data as predicted in figure 4 3 The complex demodulated signal correlation function is exponential in shape as expected from the theory developed earlier The correlation function for the clipped complex demodulated signal has a sharp peak similar to the clipped complex correlation function calculated from the statistical properties of the field Only the x channel in the clipped complex demodulation shows this sharp peak, because the y channel correlation is rounded by the off axis decorrelation The clipped complex demodulated signal has a smaller standard deviation of the correlation coefficient than the complex correlation coefficient and therefore should give more accurate velocity values for bottom velocity determination

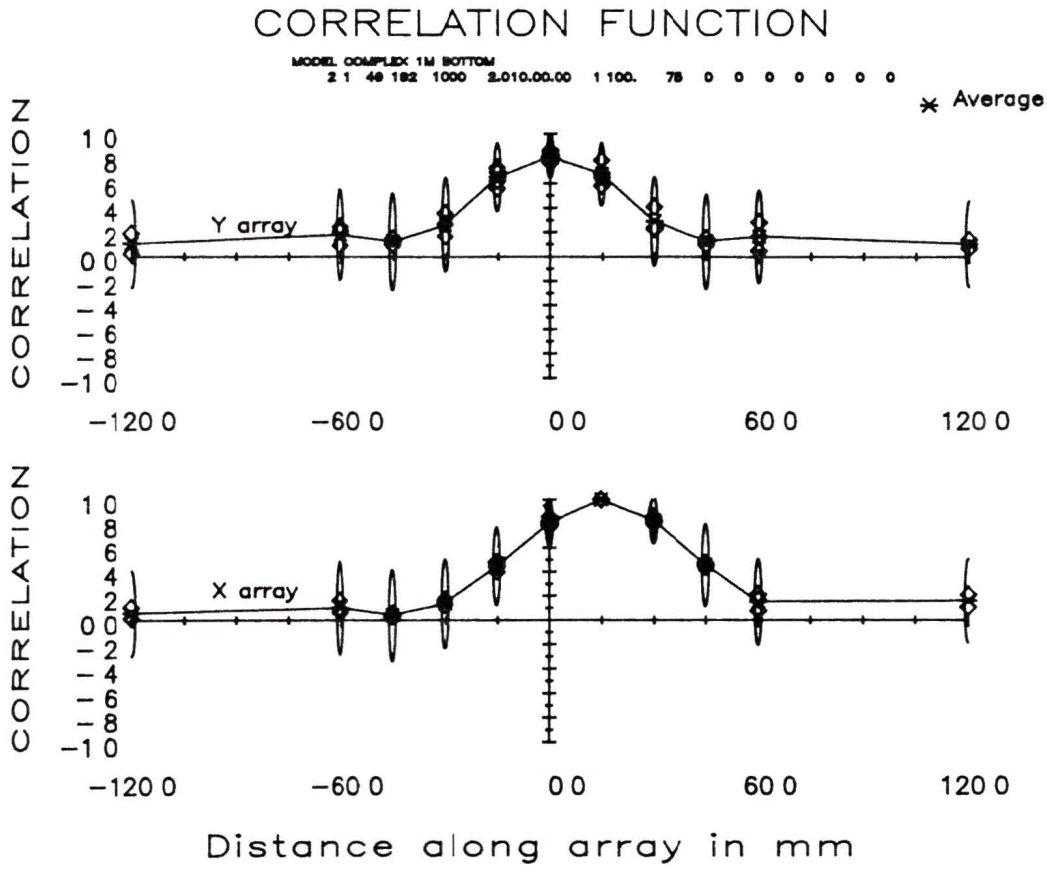

Figure 7.15

Spatial correlation function of computer model generated complex demodulated data for a 1m layer at a depth of 100m The correlation function is averaged over 20 transmissions The scatterer velocity is 0 75m/sec

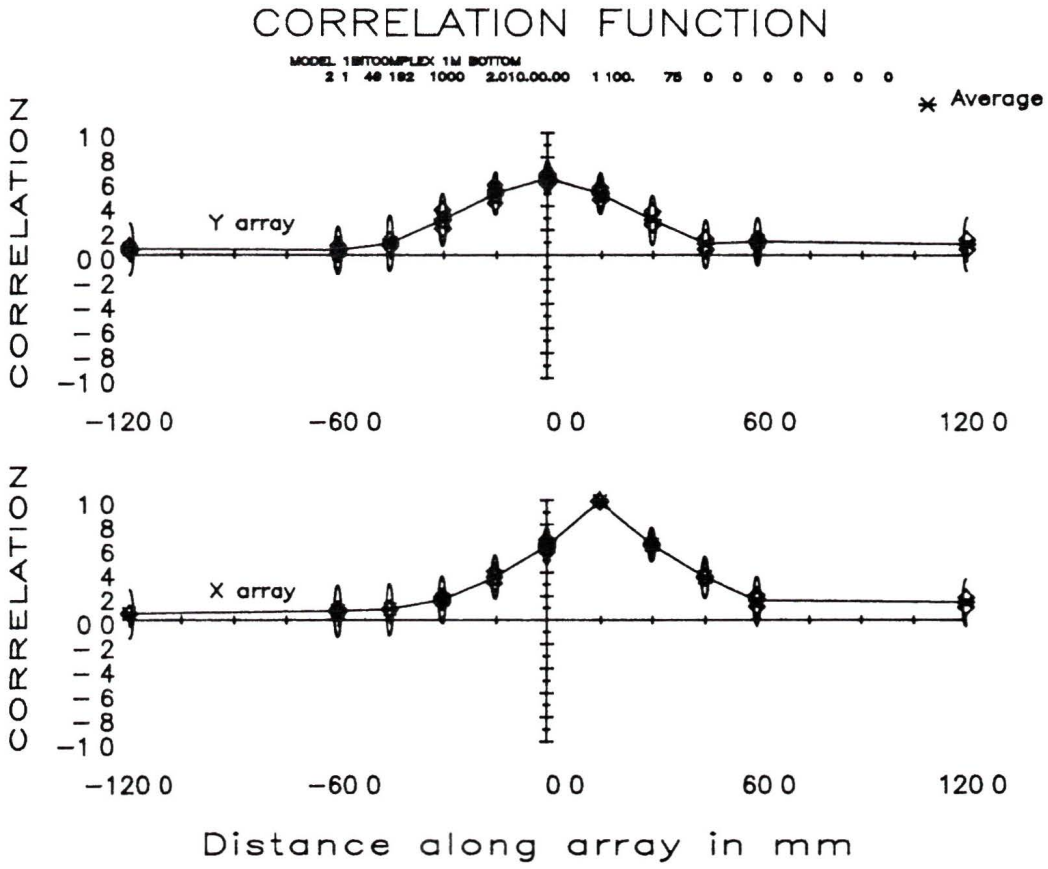

Figure 7.16

Spatial correlation function of computer model generated one bit complex demodulated data for a 1m layer at depth of 100m The correlation function is averaged over 20 transmissions The scatterer velocity is 0 75m/sec

8 ANALYSIS OF CORRELATION SONAR VOLUME DATA

Up to this point, the signal returning from the bottom or a well defined scattering layer has been discussed If the scatterers are distributed over a larger vertical distance than the separation between pulses, then the signal received on the hydrophones will be made up of the return signal from both pulses at the same time returning from different ranges This is called volume return In the correlation process the data from each pulse is required separately and the other pulse data can be treated as noise

8.1 Correlation sonar volume return

A typical correlation sonar volume return signal can be seen in figure 8 1 It was taken on the research vessel *VECTOR* heading south in Saanich Inlet from the Navy Buoy with an approximate speed of 0 75m/sec at 18 52 on June 5 1985 The x axis velocity should therefore be approximately 0 75m/sec, while the y axis velocities should be approximately zero The data are from a bin that extends from 50m to 100m in the water column A pulse length of 2msec and a pulse separation of 10 msec was used

As can be seen from the plot of the time series of the volume return, it no longer is possible to separate the two pulses visually The y array preamplifiers have a consistently higher gain than the x array amplifiers by approximately 2db The raw amplitude demodulated signal shows the presence of a large amount of noise A Fourier transform power spectrum of the noise reveals that it is concentrated around 2 7kHz (figure 8 2)

Much effort was expended in tracing the origin of this noise The transducer assembly was housed in a streamlined fiberglass shell, which appeared to resonate at this frequency When the shell was removed the 2 7khz noise decreased by about 2db, but it did not disappear The signal displayed in figure 8 1 is with the fiberglass shell removed No attempts were made to filter out the noise since filtering may affect the

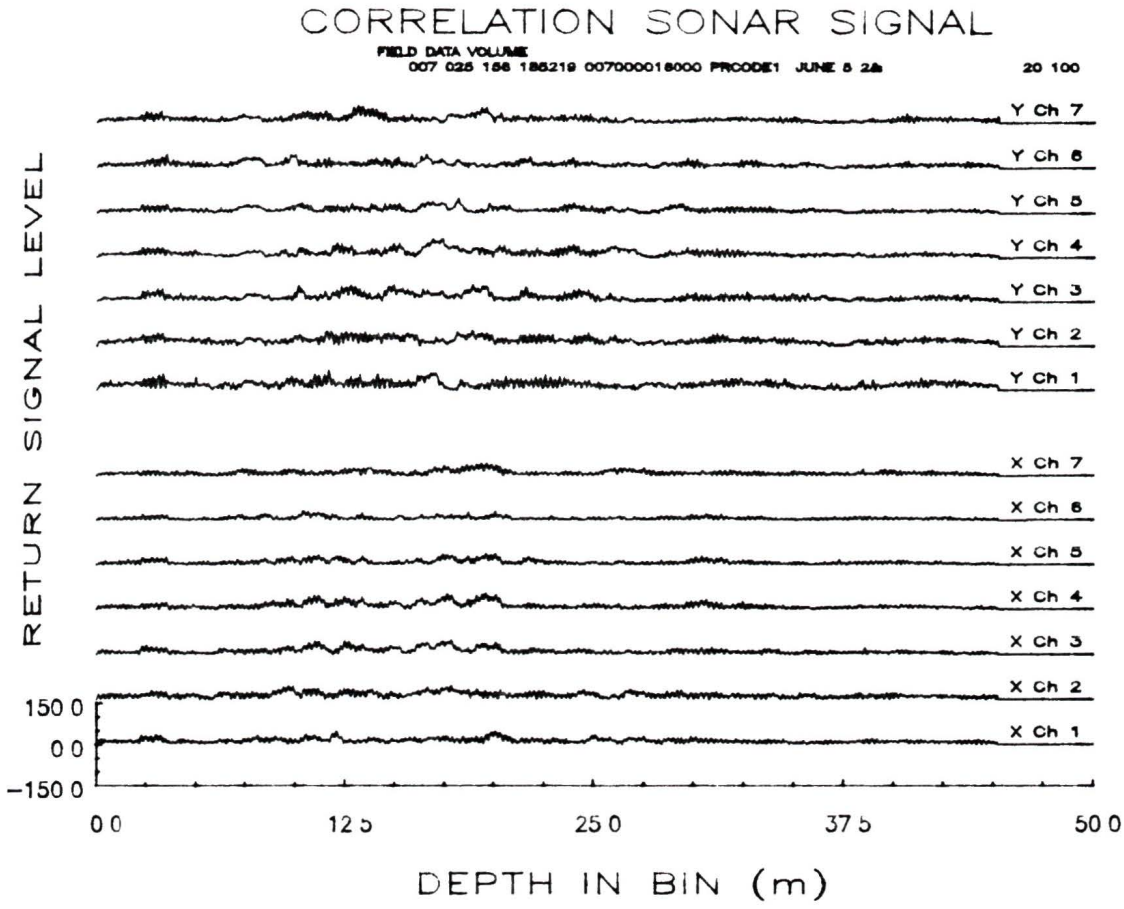

Figure 8.1

A volume return echo time series for the correlation sonar Two pulses of length 2msec were sent out with a separation of 10msec The data plotted represent the return echo from a section of water between 50m and 100m

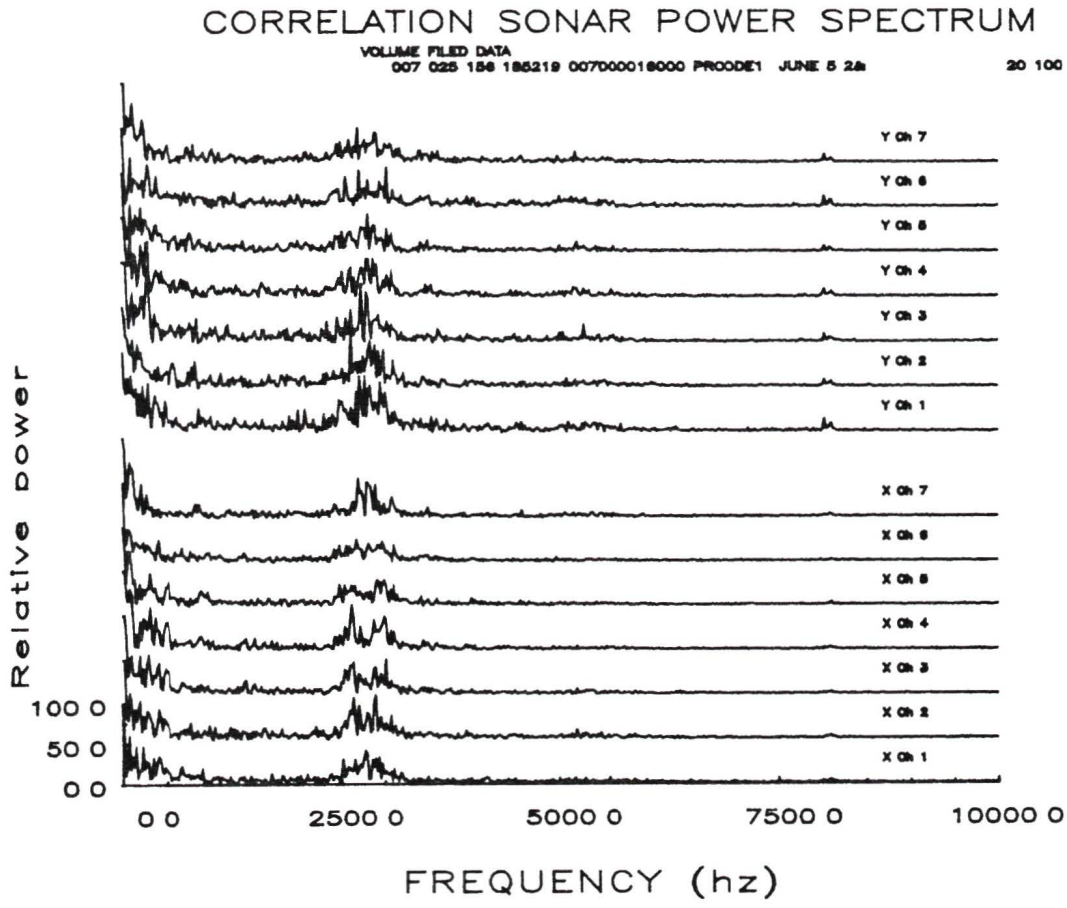

Figure 8.2

Power spectrum of the field volume return signal form figure 8 1

correlations Since the noise increases with the signal, it was caused either by the demodulation electronics or by a resonant preamplifier stage A cross correlation of the noise between the channels reveals that the noise is non coherent The received signal to noise ratio in figure 8 1 is approximately 4db

The data were collected in Saanich Inlet at a bottom depth of approximately 200m The echo sounder was operated at the same time as the correlation sonar Figure 8 3 shows the Biosonics echo sounder image displayed graphically with an EPC recorder The echo sounder image is effectively the scatterer strength as a function of depth and distance along the Inlet The image in figure 8 3 covers a time from 18 40 to 21 00 on June 5 1985 A strong scattering layer can be seen at an approximate depth of 65m in the echo sounder image The layer is caused by a large number of zooplankton, most likely Euphausia pacifica, which can be found in great concentrations in Saanich Inlet (Beamish 1971) The same scattering layer can be seen in the correlation sonar signal plot of figure 8 1 at a relative depth in the bin of 15m Since the correlation sonar data were collected from the second 50m bin, the depth of the layer from figure 8 1 also corresponds to 65m From the echo sounder image it can be seen that scatterers can be found over the whole depth of Saanich Inlet At a depth of 160m the anoxic layer starts and there is a smaller number of scatterers present The bottom is at approximately 200m

8.2 The volume return correlation function

The velocity of the scattering volume is determined by cross correlating the raw amplitude demodulated data signals between channels in each transducer bank A time lag that is the same length as the pulse separation is used between the two signals that are correlated The correlation has to be repeated at increments of the depth resolution to get a continuous correlation profile

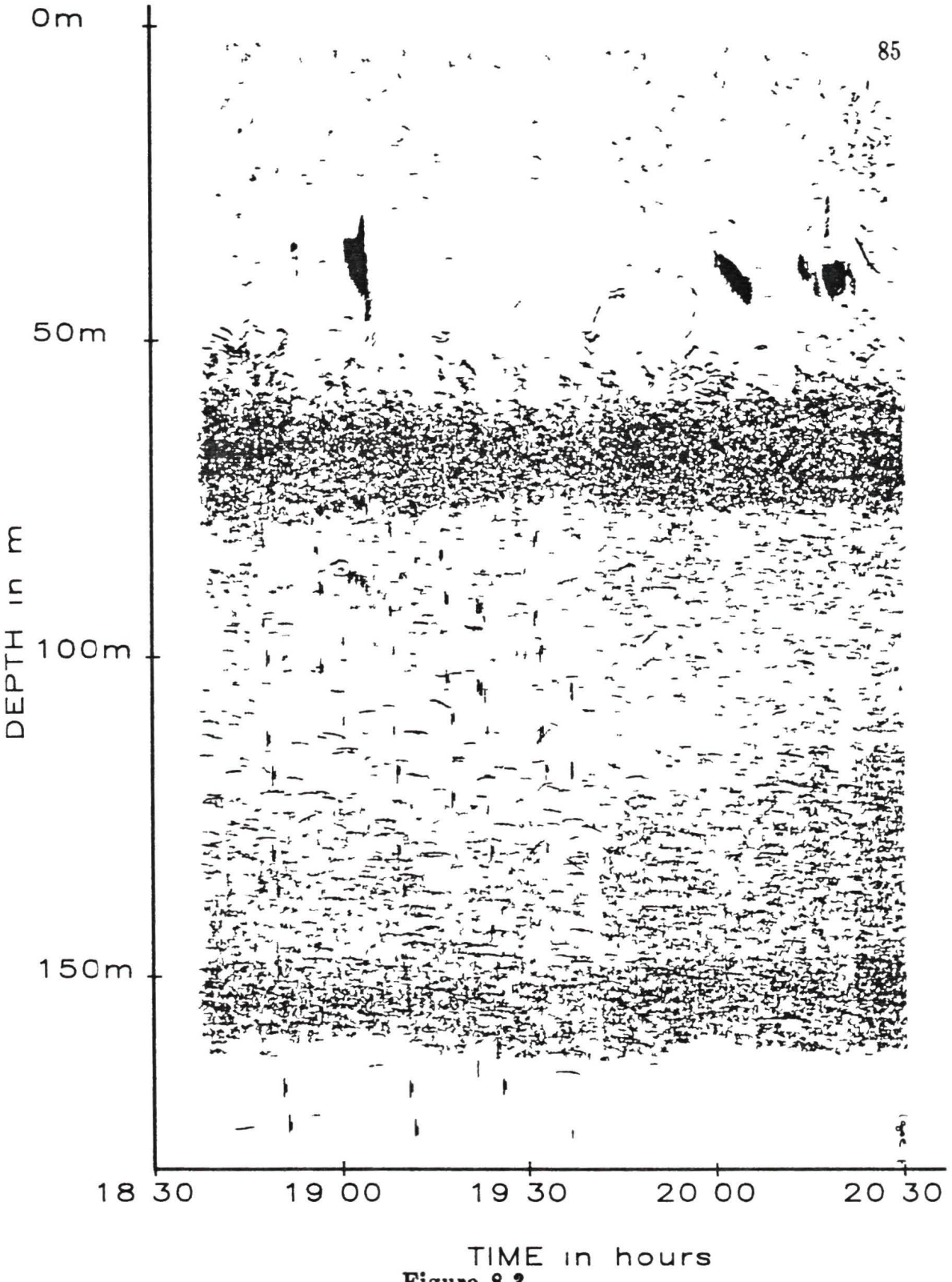

Figure 8.3

The echo sounder image of the scatterers in Saanich Inlet The bottom is found at approximately 200m and a scattering layer can be seen at 65m

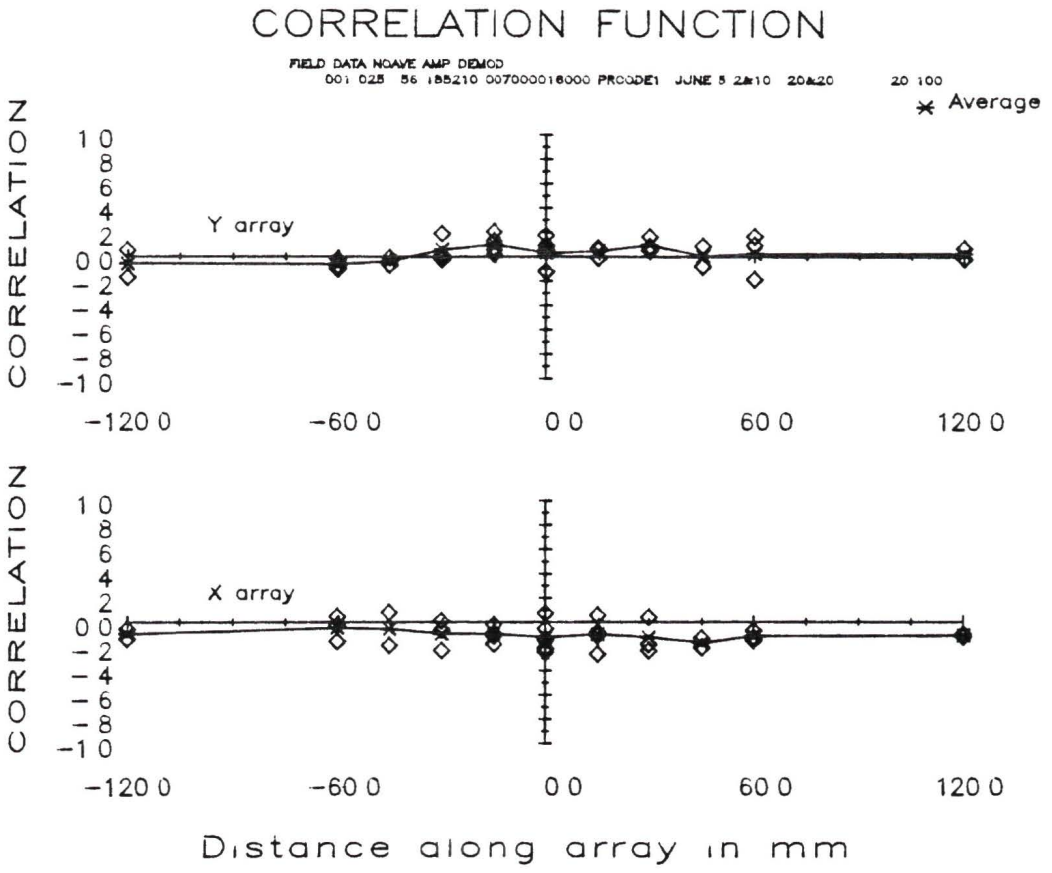

Figure 8.4

Spatial correlation function of volume amplitude demodulated field data at a depth of 75m The ship's velocity was approximately 0 75m/sec

The correlation function for a single transmission is shown in figure 8 4 at a range gate of 75m The correlation function is so noisy that the correct peak can not be determined visually The correlation values for 20 transmissions are averaged together and are plotted in figure 8 5 to obtain a better picture of the correlation function

In the averaged correlation function a peak can be seen on both the x and the y array, but the standard deviation for each correlation value is very high, and therefore there is a large uncertainty in the actual peak position The peak height is approximately 0 25 The value predicted from theory in chapter 4 is 0 23 for amplitude demodulation, which is obtained by assuming the interpulse interference can be treated as a signal with a signal to noise ratio of one The value predicted from theory agrees with the experimental data to within experimental accuracy This means that it is in fact possible to treat the interfering pulse as a noise signal, that mixes with the wanted signal in the correlation

The data were also correlated using the slope and one bit slope signal and the correlation functions can be seen in figures 8 6 and 8 7 The correlation function for the slope demodulated signal is almost identical to the amplitude demodulated signal with a peak of 0 25, while the correlation function for the one bit slope demodulated signal shows a peak of 0 5 The standard deviation for the one bit slope correlation function is about twice as large as that for the slope demodulated signal and thus the accuracy for the amplitude and one bit slope demodulated function is approximately equal

8.3 The interpulse interference

The computer model was used to generate volume return from a 30m layer at a starting depth of 100m, to investigate the exact effect of the interpulse interference The return signal from the layer is plotted in figure 8 8 The model parameters were set

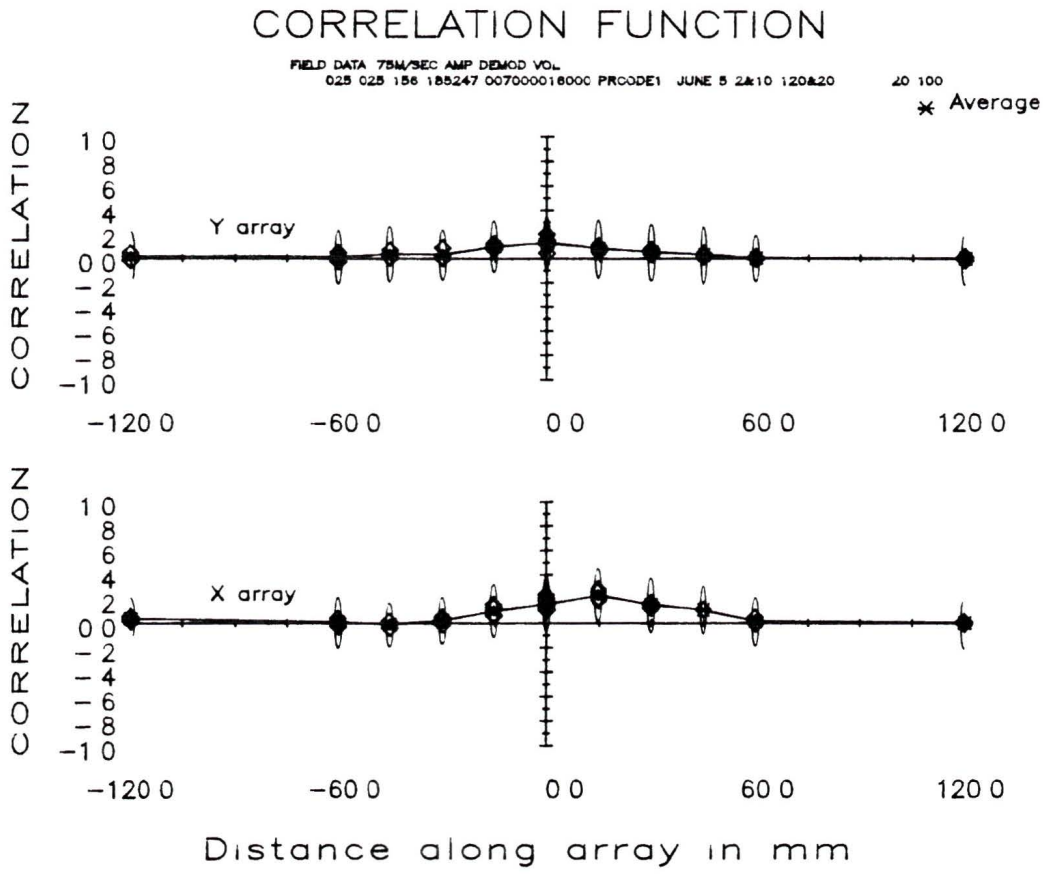

Figure 8.5

Spatial correlation function of volume amplitude demodulated field data at a depth of 75m, averaged over 20 transmissions

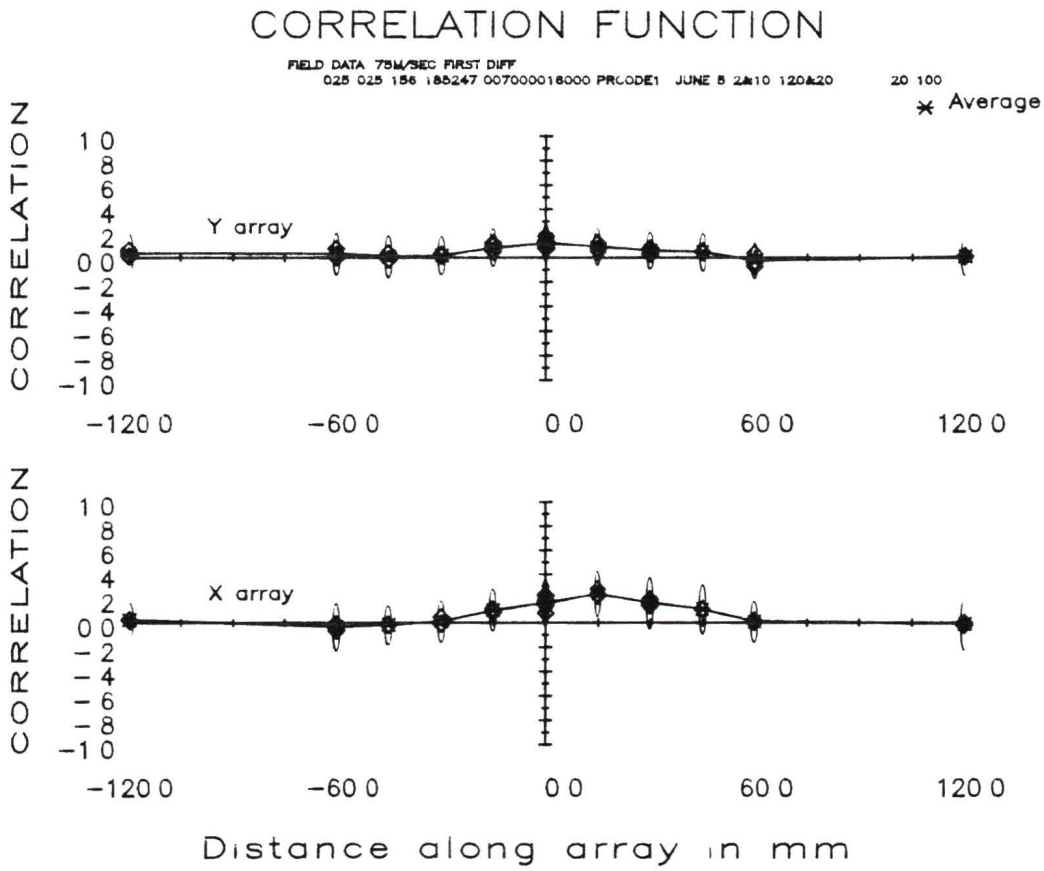

Figure 8.6

The spatial correlation function for slope demodulated amplitude signal of field volume return data at a a depth of 75m averaged over 20 transmissions

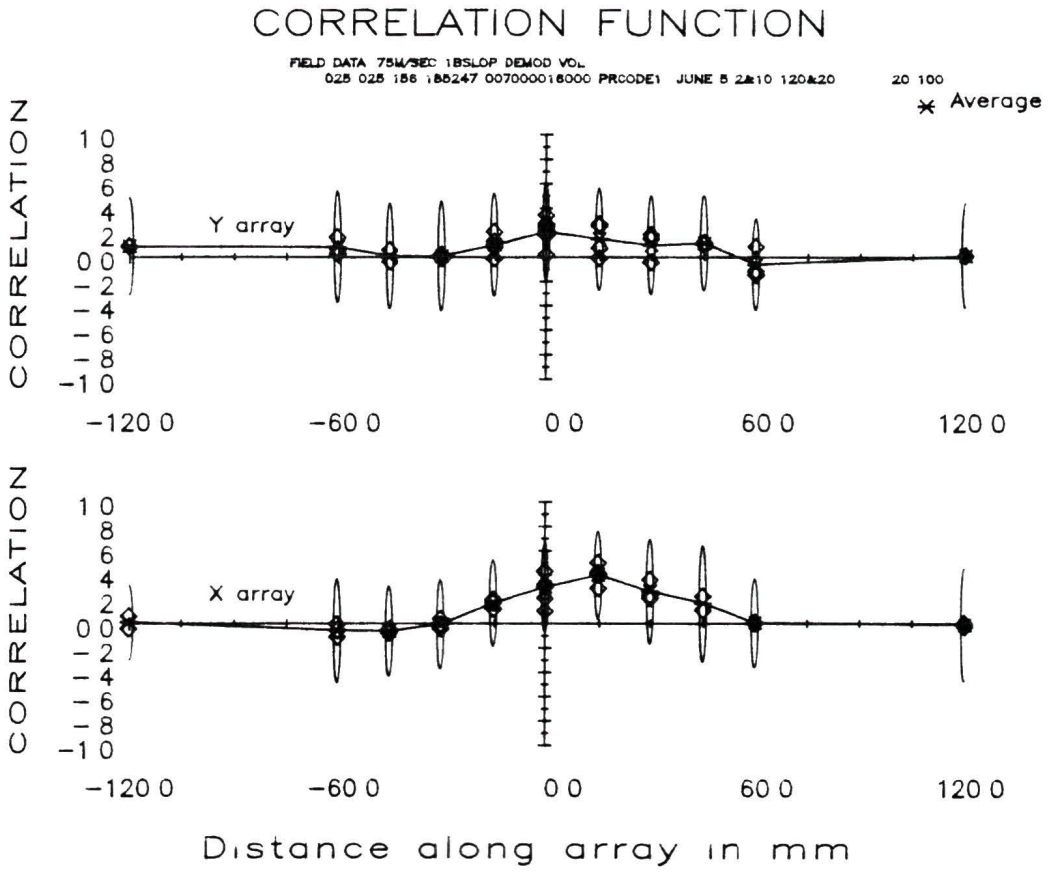

Figure 8.7

The spatial correlation function for one bit slope demodulated amplitude signal of field volume return data at a depth of 75m averaged over 20 transmissions

to the same values as used for the thin scattering layer simulations in chapter 8 The number of scatterers was increased from 1000 for the thin layer scattering, to 4000 since the water volume insonified is much greater for the volume return case Using a higher number of scatterers does not change the results, but slows the model simulations down to an unuseable level A velocity of 0 75m/sec was used in the x direction to simulate a moving scattering layer

As with the field data in figure 8 1 the individual pulses can no longer be seen in the time series due to the interpulse interference The 20 transmission average correlation function for these data is plotted in figure 8 9

The maximum correlation drops to 0 25 for the correlation function in figure 8 9, similarly to the field data correlation function in figure 8 4 A test to check if the drop in the correlation function peak was actually caused by the interpulse interference was conducted by storing the time series for the two pulses separately in the computer model The correlations were then performed on these data and averaged over 20 transmissions

The spatial correlation function for the separated data is shown in figure 8 10 A clear peak of 1 can be observed in the separated data correlation function The separated correlation function drops to zero at a distance from the peak as predicted from theory Since the x axis velocity is 0 75m/sec the correlation peak along the x array is shifted by 1 5cm The correlation along the y axis has a peak of only 0 65 due to the off axis problem discussed in chapter 8 Since separated pulse correlation function has a peak of one, while the actual correlation function of figure 8 9 has a peak of only 0 25, it can be concluded that the drop in the correlation function is caused by the interpulse interference

Several methods have been devised to improve the interpulse interference problem The use of spread spectrum codes for labeling the two pulses has been shown to be of only limited usefulness

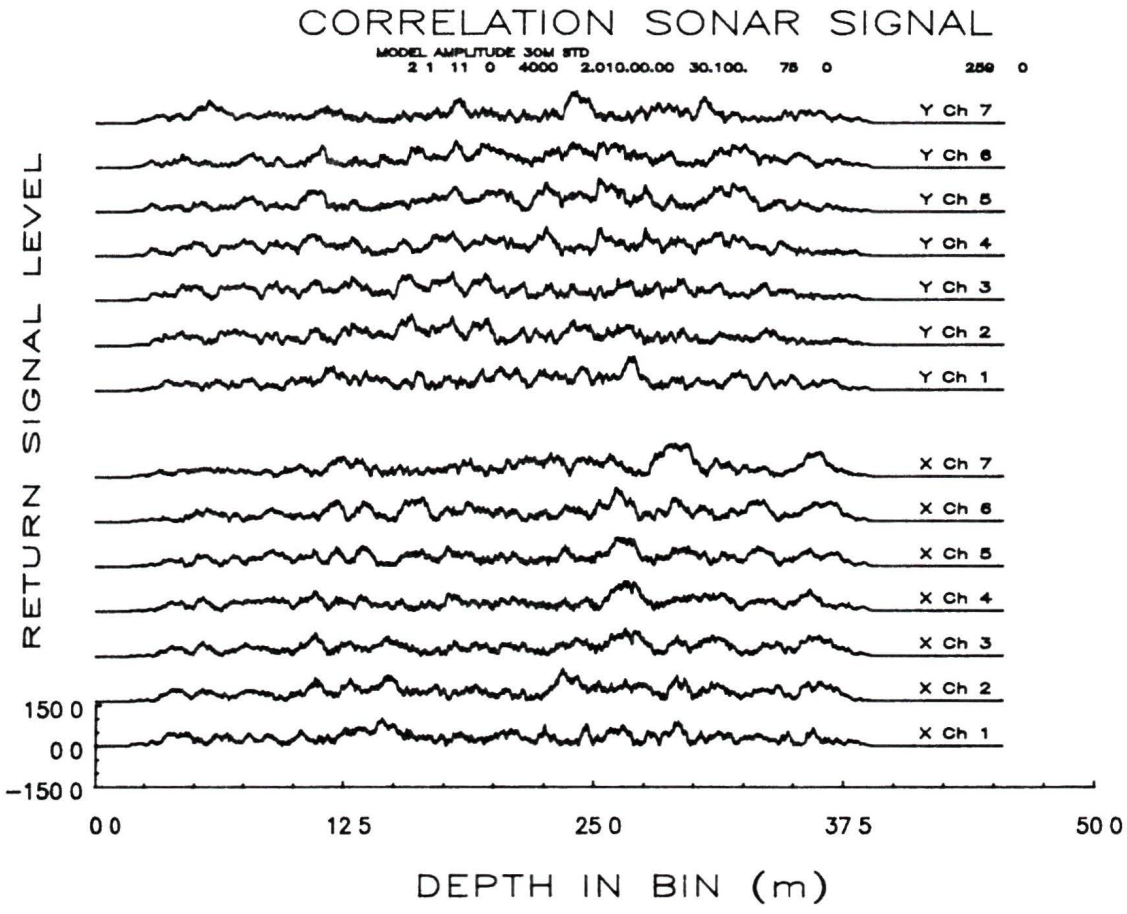

Figure 8.8

The computer model generated amplitude demodulated time series for a 30m scattering layer The layer is at a depth of 100m The pulse length was 2msec, while the pulse separation was 10msec

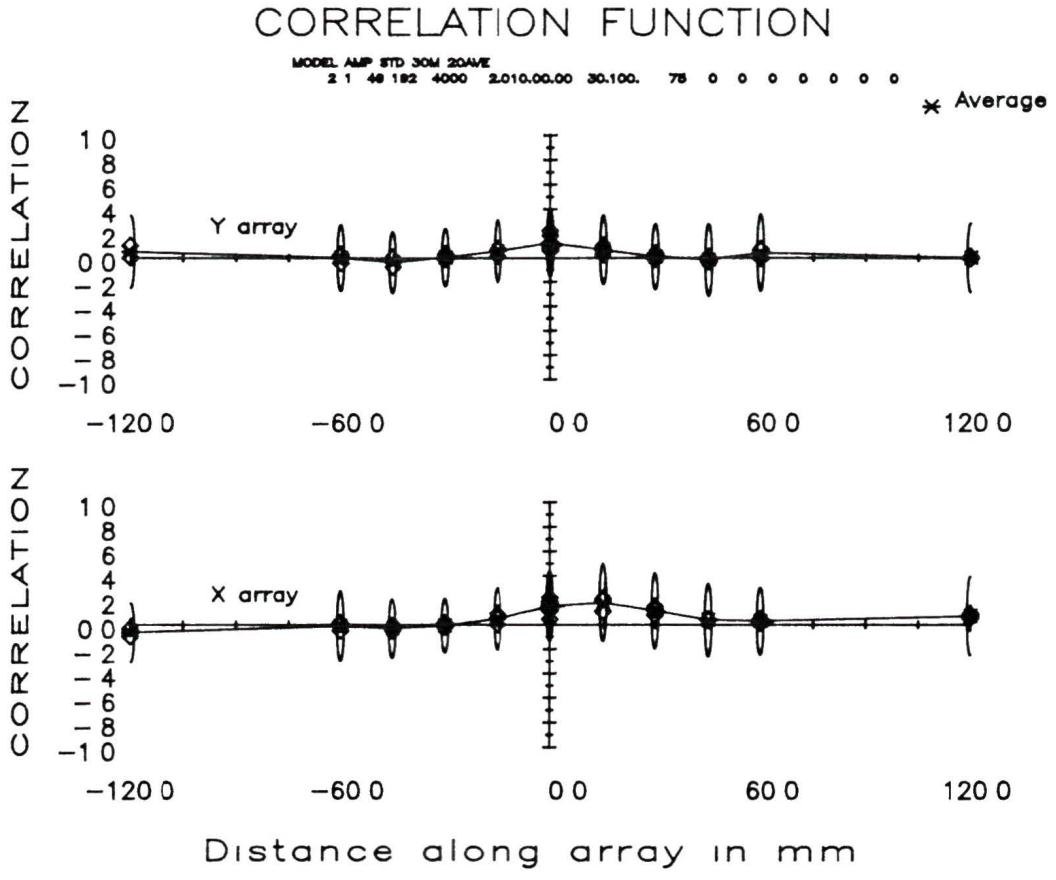

Figure 8.9

Spatial correlation function of computer model volume return data averaged over 20 transmissions at a depth of 120m

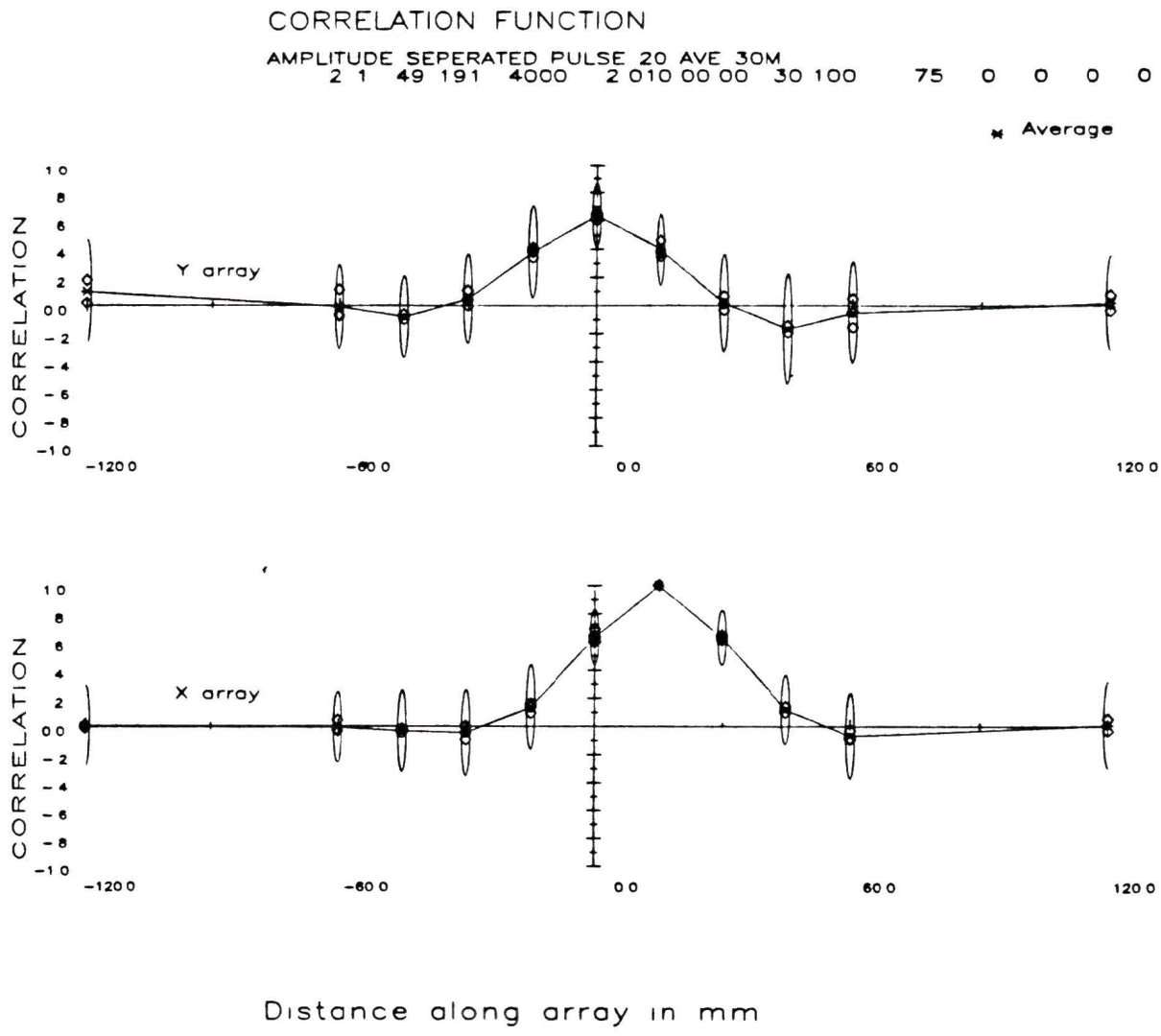

Figure 8.10

Spatial correlation function of the separated pulse volume return signal averaged over 20 transmissions at a depth of 120m

By sending each of the two pulses at a different frequency, it should be possible to separate the signals from the two returning pulses This is indeed possible, but unfortunately the actual interference pattern on which the correlations are performed is a sensitive function of frequency Thus even changing the frequency a slight amount will completely decorrelate the received signal

A bistatic correlation sonar with intersecting receiving and transmitting beams will prevent interpulse interference, but it will also severely limit system flexibility

8.4 Volume return velocity profiles

By performing the correlations at different range gates, the correlation function can be determined as a function of depth The velocities along each axis can be calculated from the location of the correlation peak The peak usually does not fall exactly on one of the transducer elements, thus some type of interpolation has to be used to locate the peak For the initial evaluation of the correlation sonar three point parabolic interpolation was used to locate the peak since it is simple to implement and has well known properties (Edward 1978)

A typical depth profile, obtained from the model data can be seen in figure 8 11 The solid line represents the velocity along the x array, while the dotted line represents the velocity along the y array The x velocity was 0 75m/sec and the y velocity was 0 0m/sec The average velocity along the x and y array are actually the expected values, but large deviations of 0 25m/sec on the x axis and 0 35m/sec on the y axis can be observed These deviations are due to the error introduced by the low peak height of the volume return correlation function The velocity profile for the separated pulse time series was plotted in figure 8 12, to see what the velocity profile would look like if interpulse interference were not present The separated pulse velocity profile is within 01m/sec of the expected value for the x axis profile, while the error on the

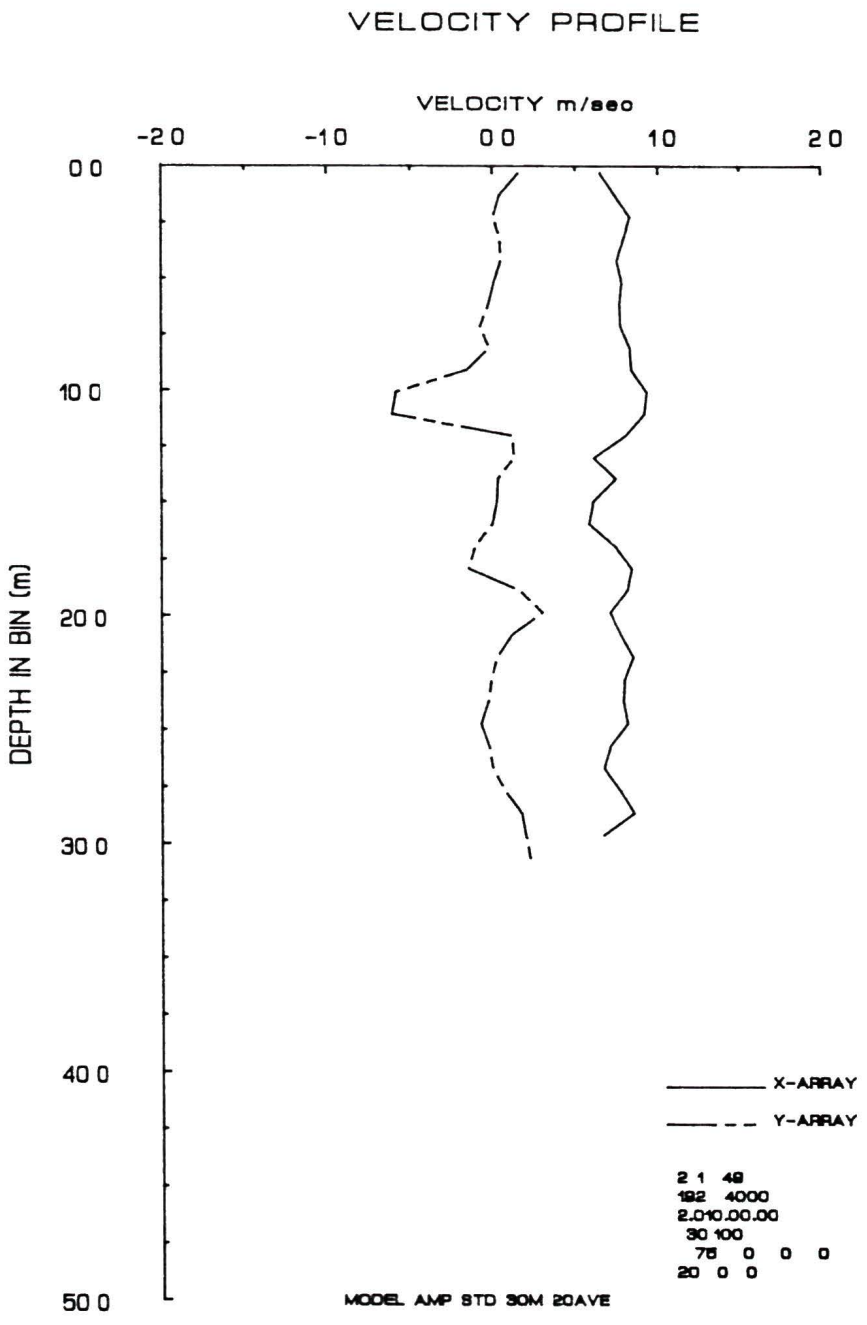

Figure 8.11

Velocity profile of the 30m model data calculated from the correlation with a depth resolution of 0 4m The correlations used to calculate the velocities were averaged over twenty transmissions The profile covers a depth starting at 100m

y axis profile is 0 05m/sec Since both the x axis and y axis profiles are calculated from the same data it is initially expected that the error should be the same in both Because of the off axis problem the correlation coefficients for the y axis correlation function are smaller than the values along the x axis and thus the velocity error on the y axis array is larger

From figure 8 12 it can be concluded then that both the off axis components and the interpulse interference will degrade the correlations and thus reduce the accuracy of the velocity estimate

For the field data from figure 8 1 the velocity profiles are plotted in figures 8 13, 8 14 and 8 15 for amplitude demodulation, slope demodulation and one bit slope demodulation respectively All three demodulation types show similar velocity profiles, and it is not possible to state that one technique gives more accurate results than another technique from the velocity profiles The accuracy, for a 20 transmission average, along the x array is approximated to be 0 2m/sec, while along the y axis it is about 0 3m/sec The y axis velocity profiles are less accurate than the x axis profiles due to the off axis decorrelation By sampling the spatial correlation function in a plane, with a redesigned transducer, the off axis decorrelation could be eliminated

8.5 Volume return complex and clipped complex demodulation

The spatial correlation function for the complex and clipped complex demodulated signals of the computer model is shown in figures 8 16 and 8 17 The peak of the complex signal correlation function is of height 0 5, while for the clipped complex correlation function the peak has an approximate height of 0 25 This is exactly what was predicted from the theory assuming the interpulse interference could be treated as being caused by a noise in the signal with a signal to noise ratio of one

The correlation function behaves exactly as predicted from theory for the different demodulation techniques The amplitude and clipped complex demodulation have a

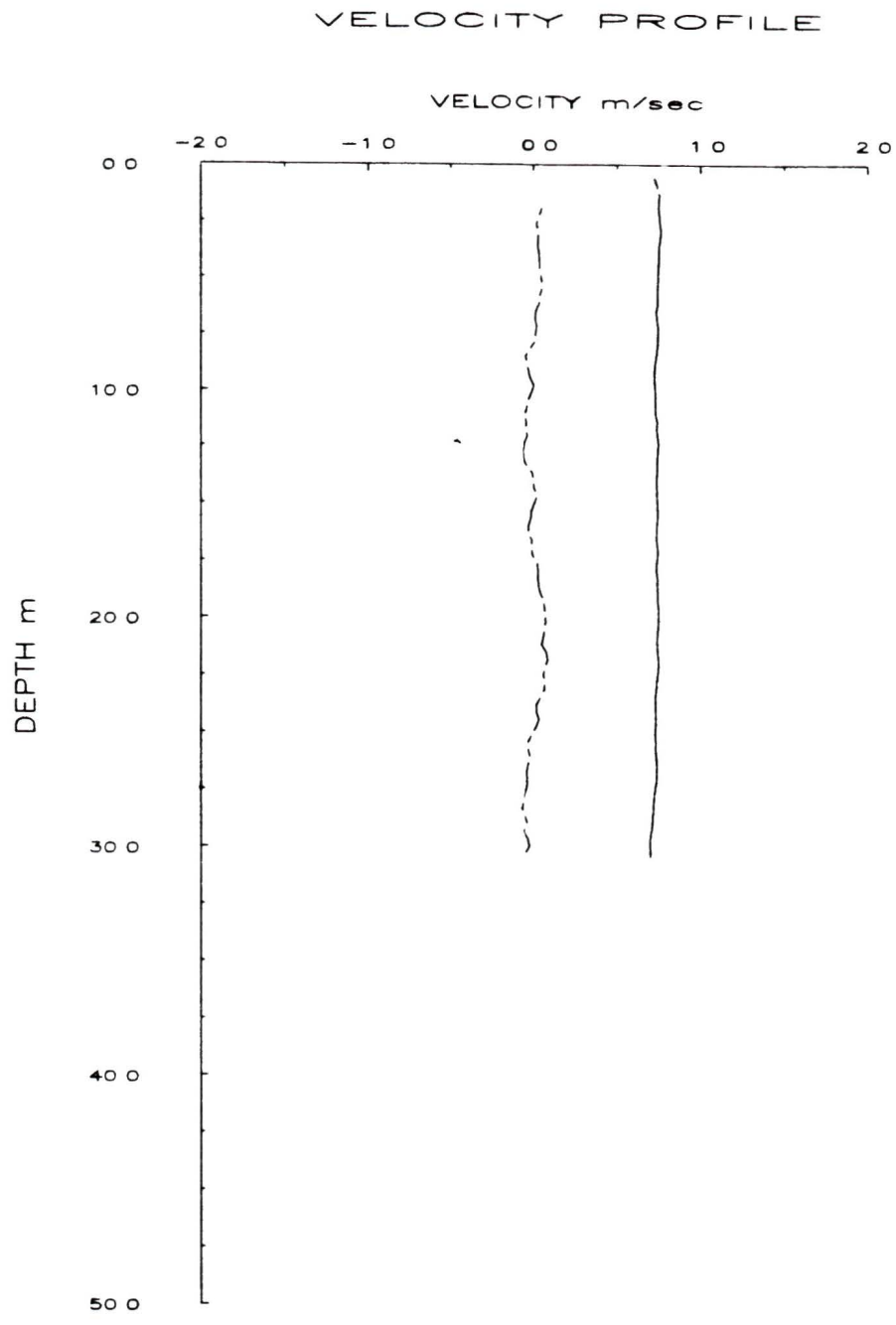

Figure 8.12

Velocity for separated pulse model data The x velocity was 0 75m/sec, while the y velocity was 0 0m/sec The profile is averaged over 20 transmissions and covers a depth starting at 100m

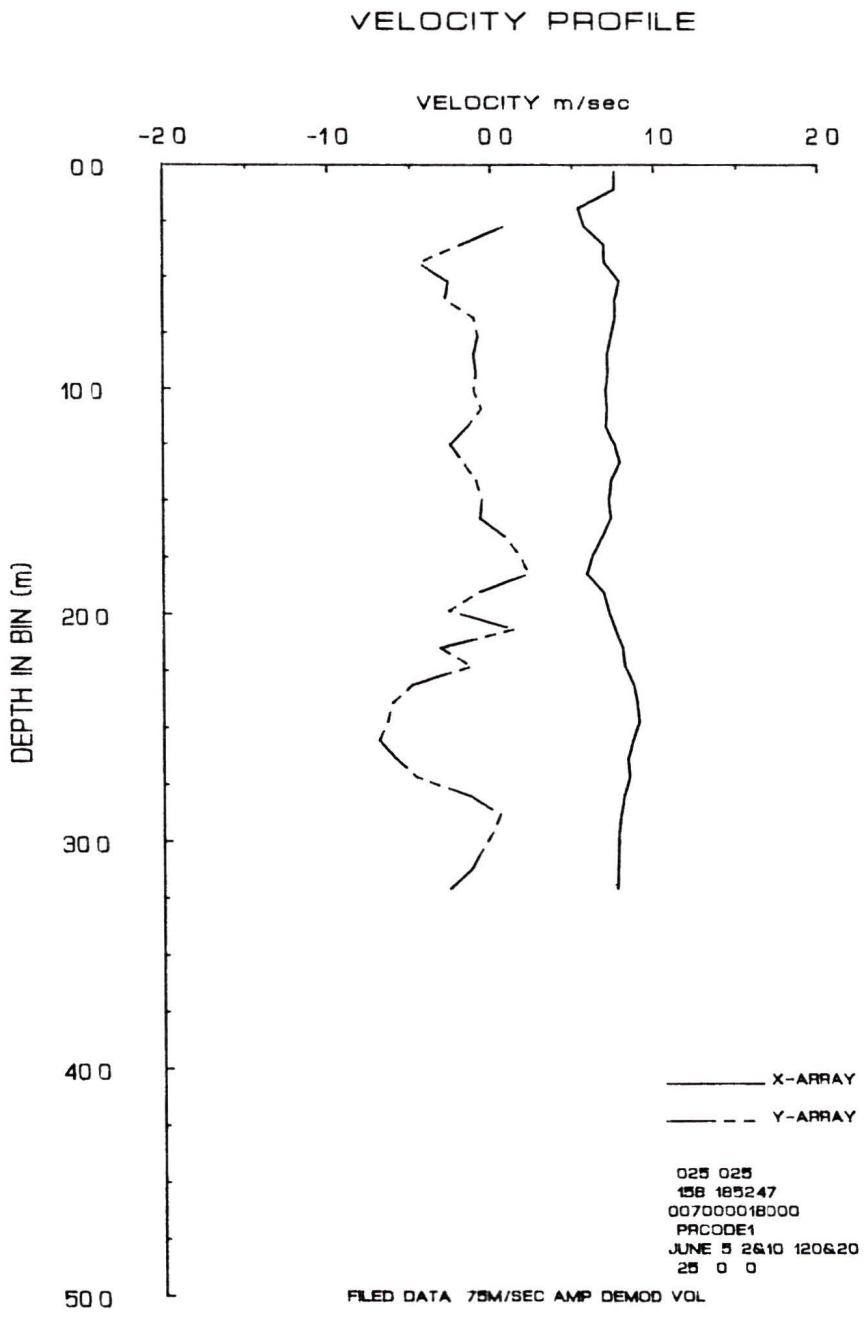

Figure 8.13

Velocity profile of amplitude demodulated field data taken with a ship velocity of 0 75m/sec The profile is averaged over 20 transmissions and starts at a depth of 50m

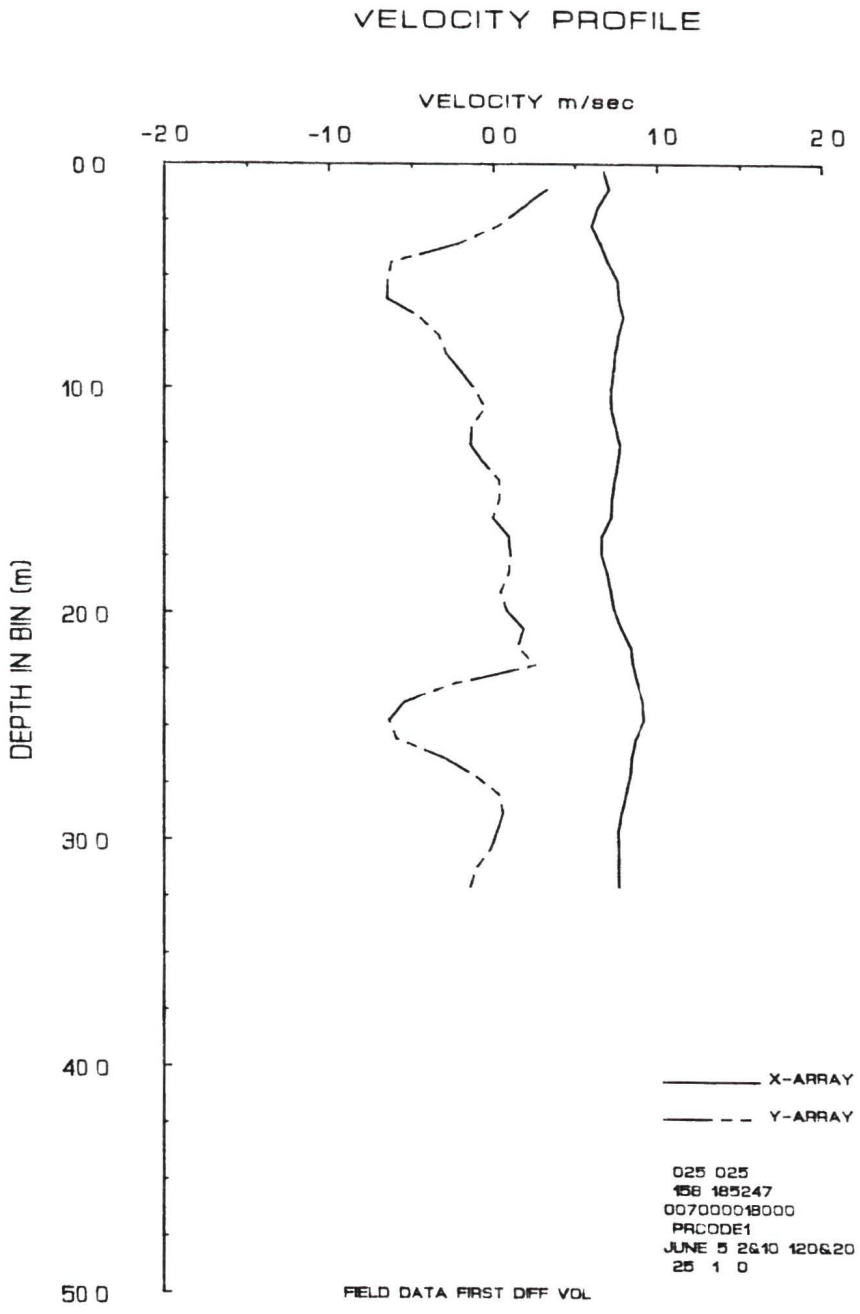

Figure 8.14

Velocity profile of slope demodulated field data taken with a ship velocity of 0 75m/sec The profile is averaged over 20 transmissions and starts at a depth of 50m

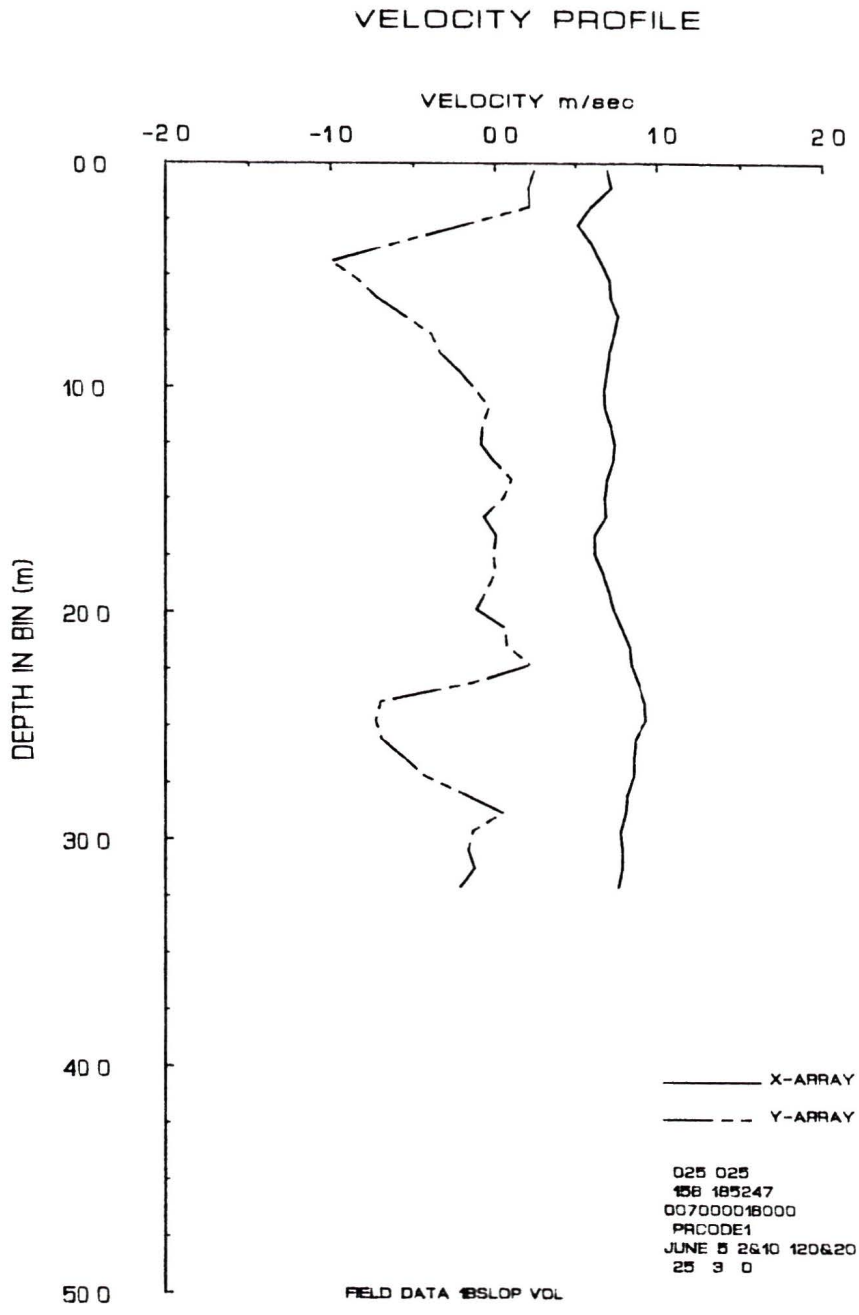

Figure 8.15

Velocity profile of one bit slope demodulated field data taken with a ship velocity of 0 75m/sec The profile is averaged over 20 transmissions and starts at a depth of 50m

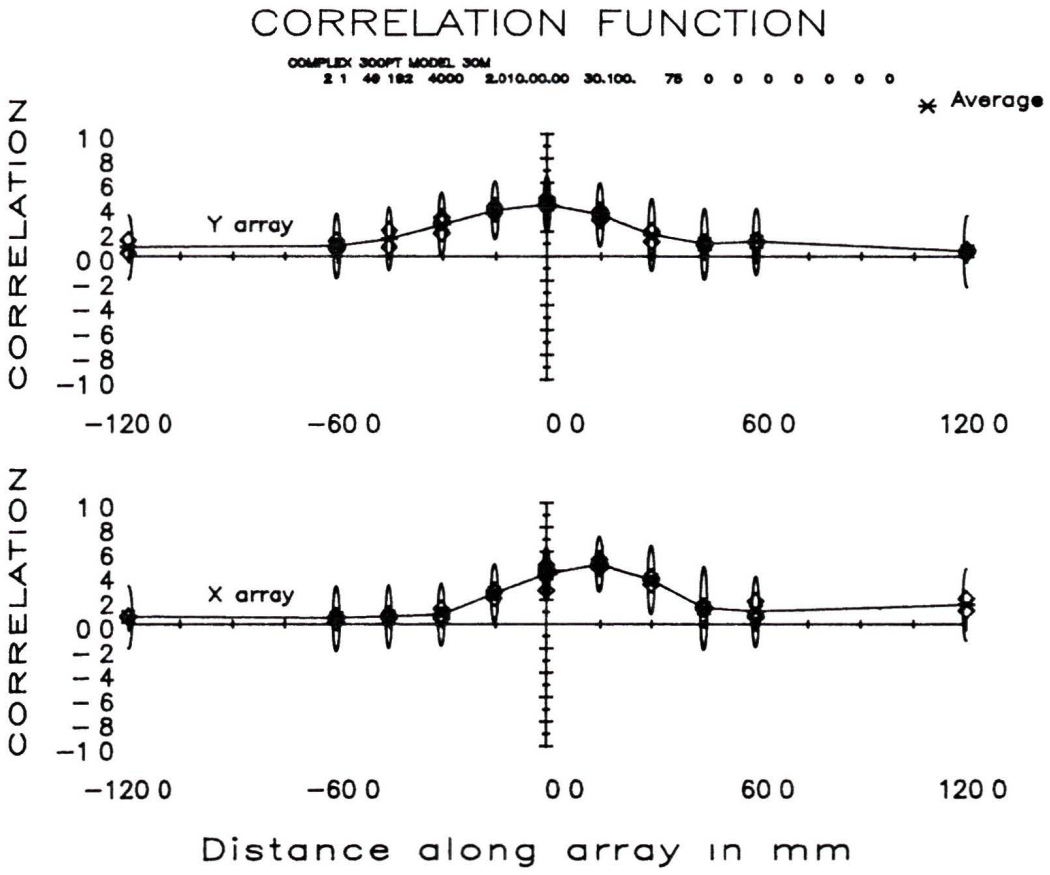

Figure 8.16

Spatial correlation function of computer model generated complex volume return signal averaged over 20 transmissions at a depth of 120m

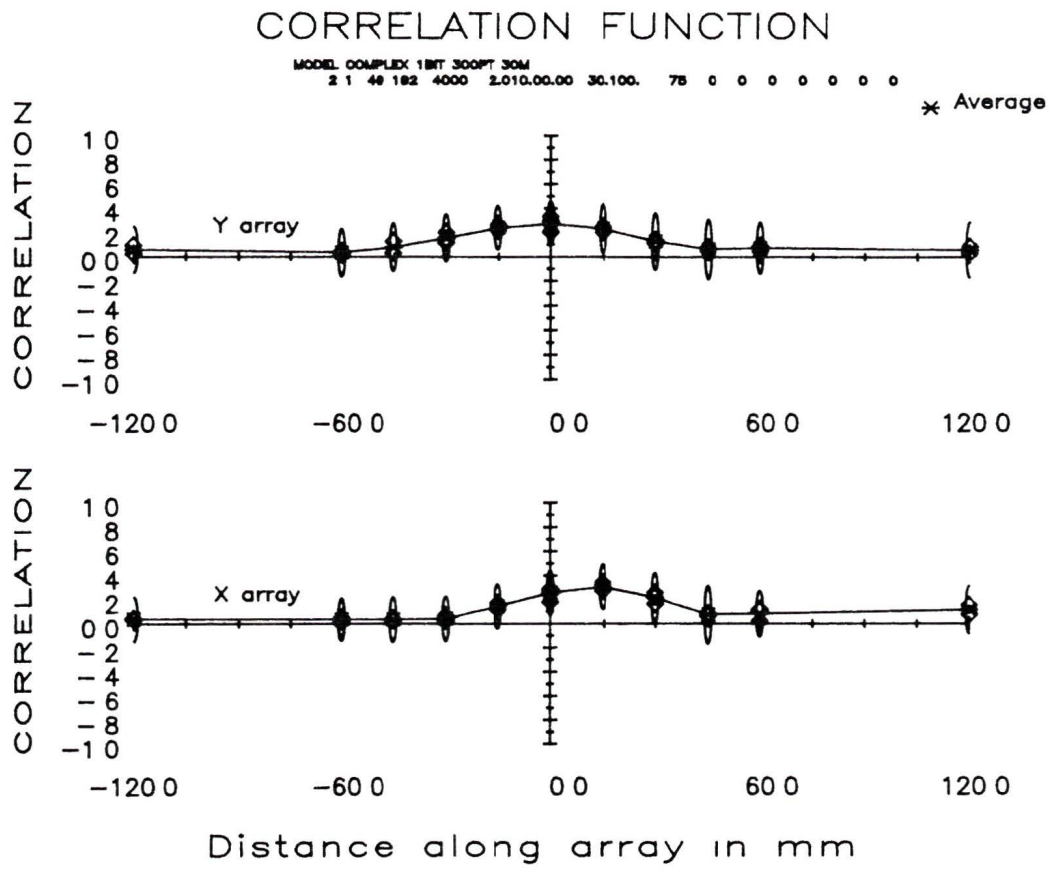

Figure 8.17

Spatial correlation function of computer model generated clipped complex volume return signal averaged over 20 transmissions at a depth of 120m

peak correlation of approximately 0 25, while the complex demodulation technique has a peak of about 0 5 The standard deviation of the amplitude demodulation correlation function is larger than that for the clipped complex correlation, thus the clipped complex correlation should perform better than the amplitude demodulated correlation The highest peak is obtained with the complex demodulated correlation function, and it will thus give the best results The spatial correlation function for the amplitude demodulated field volume return data is similar to the computer generated data, which confirms the correctness of the model

The velocity profile for the complex demodulated signal is shown in figure 8 18 It is more accurate than the velocity profile shown in figure 8 11 for the amplitude demodulated data It can therefore be concluded that complex demodulation will give a more accurate velocity profile The accuracy is approximately 0 1m/sec in the x and y directions for the 20 transmission average The velocity profile for the clipped complex demodulated data is similar to that of the amplitude demodulated data in figure 8 11

If 120 transmissions were averaged together for the complex demodulated data the velocity accuracy would be approximately 0 04m/sec This agrees with the value of 0 04m/sec predicted for the correlation sonar using Edward's equation 2 10 for the velocity standard deviation with a signal to noise ratio of one

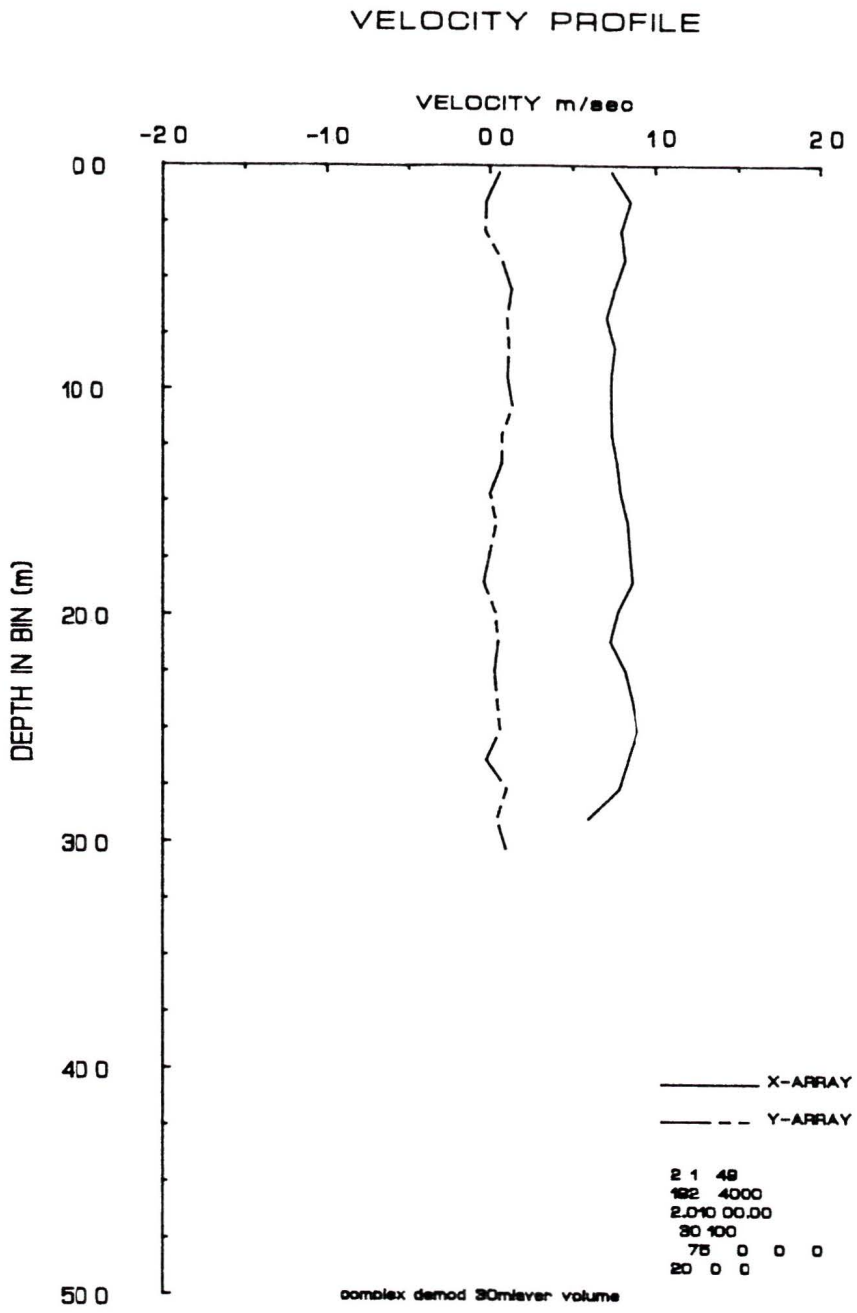

Figure 8.18

Velocity profile of complex demodulated model data of a 30m layer of scatterers at a depth of 100m averaged over 20 transmissions

9 COMPARISON OF DIFFERENT CORRELATION TECHNIQUES

To compare the effectiveness of a correlation technique, the correlation function has to be parameterized in some way In general the accuracy to which the correlation peak can be determined, at a given spatial sampling resolution, depends on two parameters The relative height of the peak of the correlation function above the off peak correlation and the size of the standard deviation of each of the correlation values A general method to compare two correlation techniques would be to calculate a correlation quality factor, which is the ratio of the peak height over the off peak standard deviation If the correlation quality factor of two correlation techniques is different by a factor of k, then approximately k^2 as many correlations would have to be averaged together to obtain similar accuracy peak location estimates In table 9 1 the different qualities are summarized An execution speed factor that gives the relative number of arithmetic operations required in the correlation is also given The execution speed for the clipped or one bit signals is given assuming that the summations are done using the same type of arithmetic as used in the other correlation types By using simple binary shift register correlation hardware the speed of correlation can be increased by a factor of ten or more for binary demodulations

The error in the off peak standard deviation given in the table may be up to 20 percent More precise values can only be obtained by taking a larger statistical sample of the correlations, which was not possible with the computing facilities available However, the values given in the table can be used to compare the different correlation techniques

The table shows the similarity between model and field data in the quality factor The quality factor is generally smaller for the field data because of the bandwidth limiting receive filters in the IOS correlation sonar Only the volume field data has a slightly higher quality factor than the model data This may be caused by the fact that the scatterers in the field data have a non uniform distribution and there was

Data Type	Correlation demodulation type	Peak height (A)	Off peak standard deviation (B)	Ratio A/B Quality	Relative execution speed
Model 1m Bottom	Amplitude	0 55	0 30	1 8 (1 6)	4
	Slope	1 00	0 20	5 0 (4 0)	4
	One bit slope	1 00	0 15	6 6 (5 5)	1
	Complex	0 90	0 30	3 0	8
	Clipped complex	0 95	0 20	4 8	4
	Amplitude wideband	1 00	0 15	6 6 (5 0)	4
	Slope wideband	1 00	0 15	6 6 (5 0)	4
	One bit slope wideband	1 00	0 12	8 3 (6 6)	1
	Complex wideband	0 90	0 08	11 2	8
	Clipped complex wideband	0 95	0 07	13 6	4
Field data 1m Bottom	Amplitude	0 65	0 40	1 6	4
	Slope	1 00	0 25	4 0	4
	One bit slope	1 00	0 18	5 5	1
	Amplitude wideband	1 00	0 20	5 0	4
	Slope wideband	1 00	0 20	5 0	4
	One bit slope wideband	1 00	0 15	6 6	1
Model 30m Volume	Amplitude	0 21	0 30	0 7 (0 9)	4
	Slope	0 20	0 18	1 1 (1 2)	4
	One bit slope	0 50	0 40	1 2 (1 2)	1
	Complex	0 50	0 25	2 0	8
	Clipped complex	0 25	0 20	1 3	4
	Amplitude separate correlation	1 00	0 25	4 0	–
	Amplitude wideband	0 30	0 15	2 0 (1 3)	4
	Complex wideband	0 50	0 10	5 0	8
	Clipped complex wideband	0 25	0 07	3 6	4
Field data 1m Volume	Amplitude	0 22	0 25	0 9	4
	Slope	0 27	0 23	1 2	4
	One bit slope	0 40	0 33	1 2	1
	Amplitude wideband	0 26	0 20	1 3	4
	Slope wideband	0 30	0 25	1 2	4
	One bit slope wideband	0 40	0 30	1 3	1

Table 9.1

The quality of various correlation and demodulation techniques in terms of accuracy of the peak location and the speed of correlation The values beside the model data in brackets, are for field data, to facilitate easy comparison between model and field data

a strong scattering layer present at 75m depth where the correlation values are compared The signal to noise ratio may consequently have been slightly greater than 1 for the field data volume return

The table shows the increase in accuracy of the correlation coefficients by using a wideband transmitted pulse for both the model and field data The increase in accuracy when using wideband signals is greater for the model data than for the field data, especially for the volume return, because the model does not have a restricted bandwidth demodulator This means that the model signal will have a bandwidth of about 10kHz, while the field data are restricted to 4kHz with bandpass filters

The values for the correlation peak heights are, within experimental uncertainty, as predicted from theory earlier in this thesis for both model and field data The quality factor of the different correlation techniques for the model and field data also agree to within experimental uncertainty The quality factor values in brackets shown in table 9 1 are for the field data, beside the values for the model data Since the model data agree with the field data, where comparison is possible, the optimum signal processing technique for a two pulse correlation sonar can be determined, from an extension of the model to cases where field data is not available The best accuracy for volume return correlations can be achieved using complex demodulation of the received signal For complex demodulation of a volume return signal, the ratio of relative peak height over off peak standard deviation is about 2 0, while the ratio is about 0 8 for amplitude demodulated signal volume return This means that more than four times as many correlations would have to be averaged together for the the amplitude demodulated correlation function, than for the complex demodulated correlation function, to get similar accuracy If wide bandwidth pulses are used for transmission, the increase in accuracy is even more pronounced for complex demodulation The accuracy of the clipped complex demodulation for volume return, is better than that of amplitude demodulation while, it is worse than that of complex demodulation For the same number of pings the complex demodulation would therefore give more accurate velocity estimates than either of the clipped complex or amplitude demodulated signal

10 SUMMARY OF RESULTS

A correlation sonar allows acoustic remote sensing of current profiles with temporal and spatial resolutions not obtainable with in situ methods such as moored current meters A correlation sonar operates by reflecting acoustic energy off scatterers suspended in the water volume of interest By obtaining the correlation function of the reflected signal at a receiving hydrophone array at the ocean surface or bottom it is possible to infer the scatterer and thus the water velocity

A characteristic of the correlation sonar is that it uses wide bandwidth transmission pulses and a wide beamwidth A related velocity sensing apparatus, the Doppler sonar, uses narrow beamwidth and long pulses for accurate velocity measurement Smaller transducer size and depth resolution are some of the advantages of the correlation sonar over the Doppler sonar

The shape of the spatial correlation function of the received signal was shown to be gaussian with a width $W \approx \frac{c}{f_o \theta_o}$, where c is the speed of sound in the water, f_o the acoustic frequency and θ_o the width of the transmitting and receiving beams In any practical correlation sonar system, the correlation function can be sampled only at discrete points in space If the transducers are arranged in the form of two linear perpendicular arrays, correlations performed on the two arrays will give the spatial correlation function along two perpendicular lines segments A new investigation revealed that a high velocity along one of the two axes will cause a lowering of the correlation along the other axis A lower correlation peak always means a less accurate velocity estimate The lowering of the off axis correlation value was observed in all the data collected from the IOS correlation sonar and the computer model that simulated the correlation sonar operation The spatial correlation function must be sampled in a plane, to prevent the off axis decorrelation, not just along two axis By using a receiving transducer layout in the form of an U or T shape, the spatial correlation function can be obtained in a plane, if cross correlations between all elements are performed

The accuracy of the correlation sonar velocity estimate depends on many parameters The bandwidth in the received signal and the signal to noise ratio of the received signal are the two most important parameters for a volume return correlation sonar The accuracy to which the velocity can be determined is limited by the height of the correlation peak and the error on each of the correlation values The correlation peak height is determined by the signal to noise ratio of the received signal, while the error on each of the correlation values is related to the number of independent samples in the received time series The number of independent samples is the integration-time bandwidth product A wider bandwidth transmission pulse and a lower signal to noise ratio will give more accurate velocity measurement

The signal received on each hydrophone can be demodulated using several different techniques Complex demodulation uses quadrature demodulation to recover all the received information Clipped complex demodulation uses the complex demodulated signal digitized to one bit accuracy and thus only recovers the sign of the complex signal Amplitude demodulation uses the amplitude information embedded in the complex signal A new type of demodulation, slope demodulation, is the first difference amplitude demodulated signal, while one bit slope demodulation uses the clipped slope demodulated signal The correlation function for clipped complex and one bit slope demodulated signals is self normalizing, which allows the use of simple correlation hardware to speed up the correlation process Complex, amplitude and slope demodulation require high resolution digitizers to sample the received signal, which require large memories for storage and accurate gain control New experimental and computer data showed that one bit slope demodulation will give more accurate results than amplitude demodulation for bottom return correlations

For volume return scattering the received in-phase and quadrature components of the acoustic field have a normal probability distribution This means that the phase of the demodulated signal is uniformly distributed over 2π and that the amplitude signal has a Rayleigh distribution The signal received on each hydrophone will contain

energy from both pulses that are present in the water at the same time In the correlation process the signal from a single pulse is required A newly developed theory showed that, since the two received pulses cannot be separated, the other contaminating pulse must be considered noise of equal amplitude to the signal The signal to noise ratio can therefore never be greater than one for complete volume return Electronic and system noise can usually be controlled to be much better than a signal to noise ratio of one, and therefore the important noise contribution will come from interpulse interference

The potential for pulse labeling using spread spectrum techniques has been analyzed in this thesis using a newly developed theory Although the use of spread spectrum codes is a suitable method of generating broad band signals, which improve the time-bandwidth product of the correlations, it is shown that the improvement in the signal to noise ratio due to interpulse interference is only a factor of 1 4 for a 127bit maximal linear sequence The low increase of the signal to noise ratio combined with the limitations placed on the usable vertical velocity makes pseudo random noise codes impractical for labeling the correlation sonar pulses

A new study showed that the different correlation techniques will behave differently for a given signal to noise ratio It was shown that, for a noise free bottom return signal, the correlation peak will always be one since the two signals that are correlated at the peak are equal For volume return the two equal signals will be contaminated by noise with an effective signal to noise ratio of one The correlation peak of a complex demodulated signal is 0 5 for a signal to noise ratio of one A new theory shows that the clipped complex correlation coefficient will drop to 0 25 and the amplitude demodulated correlation coefficient will drop to 0 23 under similar circumstances Complex demodulation will therefore perform better than clipped complex demodulation or amplitude demodulation This can be observed in both computer model data and field data from Saanich Inlet Velocity profiles can be obtained from the correlation sonar data by repeating the correlation process at different range gates Velocity

profiles obtained with the computer model and the IOS correlation sonar show the effect of both the interpulse contamination and the off axis correlation, and confirm the theoretical predictions

The accuracy of the correlation values can be improved by sending a wide bandwidth transmission pulse into the water column, using pseudo random sequences, and increasing the bandwidth of the receiving electronics This increase in accuracy is observed in both the computer model and field data

Theory, the data from the computer model and the data collected in the field show that the two pulse correlation sonar principle works and that it can be used for water current measurement Given that the field data support the computer model data for those cases that can be tested, the computer model can be used to postulate a optimum approach for the design of a current measuring correlation sonar As a result of what has been identified in this thesis, the following is a description of an implementation of the two pulse correlation sonar method which would allow the measurement of ocean currents from a moving platform such as a ship

An acoustic frequency of 100kHz should be used since it is a good compromise between range attenuation and scattering strength It was shown in this thesis, that the correlation function must be sampled in a horizontal plane, to prevent off axis decorrelation This can be accomplished by using a U shaped array of receiving hydrophones It can be shown that all the vector separations in a plane can be obtained from a U shaped array

The data collected in the field showed that the ship's forward velocity will usually be a large component of the measured velocity The hydrophone array must therefore be able to track larger velocities in the direction of the ship's heading than perpendicular to it At 100kHz, a correlation function width of 4cm dictates a transducer spacing of 1 5cm or less The field data showed that a pulse separation of 10msec is optimum, which requires 5 transducers to track a velocity range from 0 to 2 5m/sec

If the ship's velocity is 0 to 3 5m/sec, the U shaped array should have 12 transducers along the base of the U, pointing in the direction of the ship's heading, and 5 transducers in each of the arms of the U This means that the total number of transducers is 20

Data from the computer model and the field indicated that correlations will only have to be performed for those elements which give a current velocity range of $+/-2$ 5m/sec since the ship's velocity can be determined by tracking the bottom The number of cross correlations is therefore 81, which results in an 9 by 9 array of correlations A two dimensional gaussian must be fitted to the 9 by 9 array to determine the exact displacement of the peak

A suitable hydrophone array can be constructed using newly developed plastic-film transducers, which can be easily formed into an array Each hydrophone element should be round for symmetry A investigation with the computer model revealed that any other transducer element shapes, such as square or rectangular, will result in decorrelation for off axes currents Model investigation also indicated that the transmitter should have a beamwidth of approximately 20 degrees, while the receiving hydrophone beamwidth should be slightly larger than this

The transmit pulse must be phase modulated with a bit length of 50μsec, which will result in a signal bandwidth of 20kHz Computer model and field data both showed that a high bandwidth will give a more accurate velocity estimate

The results from the computer model agreed with the field data for those cases that could be tested The model can therefore be used to postulate the best possible signal demodulation technique The signal must be complex demodulated by mixing it with a in-phase and quadrature carrier and low pass filtering, to give the largest possible correlation peak The resulting two in-phase and quadrature channels should be sampled at a rate of 20kHz using a 16bit analog to digital converter to cover the large dynamic range required

Results from the IOS correlation sonar showed that each receiving hydrophone must have its own highly sensitive pre-amplifier to minimize noise The 100kHz signal may be mixed down to 20kHz in the transducer housing before it is sent to the deck unit for demodulation and digitizing The gains of the amplifiers should be adjustable so that the strongest return signal will just be clipped The strong clipped signal will still give proper, although slightly lower, correlations, while the weak return signals will be within range of the digitizer Data from the IOS correlation sonar indicated that a high resolution digitizer is essential to allow the digitization of the whole water column without switching gains

From experience with the IOS correlation sonar it was found that the control processor must have enough memory available to store 0 5sec of data for a 350m range, which is equivalent to 800 kilobytes Since it will not be possible to balance the gains of the receiving hydrophones, the fully normalized complex correlation calculation must be used By observing the amount of processing required for computer model data, it was found that a velocity profile with a 5m resolution and a correlation integration time of 15msec requires 14 million floating point operations Once the correlation peak has been located, a time lagged correlation which locates the correlation peak in the time domain will give the vertical velocity Edward (1978) demonstrated that the vertical velocity will usually be more accurate than the horizontal velocity For real time calculation of the three dimensional velocity profile at 2 transmissions per second, 30 million floating point operations per second are required with two banks of memory, one for performing the correlations, while the other one is used to collect the digitized data

Since real time operation is essential, the large number of arithmetic operations required could either be obtained using a single high speed array processor, or several smaller low cost vector signal processing devices such as the newly developed Zoran corporation (Zollo 1986) VSP processor Twenty VSP processors operating in parallel should be able to perform the necessary calculations in real time

Using dedicated signal processing devices for the correlation calculation would allow the control processor to perform some high level processing such as averaging of the velocity profiles and displaying the velocity profiles in real time to the operator The resulting data could then be stored on nine track magnetic tape or hard disk

Using a two pulse correlation sonar with the above design parameters, it should be possible to obtain a 120 transmission average velocity profile every minute, with a velocity range of 0 to 2 5m/sec and an accuracy of 0 04m/sec

REFERENCES

Andermo, N I and Mosrelıez, K 1978 *Acoustıc log* Unıted States Patent, No 4068207

Barrodale, I , Roberts, D K , and Ehle, B L , 1971 *Elementary computer applıcatıons*, John Wıley & Sons Inc , New York

Beamısh, P , 1971 "Quantıtatıve measurements of acoustıc scatterıng from zooplanktonıc organısms" *Deep-Sea Research*, vol 18, pp 811-822

Booth, A D 1985 *The development of a sımulator for correlatıon sonar data generatıon and ıts use for system evaluatıon and redesıgn* Report prepared for Seastar Instruments, 2045 Mills road, Sıdney BC

Brıggs, B H 1980 "Radar observatıons of atmospherıc wınds and turbulence a comparıson of techniques" *Journal of Atmospherıc and Terrestrıal Physıcs*, vol 42, pp 823-833

Churnside, J H and Yura, H T 1981 "Velocity measurement usıng laser speckle statıstıcs" *Applıed Optıcs*, Vol 20, No 20, pp 3539-3541

Davenport, W B , Jr , and Root, L R 1958 *An ıntroductıon to the theory of random sıgnals and noıse* McGraw-Hill book company Inc , Toronto

Dıckey, F R , Jr , 1958 "The correlatıon Aırcraft Navıgator, a vertıcally beamed Doppler radar" Proceedıngs of the Natıonal Conference on Aeronautıcal Electronıcs

Dıckey, F R , Jr , 1981 *Velocıty measurıng correlatıon sonar* Unıted States Patent, No 4244026

Dıckey, F R , Jr and Bookheımer, W C 1983 *Implementatıon and testıng of a deepwater correlatıon velocıty sonar* Offshore Technology Conference, Houston, pp 437-445

Dickey, F R , Jr and Edward J A 1978 *Velocity measurement using correlation sonar* Location and Navigation Symposium, San Diego CA, pp 255-264

Edward, J A 1978 *Accuracy relationship in a Correlation Sonar System for the Remote Measurement of Water Currents* Report by General Electric Company, Heavy Military Equipment Department, Syracuse, NY Prepared for U S Department of Commerce/NOAA (Private communication available through courtesy of the author)

Edward, J A 1979 "Remote Measurement of Water Currents Using A Correlation Sonar" *Journal Acoustic Soc Am , Supplement* , Vol 66, p557

Farley, D T 1982 *Pulse compression using binary phase codes* Internal report, School of Electrical Engineering, Cornell University, Ithaca, NY 14853

Farmer, D M , Booth, A D and Kamitakahara, G 1981 "Preliminary considerations in the design of a correlation sonar for remote velocity profile measurements in the ocean" *Proceedings of international Synopsium on Acoustic Remote Sensing of the Atmosphere and Oceans* (University of Calgary Printing Services, 1981)

Farmer, D M and Crawford, G B 1983 "Measurement of acoustic correlation in the ocean with a high frequency echo sounder" *Nature*, Vol 301, No 5902, pp 698-700

Golay, J E 1961 "Complementary series" *IRE Transactions on information theory*, IT-7, pp 82-87

Gray, R W and Farley, D T 1973 "Theory of incoherent-scatter measurements using compressed pulses" *Radio Science*, Vol 8, No 2, pp 123-131

Hoel, P G 1954 *Introduction to Mathematical Statistics* John Wiley & Sons Inc , New York

Huston, D 1986 Private communication

Ishimaru, Akira 1978 *Wave propagation and scattering in random medium* Academic press, New York, Volume 1

Junger Instruments 1976 *SAL-ACCOR Marine Log* Junger Instrument Marine division manual for SAL-ACCOR Marine Log, Svetsarvagen 15, Stockholm, Sweden

Lawson, J L and Uhlenbeck, G E 1950 *Threshold Signals* Dover Publications Inc , New York

Pinkel, R 1980 "Acoustic Doppler Techniques" Reprinted from *Air Sea Interactions*, Plenum Publishing corp , New York

Stanton, T K 1986 "Sonar echo statistics as a remote sensing tool Volume and Seafloor" *IEEE Journal of oceanic engineering*, Vol OE-11, No 1

Woodman, R F 1980 "High altitude resolution stratospheric measurement with the Arecibo 430-MHz radar" *Radio Science*, Vol 15, No 2 pp 417-422

Woodward, W E and Gerald, F A 1986 "Current velocity measurement using acoustic Doppler backscatter A review" *IEEE Journal of oceanic engineering*, Vol OE-11, No 1 , pp 3-6

Zedel, J 1985 *Evaluation of an acoustic Doppler profiler with applications to flow in a Fjord* Master of Science Thesis, University of Victoria

Zedel, J 1986 Private communication

Ziemer, R E and Peterson, L P 1985 *Digital communications and spread spectrum systems*, Macmillan publishing company, New York

Zollo, S 1986 "A new class of DSP chip The Vector Signal Processor" *Electronics*, Vol 59, No 27, pp 59-66

VITA

Surname Huber Given Names Benedikt Theodor

Place of Birth Munich W Germany Date of Birth Feb 28 1959

Educational Institutions Attended with Dates of entering and Leaving

University of Victoria, BC 1979 to 1983

University of Victoria, BC 1984 to 1986

Degrees, Diplomas, Awarded, with Dates and Names of Institutions

B Sc (Honors) 1983 University of Victoria, BC

Honors and Awards

University of Victoria Presidents Entrance Scholarship 1978

University of Victoria Presidents Scholarship 1979

BC Postsec Scholarship 1986

N S E R C Scholarship 1984/1985, 1985/1986

PARTIAL COPYRIGHT LICENSE

I hereby grant the right to lend my thesis (the title of which is shown below) to users of the University of Victoria Library, and to make single copies only for such users or in response to a request from the Library of any other University, or similar institution, on its behalf or for one of its users I further agree that permission for extensive copying of this thesis for scholarly purposes may be granted by me or a member of the University designated by me It is understood that copying or publication of this thesis for financial gain shall not be allowed without my written permission

Title of Thesis

INVESTIGATION OF THE TWO PULSE CORRELATION SONAR TECHNIQUE FOR WATER CURRENT MEASUREMENT

Author [redacted]

Benedikt Huber

Nov 27 1986